INDUCTION OF PLASTICITY IN SUBCORTICAL STRUCTURES AND ITS APPLICATION IN SPINAL CORD INJURY

Maria Germann

Thesis submitted for the degree of

Doctor of Philosophy

Institute of Biosciences

Faculty of Medical Sciences

Newcastle University

Supervisors

Prof Stuart N. Baker

Dr Mark R. Baker

March 2022

Abstract

Most current non-invasive plasticity protocols target the motor cortex and its corticospinal projections. Approaches for inducing plasticity in sub-cortical circuits and alternative descending pathways such as the reticulospinal tract (RST) are less well developed.

The overall aim of this thesis was to gain a better understanding of the extent to which corticospinal transmissions are altered after spinal cord injury (SCI) and to explore the mechanisms of non-invasive stimulation protocols at the cortical and subcortical level.

In the first study, transcranial magnetic stimulation was used to elicit motor-evoked potentials (MEPs) in the biceps brachii using different coil orientations, which allows for preferential activation of different neural elements. Analysis of MEP latencies suggests that differences between MEPs elicited by specific coil orientations may not be fully preserved in humans with cervical SCI, both in the biceps and in more distal muscle groups.

In a second study, we developed a novel associative stimulation paradigm, which paired loud acoustic stimuli with transcranial magnetic stimulation over the motor cortex in healthy participants and observed enhanced motor output after stimulus pairing ended. Electrophysiological measurements in humans and direct measurements in monkeys undergoing a similar protocol implicate corticoreticular connections as the most likely substrate for the plastic changes.

Finally, we used a custom built device to deliver precisely paired auditory clicks with electric stimulation to the muscle. We observed changes in electrophysiological measurements consistent with the induction of sub-cortical plasticity in the biceps muscle. We then used the same protocol to target the triceps muscle in individuals with SCI over the course of 4 weeks. Notably, we did not observe the same changes as in the biceps muscle, suggesting that elbow flexors and extensors have a different potential for plasticity, perhaps due to a differential control of flexor and extensor motoneurons by corticospinal and reticulospinal pathways.

Acknowledgements

The work presented in this thesis would not have been possible without the help and support from many people.

First and foremost, I would like to thank my supervisor Stuart Baker, for his exceptional encouragement, enthusiasm and continuous support and patience throughout the entire process. His unwavering belief in my abilities has helped me expand my comfort zone in all the best ways.

A special thanks to Mark Baker, for his tireless support and advice, and for always providing a link between basic science and clinical expertise with a bottomless repertoire of anecdotes.

I am grateful to the International Spinal Research Trust, for funding this work.

I would like to thank all the people outside of Newcastle, whom I had the pleasure of working with over the past few years. To Monica Perez, for welcoming me during my stay in her lab in Chicago and Hang Jin, who stepped up to help with the project. To Supriyo Choudhury, Robin and Tapati Sengupta, for an unforgettable time in India. To Jane Symonds, Harvey Sihota and the entire NeuroKinex team, for hosting me at their gym in Hemel Hempstead and for helping me complete my project there with an inspiring positivity. To Jason and Marco, for being wonderful students under my supervision and helping me collect data.

I'm thankful to Norman Charlton for designing and building virtually every piece of my equipment.

This would have been a much harder and gloomier experience without the uplifting and joyful environment made possible by the Bakerlab members. Thanks to all present and former members of the lab, as well as the extended Cheese & Wine community.

I am grateful to all my study participants, who volunteered their time for science and made this work possible.

Finally, I would like to thank my family for providing me with their constant support, even across countries, and my friends for providing me with a family away from home. And to Beshoy and Matthew, for taking me in during the lockdowns and weathering these strange times with me.

Table of Contents

List of Figures and Tables

Abbreviations

1DI	First dorsal interosseous
AE	Adverse event
ADM	Abductor digiti minimi
AMT	Active motor threshold
ANOVA	Analysis of variance
AP	Anterior-posterior
ASIA	American spinal injury association
AUC	Area under the curve
CMEP	Cervicomedullary motor evoked potential
CST	Corticospinal tract
CUE	Capabilities of upper extremity
EMG	Electromyography
FDS	Flexor digitorum superficialis
IN	Interneuron
IZ	Intermediate zone
LAS	Loud acoustic stimulus
LED	Light-emitting diode
LLSR	Long latency stretch reflex
LM	Lateral-medial
LTD	Long-term depression
LTP	Long-term potentiation
MDC^2	Mahalanobis distance squared

MEP	Motor evoked potential
MN	Motoneuron
MVC	Maximal voluntary contraction
PA	Posterior-anterior
PAS	Paired associative stimulation
PT	Pyramidal tract
RF	Reticular formation
RST	Reticulospinal tract
SCI	Spinal cord injury
SCM	Sternocleidomastoid muscle
STDP	Spike timing-dependent plasticity
TES	Transcranial electrical stimulation
TMS	Transcranial magnetic stimulation
VART	Visual-auditory reaction time
VRT	Visual reaction time
VSRT	Visual-startle reaction time

Publications

Papers

Germann M, Baker SN (2021) Evidence for Subcortical Plasticity after Paired Stimulation from a Wearable Device. J Neurosci 41:1418-1428.

Germann M, Poll A, Raditya M, Siong JT, Baker SN Pairing Transcranial Magnetic Stimulation and Loud Sounds Produces Plastic Changes in Motor Output. *Submitted to the Journal of Neuroscience.*

The following work is based on secondary data analysis and will otherwise not be presented in this thesis:

Habekost B, **Germann M**, Baker SN (2021) Plastic changes in primate motor cortex following paired peripheral nerve stimulation. J Neurophysiol 125:458-475.

Foysal KMR, **Germann M**, Baker SN Paired associative stimulation does not induce plasticity in cutaneomuscular reflexes. *To be submitted.*

Abstracts

Germann M, Habekost B, Baker SN. Long-term changes in the neural coding of primate finger movements induced by paired nerve stimulation. *UK Sensorimotor Conference, London, 2019*.

Germann M & Baker SN. Improving grasp in spinal cord injury via a wearable electronic device. *International Spinal Research Network Meeting, London, 2019.*

Germann M, Habekost B, Baker SN. Long-term changes in the neural coding of primate finger movements induced by paired nerve stimulation. *Society for Neuroscience, Chicago, 2019.*

Germann M & Baker SN. Improving grasp in spinal cord injury via a wearable electronic device. *North East Postgraduate Conference, Newcastle upon Tyne, 2019.*

Germann M & Baker SN. Improving upper arm mobility after spinal cord injury via a wearable device. *I-OSCIRS & International Spinal Research Trust Seminar, Online, 2021.*

CHAPTER I – GENERAL INTRODUCTION

Descending Motor Pathways

The seminal work of Lawrence and Kuypers has shaped our understanding of the anatomy and function of the descending pathways (Lawrence and Kuypers, 1968a, Lawrence and Kuypers, 1968b). In addition to the corticospinal tract (CST), which is believed to be the dominant pathway in primates, Kuypers' lesion studies demonstrated that subcortical pathways can also generate a wide range of movements. They grouped these brainstem pathways into ventromedial and dorsolateral brainstem pathways, depending on whether they terminate in the ventral or dorsal horn in the spinal cord (see Figure 1.1).

The dorsolateral brainstem pathways include the rubrospinal tract, arising from the red nucleus (Kennedy, 1990). It descends contralaterally through the dorsolateral column and terminates in the dorsolateral regions of the intermediate zone (IZ) of the spinal cord grey matter. However, there is little evidence supporting a rubrospinal tract in humans (Nathan and Smith, 1955, Onodera and Hicks, 2010). On the other hand, the ventromedial brainstem pathways include the reticulospinal, bulbospinal, tectospinal and vestibulospinal pathways, originating in the pontine and medullary reticular formation, the superior colliculus and the vestibular complex respectively (Matsuyama and Drew, 1997, Shinoda et al., 1992, Lemon, 2008). These pathways descend in the ventrolateral column of the spinal cord and terminate bilaterally in the ventromedial regions of the IZ. Although they arise from the brainstem, these pathways receive significant cortical projections (Berrevoets and Kuypers, 1975, Jinnai, 1984, Lemon, 2008).

The corticospinal tract originates mostly from the primary motor cortex, though it also gets contributions from other motor and somatosensory cortices (Murray and Coulter, 1981, Galea and Darian-Smith, 1994, Lemon, 2008). The CST mostly projects onto interneurons in the intermediate zone of the spinal cord. Notably, CST axons can form monosynaptic corticomotoneuronal connections in primates (Bernhard and Bohm, 1954) and it has been suggested these connections are responsible for the exceptional manual dexterity of primates (Kuypers, 1981a). The majority of axons decussate at the medulla and descend contralaterally through the dorsolateral funiculus (Kuypers, 1981a). Approximately ~1-10% of fibres descend ipsilaterally through the dorsolateral and ventromedial funiculus (Lacroix et al., 2004, Yoshino-

Saito et al., 2010). The CST can therefore be considered a predominantly unilateral pathway, as opposed to the bilateral ventromedial brainstem pathways.

Lawrence and Kuypers (1968b) have identified the main functions of the ventromedial pathways as being postural adjustment and gross limb movements. Subsequent studies in cats have supported the role of the reticulospinal tract (RST) in locomotion (Drew et al., 1986, Matsuyama and Drew, 2000), postural control (Prentice and Drew, 2001, Schepens and Drew, 2004) and reaching actions (Schepens and Drew, 2004, Schepens and Drew, 2006), but evidence in humans remained limited due to the invasive nature of the experiments required.

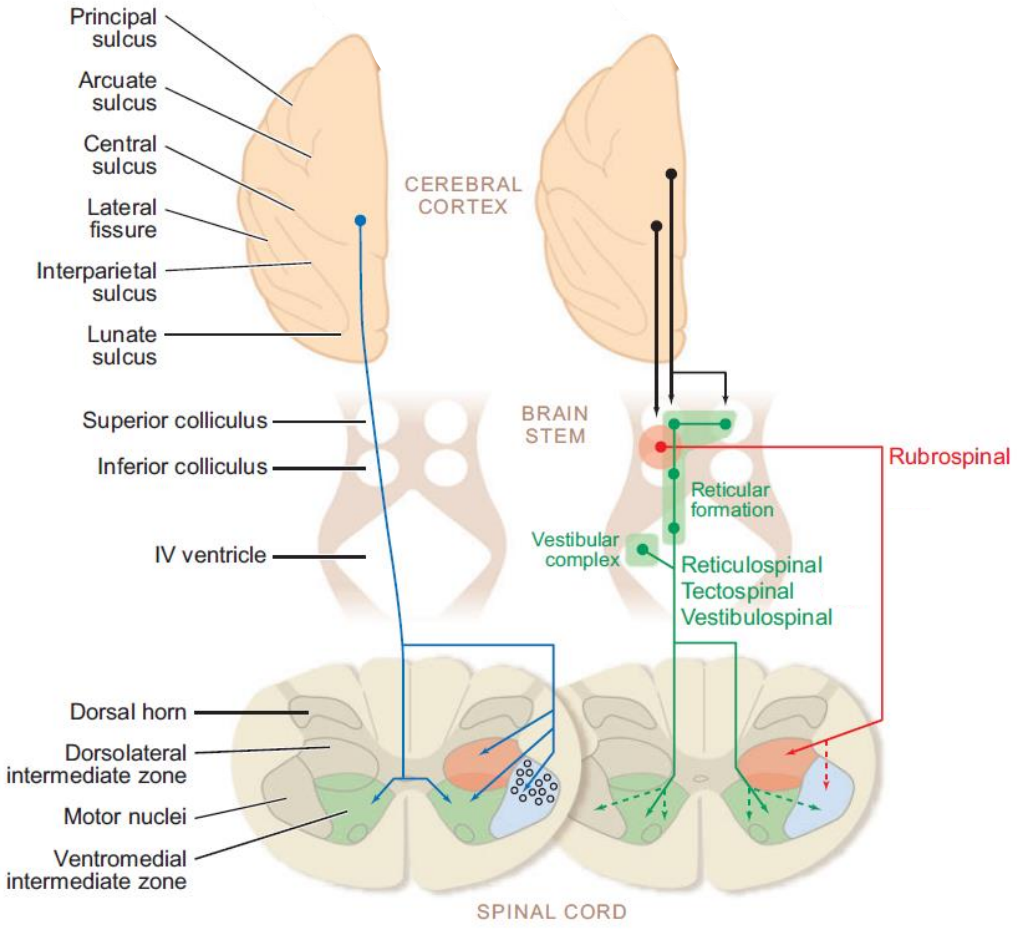

Figure 1.1: *Schematic representations of the descending motor tracts.*
Corticospinal projections are shown to the left (blue) and brainstem pathways are shown on the right-hand side. The ventromedial brainstem pathways (reticulsopinal, tectospinal, vestibulospinal) are depicted in green and the dorsolateral pathway (rubrospinal) in red. Figure adapted from Lemon (2008).

The loss of grasping function and independent finger control with dorsolateral and CST lesions implies that hand function is predominantly mediated by these other pathways. However, macaques with both bilateral pyramidal tract and dorsolateral lesions were still able to climb the bars of their cages, suggesting a degree of hand function persists and must therefore be mediated by the only remaining descending system, the ventromedial pathways (Lawrence and Kuypers, 1968b).

Evidence supporting the role of the RST in distal limb function has accumulated in recent years. Using intracellular recordings in anaesthetised macaques, Riddle et al. (2009) identified mono- and di- synaptic connections between the RST and antidromically identified motoneurons projecting to wrist and digit muscles (Riddle et al., 2009). Furthermore, many interneurons are under shared control of both CST and RST, implying a high degree of convergence of these two pathways (Riddle and Baker, 2010). Also, reticular formation cells modulate their discharge during fine finger movements at least as much as corticospinal neurons in M1 (Soteropoulos et al., 2012).

All of this suggests that in primates, distal and proximal muscles are innervated by both the CST and RST. However, it is unlikely these pathways represent redundancy in the motor system. Rather the CST and RST are both functionally relevant, each contributing uniquely to the motor system.

One clear difference between CST and RST is fractionation. CST axons diverge to a small number of motoneuron pools (Buys et al., 1986). On the other hand, RST axons branch extensively and may even make contacts at both the cervical and lumbar level of the spinal cord (Peterson et al., 1975, Matsuyama and Drew, 1997, Matsuyama et al., 1999).

A second quantitative difference between the RST and CST is the relative strength of their inputs to extensors and flexors. Corticospinal axons show little flexor/extensor bias with extensor inputs being marginally stronger (Cheney et al., 1991). Conversely, the RST facilitates extensors and suppresses flexors contralaterally, and vice versa on the ipsilateral side (Davidson and Buford, 2006, Davidson et al., 2007). These biases are clinically relevant with stroke patients often presenting with weak extensors and overactive flexors (Kamper et al., 2003).

As mentioned previously, one of the major differences between CST and RST is their laterality, with the CST being a primarily crossed pathway and the RST being bilateral at both the level of the pathway and single axons (Schepens and Drew, 2006, Davidson et al., 2007, Jankowska et al., 2003).

Lawrence and Kuypers (1968b) emphasised the importance of the rubrospinal tract in mediating the recovery of hand function in monkey. However, there is little evidence supporting a rubrospinal tract in humans (Nathan and Smith, 1955, Onodera and Hicks, 2010), leaving the reticulospinal tract of particular interest as a rehabilitative target in patients who have suffered CST lesions. Indeed, it has already been shown that RST connections to motoneurons can strengthen after CST lesions, partially restoring lost synaptic drive and forming some of the substrate for recovery (Zaaimi et al., 2012).

Non-invasive brain stimulation

In recent years, considerable knowledge has been accumulated about the physiology of motor function at a systems level in the intact human brain, thanks to the rise of safe non-invasive brain stimulation techniques. This was first achieved with transcranial electrical stimulation (TES), which is believed to directly excite descending corticospinal axons (Merton and Morton, 1980, Day et al., 1989). This stimulus evokes contralateral muscle twitches, known as motor evoked potentials (MEPs). Measurement of MEP size can therefore be used to provide a measure of corticospinal output. However, application of TES can be limited by the discomfort associated with its use since the high currents required to penetrate the skull result in unpleasant stimulation of the scalp muscles and sensory receptors in the skin.

Transcranial magnetic stimulation (TMS) developed by Barker et al. (1985) overcame this major drawback and is now a widely used brain stimulation technique that allows non-invasive examination of the motor system in humans. TMS uses an electromagnetic coil which generates a magnetic field that can painlessly penetrate the skull and evoke currents in the brain. The current will cause neurons to depolarize and if applied over the primary motor cortex will elicit MEPs in the contralateral muscles, which can be recorded with surface electromyography (EMG) electrodes and provide a measure of corticospinal excitability. At which point the stimulation will take place depends mostly on the gradient of the induced current. Straight axons are stimulated at the strongest point of the electric field gradient,

whereas curved axons are preferably stimulated at the bends, where currents have their maximum impact (Amassian et al., 1992). Therefore, for all neurons present within the cortex, activation with TMS depends upon the direction of the current relative to the geometry of the axons. Evoked responses thus depend not only on the intensity of the stimulus, but also on coil orientation, the wave form of the stimulation pulse and the shape of the coil (Di Lazzaro et al., 2008). With a figure of eight coil, TMS can be used focally since this configuration generates the largest current density directly below the centre of the coil (Ueno et al., 1988).

TMS stimulates cells within the motor cortex both directly and indirectly (trans-synaptically), leading to a series of high frequency volleys that descend through the spinal cord (Patton and Amassian, 1954, Rothwell et al., 1991). These volleys differ in latency, activation threshold and most likely arise at least in part from different neural circuits (Di Lazzaro et al., 2012, Di Lazzaro et al., 2018, Di Lazzaro and Ziemann, 2013, Di Lazzaro and Rothwell, 2014).

The earliest wave is thought to originate from the direct activation of the corticospinal neuron at or near the initial segment and is termed D-wave. The latency of D-waves correspond to MEPs elicited via transcranial electrical stimulation (Day et al., 1989, Di Lazzaro et al., 2018). The later response, termed I1-wave, is dependent upon the integrity of the grey matter, implying that it originates from indirect, trans-synaptic activation of corticospinal neurons by intracortical circuits (Patton and Amassian, 1954). At higher stimulus intensities, later volleys (I2 and I3) appear at intervals of approximately 1.5ms. The interval between I-waves from intracellular recordings from pyramidal tract (PT) neurons in primates and evoked with TMS in humans is comparable (Kernell and Chien-Ping, 1967, Amassian et al., 1987, Edgley et al., 1997, Maier et al., 1997, Di Lazzaro et al., 1998a, Di Lazzaro et al., 2001).

These early and late I-waves likely differ in their mechanism of action and their origin (Di Lazzaro et al., 2012). While cortical networks likely contribute to the generation of the first TMS-induced peak (Ziemann et al., 1998b, Ilic et al., 2002), there is increasing evidence for the involvement of subcortical sources for the later I-waves (Tokimura et al., 1996, Ziemann et al., 1998a).

Another non-invasive technique to probe the motor pathways is electrical stimulation at the level of the cervicomedullary junction (Ugawa et al., 1991, Berardelli et al., 1991, Gandevia et al., 1999). Two adhesive electrodes are fixed over the mastoid processes and a pulse of high-voltage current (usually 50-100 μs, up to 750 V) is passed between them. This will elicit a single

descending volley (Berardelli et al., 1991, Rothwell et al., 1994), which activates motoneurons directly and evokes a short-latency response in the muscles of the upper limb. The elicited responses are termed cervicomedullary motor evoked potentials (CMEPs) and can be used to test motoneuron excitability. Since TMS involves the stimulation of synapses at both the cortical and spinal level, the size of MEP depends on the excitability of both. On the other hand, CMEPs are unaffected by changes in cortical excitability and therefore offer the most appropriate comparison to allow interpretation of changes in recorded MEPs (Taylor, 2006). However, similar to TES, a major drawback of using CMEPs is that the stimulus is uncomfortable for the subject. Another problem of cervicomedullary junction stimulation is that the stimulus intensity required to evoke a CMEP in some subjects can additionally activate the ventral roots (Ugawa et al., 1991). Such direct motor root activation will lead to contamination of the CMEP, meaning the response no longer reflects motoneuron excitability accurately. The presence of motor root activation can be identified in an abrupt decrease of ~2 ms in the latency of the recorded response (Ugawa et al., 1991).

Non-invasive measures of reticulospinal function

Although TMS can activate reticular neurons (Fisher et al., 2012), it is unlikely to provide a reliable reticulospinal assessment on its own, since any responses observed are presumably dominated by the much larger corticospinal activation. Instead, reticulospinal function in humans has to be inferred in less direct ways, for example by using sensory stimuli known to target the reticular formation.

One technique available is galvanic vestibular stimulation (Fitzpatrick and Day, 2004), which uses electrical currents over the mastoid processes to induce EMG sway responses that are thought to be mediated by reticulospinal pathways (Rothwell, 2006). Then there is some evidence that supports a reticular role in the long latency stretch reflex (LLSR; Fellows et al., 1996, Kurtzer, 2014).

Further methods to quantify RST function are listed below. It is important to note that none can provide a pure measure of RST output, but convergent results using multiple measurements allows for a more convincing interpretation.

Startle Pathway - StartReact

One promising method of studying RST function is the startle reflex. Startle is the fast, involuntary response to an unexpected startling stimulus which causes a rapid, stereotyped contraction of face and limb muscles in a caudo-rostral pattern. A loud auditory stimulus (LAS) evokes a startle via activation of the caudal brainstem (Brown et al., 1991). Animal studies in particular implicate the nucleus reticularis pontis caudalis as the main origin of the acoustic startle response (Hammond, 1973, Leitner et al., 1980, Davis et al., 1982), and there is evidence that the same is true for humans (Brown, 2002).

The onset latency of the EMG responses in the startle depends upon the type of stimulus, the intensity of the stimulus and the expectancy of the subject (Brown et al., 1991, Wilkins et al., 1986, Chokroverty et al., 1992, Matsumoto et al., 1992). The startle response begins with an activity in the sternocleidomastoid muscle around 60 ms and can be measured in the biceps at around 75 ms (Rothwell, 2006).

Voluntary reaction time can be shortened dramatically by an acoustic startling cue, a phenomenon termed StartReact. Typically, voluntary reaction times are around 150ms, but under a StartReact paradigm these can be reduced to less than 70ms (Valls-Sole et al., 1999b, Valls-Sole et al., 1995). These responses are too fast to be considered cortical and evidence suggests that the loud acoustic stimulus somehow releases the planned movement, bypassing cortical circuitry and using the same pathways as the startle reaction itself.

There are several lines of evidence supporting the reticular formation as the subcortical structure involved in StartReact. Firstly, reticular formation dysfunction is thought to be the cause of gait freezing in Parkinson's disease, with these patients also experiencing reduced StartReact responses (Nonnekes et al., 2014a). Secondly, patients with loss of CST fibres due to hereditary spastic paraplegia type 31 present with enhanced StartReact effects, possibly due to compensatory action by the reticulospinal pathway (Fisher et al., 2013). Thirdly, the StartReact effect remains intact in patients with damaged CST (Honeycutt and Perreault, 2012, Choudhury et al., 2019, Nonnekes et al., 2014b).

Startle Pathway – conditioned TMS & CMEP responses

In addition to its effect on reaction time, a loud startling sound has also been shown to transiently modulate motor responses to TMS and TES (Furubayashi et al., 2000, Tazoe and

Perez, 2017). A loud auditory stimulus suppresses EMG responses to TMS when it precedes the magnetic stimulus by 30-60 ms (Figure 1.2), whereas it does not affect responses to electrical stimulation. Loud sounds facilitate the H-reflex at intervals larger than 50ms (Rossignol and Jones, 1976, Rudell and Eberle, 1985, Nakashima et al., 1994, Delwaide and Schepens, 1995), indicating an increase in motoneuronal excitability. This suggests that the suppression effect of the LAS at a 50 ms interval occurs at a cortical level.

In contrast, responses to electrical stimulation and H-reflexes are significantly facilitated by the loud sound at an interstimulus interval of 80 ms, whereas responses to TMS are not affected at this interval. This late facilitation is therefore considered to be a subcortical effect. The fact that the LAS has no effect on responses evoked by TMS at late intervals may be explained by the speculation that the persisting spinal facilitation at these intervals is cancelled out by simultaneous cortical inhibition (Furubayashi et al., 2000). Using the results from Furubayashi et al. (2000), it is possible to select the intervals that give the largest suppression or facilitation, to study the contributions of CST and RST drive respectively, though interpretation of the net responses need to take into account the multiple overlapping processes.

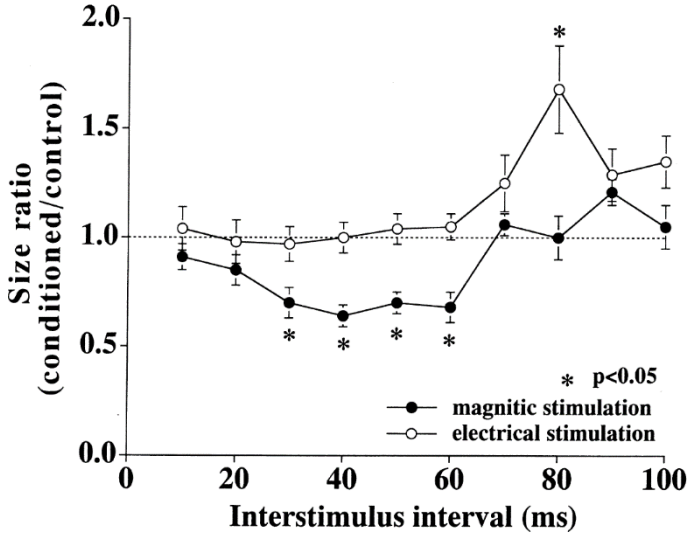

Figure 1.2: *Effect of a loud acoustic stimulus on evoked responses.*
Effect of a loud acoustic stimulus on responses to TMS (black) and TES (white) at different interstimulus intervals. Taken from Furubayashi et al. (2000).

TMS Coil Orientations

As described above, TMS evokes multiple descending volleys (Patton and Amassian, 1954, Rothwell et al., 1991). These volleys differ in latency, activation threshold and most likely arise at least in part from different neural circuits (Di Lazzaro et al., 2012, Di Lazzaro et al., 2018, Di Lazzaro and Ziemann, 2013, Di Lazzaro and Rothwell, 2014).

Several studies suggest that different neural elements in the cortex can be activated preferentially by changing the direction of induced currents (Werhahn et al., 1994, Sakai et al., 1997, Ni et al., 2011). The earliest wave (D-wave) reflects the direct activation of the corticospinal neuron near the initial segment and is preferentially recruited through LM currents (Di Lazzaro et al., 2008). A PA current will preferentially recruit early I-waves (I1, I2). An AP orientation produces preferentially longer latency late indirect waves (I3) (Sakai et al., 1997, Di Lazzaro et al., 2001, Jung et al., 2012).

While cortical networks likely contribute to the generation of the first TMS-induced peak (Ziemann et al., 1998b, Ilic et al., 2002), there is increasing evidence for the involvement of subcortical sources for the later I-waves (Tokimura et al., 1996, Ziemann et al., 1998a). Thus by measuring responses to PA and AP currents, some inference can be made about the neural structures involved.

Plasticity

Natural, altered or artificial physiological conditions can modify synaptic connections within the motor system. Such plastic changes underlie skilled motor learning and recovery after injuries, as well as a variety of neuromodulation paradigms in laboratory settings.

Paired associative stimulation (PAS) refers to a known protocol to experimentally induce neural plasticity based on the basic principles of Hebb's model of neural plasticity (Hebb, 1949, Bi and Poo, 2001). First described by Stefan et al. (2000), the original PAS approach combined peripheral electrical stimulation of the median nerve paired with single pulse TMS over the hand area of M1. This led to a long-lasting but reversible increase in corticomotor excitability, if the two inputs were paired repeatedly at a distinct interstimulus interval that is adjusted such that the afferent volley arising from the peripheral nerve reaches the motor cortex near synchronously with the magnetic stimulation. These changes in excitability are thought to

occur mainly on a cortical level, as there is no change in motoneuron excitability as assessed by F- waves (Stefan et al., 2000).

Since then, several PAS studies have been reported in literature which showed that plasticity can be induced by repetitive TMS (Huang et al., 2005), or by pairing TMS with a peripheral stimulus (Stefan et al., 2000, Taylor and Martin, 2009, Urbin et al., 2017), with natural activity generated during voluntary movements (Buetefisch et al., 2015, Edwardson et al., 2014, Thabit et al., 2010), or with motor imagery (Foysal and Baker, 2020, Kraus et al., 2016).

These studies have shown that the direction of change induced by paired stimulation depends on the order of activation of the pre- and postsynaptic neuron. Synchronous or associative stimulation generates long-term potentiation (LTP) processes, if the two independent afferent inputs reach the same target in synchrony (Buonomano and Merzenich, 1998). On the other hand, asynchronous or non-associative stimulation is followed by long-term depression (LTD). The temporal order of pre- and postsynaptic spiking is in the order of tens of milliseconds (Markram et al., 1997, Bi and Poo, 1998, Sjostrom et al., 2001) and is now referred to as spike timing-dependent plasticity (STDP; Bi and Poo, 2001).

A major disadvantage of these protocols is the reliance of bulky and expensive TMS machines, which limits their application to short laboratory visits. However, larger plastic changes might be generated by more stimuli (Fitzpatrick et al., 2016), which could be why such methods have not entered routine clinical practice (Rothwell, 2016).

Alternative protocols do not rely on TMS stimulation and include the stimulation of the motor point of two muscles (McDonnell and Ridding, 2006, Pyndt and Ridding, 2004, Ridding and Uy, 2003, Schabrun and Ridding, 2007), or of two peripheral nerves (Charlton et al., 2003, McKay et al., 2002, Ridding et al., 2000, Ridding et al., 2001), all of which have demonstrated plastic changes in motor output.

For this project, a portable device capable of delivering stimuli to the motor point of a muscle paired with an auditory click was used to induce plastic changes in motor output (Foysal et al., 2016, Germann and Baker, 2021). Given that reticulospinal neurons receive extensive afferent input (Leiras et al., 2010), auditory stimuli have been shown to excite reticular neurons (Irvine and Jackson, 1983, Fisher et al., 2012) and the interstimulus interval of the two inputs can induce bidirectional changes in LLSR (Foysal et al., 2016), it is most likely that STDP mechanisms are responsible for the plastic changes in motor output. The device has the

advantage to be worn during the day, outside of the laboratory, over several weeks, to deliver a large number of stimuli during everyday activities.

Electronic Wearable Device

The wearable electronic device (Figure 1.3) was designed to deliver electrical and auditory stimuli outside the lab, allowing continuous stimulation over many days. It is housed in a custom plastic case that can be attached to an optional belt clip and has an overall size comparable to a common smartphone. The device includes an electrical stimulator, an audio amplifier, a real time clock and is powered by an internal battery which can be recharged via a standard microUSB port that lasts for at least ~12 hours per charge. An inbuilt flash memory logs the times when the device is turned on, as well as the number of stimuli given during that time, allowing post-hoc checking of compliance. The wearable device generates constant-current electrical stimulation to the target muscle through surface electrodes (220 V compliance, 0.15 ms pulse width, with the more proximal electrode negative). A knob on the device allows adjustment of the stimulus intensity, which is set to be just below the motor threshold (defined as a visible muscle twitch). Auditory stimuli are generated by delivering a 0.1ms wide, 12-V square excitation pulse into a miniature earpiece; this produces a brief click with an intensity of 110-dB SPL.

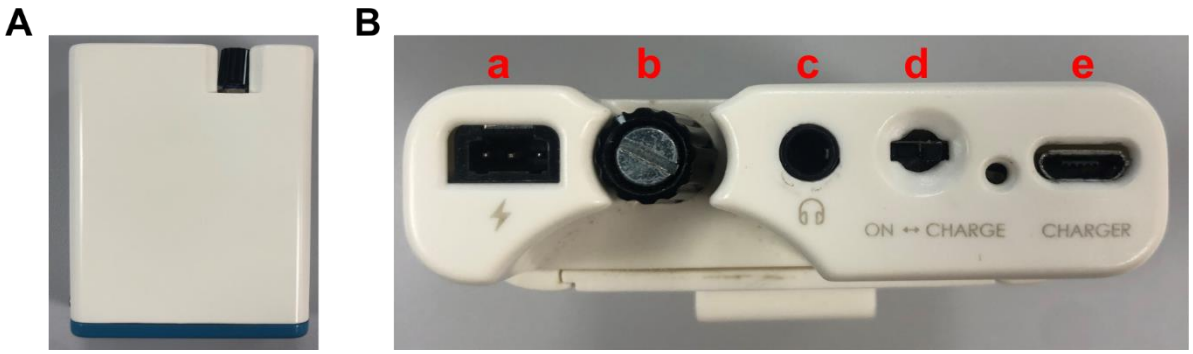

Figure 1.3: *Wearable electronic device.*
(A) Photograph of the wearable electronic device. **(B)** Controls and connections on the device. a, stimulus output port; b, stimulus intensity adjustment; c, audio output; d, on/charge switch; e, microUSB charge connection.

Based on calculations provided by (Rosengren et al., 2010) and (Foysal et al., 2016), this intensity corresponds to an A-weighted intensity of 68 dB L_{Aeq} when deliverd at 0.66 Hz, and 71 DB L_{Aeq} when delivered at 1.32 Hz; assuming device usage for at least 8 hours. This is well below the recommended safe limit for noise exposure of 85 dB L_{Aeq} given by the UK's Control of Noise at Work Regulations (The Stationery Office, 2005). The device can therefore potentially be used every day at these levels for at least 8 hours a day without concern. For all but one experiment, the earpiece was placed in the ear contralateral to the muscle stimulation.

The device works by precisely timing the electrical and auditory stimulation, in order to generate spike timing-dependent plasticity. Reticulospinal neurons receive extensive afferent (Leiras et al., 2010) and auditory input (Hammond, 1973, Leitner et al., 1980, Davis et al., 1982, Irvine and Jackson, 1983). Using invasive recordings in monkey, it was discovered that loud auditory clicks can powerfully activate RST cells (Fisher et al., 2012). This opened the exciting possibility that reticulospinal systems could be non-invasively activated by clicks.

The wearable device has previously been used to deliver clicks paired with electrical stimulation of the biceps muscle in healthy humans (Foysal et al., 2016). Depending on the inter-stimulus interval used, the long-latency stretch reflex in the biceps could be enhanced or suppressed, which may partly depend on RST output. Using the device for stroke survivors produced a small but significant improvement in upper limb function (Choudhury et al., 2020).

Spinal Cord Injury

Spinal cord injury (SCI) can be caused by contusion, compression, penetration or maceration of the spinal cord, resulting in profound changes in the central nervous system. Demyelination of long motor axons in the white matter (Griffiths and Mcculloch, 1983, Bunge et al., 1993, Totoiu and Keirstead, 2005) impairs impulse conduction after SCI and results in a complex range of disabilities associated with loss of muscle function, loss of sensation, and loss of autonomic function below the level of the injury. Each lesion is highly individualized with regard to location, severity and to which extent descending tracts are either spared or able to recover (Kakulas, 2004).

SCI is typically classified as complete or incomplete, with only the latter having prospects of motor recovery. The majority of spinal cord injuries are due to preventable causes such as

falls, road traffic accidents or sports injury. More than 2.5 million people worldwide live with paralysis caused by spinal cord injury and slightly more than half of all injuries result in tetraplegia (Thuret et al., 2006). In surveys of patients with SCI, restoration of upper limb function is selected as the most important target for therapy (Anderson, 2004).

A literature review of articles related to the interests and concerns of individuals with SCI similarly found that mobility remains the area of greatest interest (Estores, 2003). Physical functioning, societal participation and independence are the biggest predictors for quality of life in individuals with SCI (Tate et al., 2002). This appears to be true for spinal cord injuries resulting in either paraplegia or tetraplegia. However, while individuals living with paraplegia rank sexual function, bladder & bowel management and chronic pain as their top physical concerns (Anderson, 2004), people living with quadriplegia overwhelmingly rank arm and hand function as their highest priority (Anderson, 2004). Many community reports asking individuals with SCI about their concerns, pool their results regardless of injury level, resulting in shared concerns such as bladder & bowel management overshadowing the specialised need of upper limb function only pertaining to tetraplegics. Compared to paraplegics, tetraplegic individuals are usually in need of more expensive and bulky electric wheelchairs, rely more heavily on carers for everyday tasks such as using the restroom and have significantly less prospects in the workplace. Even a small improvement in upper limb function could have a huge impact on their quality of life.

Despite the lack of treatment options currently available for SCI, patients suffering incomplete injury are often able to achieve extensive functional recovery. In the absence of significant axonal regeneration (Blesch and Tuszynski, 2009), these improvements are associated with spontaneous plasticity of pre-existing circuits (Curt et al., 2008). Spinal cord injury may result in selective lesioning of the CST with the possibility of relative sparing of the RST. Although the RST does not constitute a parallel pathway to the CST, it is likely that the motor deficits experienced following spinal cord injury could to some extent be improved by upregulating reticulospinal function (Baker, 2011, Baker et al., 2015). Reticulospinal adaptation following corticospinal injury has been demonstrated in primate lesion studies (Zaaimi et al., 2012, Darling et al., 2018) and individuals with spinal cord injury show signs of increased reticulospinal function (Baker and Perez, 2017). Although it appears that plastic changes occur in the RST following corticospinal injury, the full potential of this pathway to compensate for

the loss of descending drive associated with conditions such as stroke and spinal cord injury remains to be elucidated.

Thesis Objectives

The overall aim of this thesis was to explore the mechanisms behind custom non-invasive stimulation protocols at the cortical and subcortical level and their potential beneficial effect for spinal cord injury survivors.

In line with this, we also aimed to gain a better understanding of the extent to which corticospinal transmissions are altered after SCI and the effects of loud acoustic stimuli on motor output, especially on the RST.

Objective 1: Optimise non-invasive measures of sub-cortical outflow, to detect plastic changes following wearable device stimulation

In order to be able to quantity the effects of plasticity protocols following wearable device stimulation, non-invasive methods to assess plastic changes are needed. While measuring long-latency stretch reflexes or MEPs can tell us that overall motor output has or has not changed, the site of plasticity remains unclear. We therefore need non-invasive assessments that can differentiate between CST and sub-cortical contributions, to investigate how the different pathways might contribute to the plastic changes in humans.

The first objective of this project thus focused on implementing reliable and consistent non-invasive assessments of sub-cortical inputs to motor control in humans. The rationale behind each assessment is based on existing literature (see general introduction). These include:

- Effect of a loud acoustic stimuli on MEPs and CMEPs
- Effects of different coil orientations to induce anterior-posterior and posterior-anterior currents in the brain during TMS
- StartReact paradigm (effect of sound on reaction time)
- Analysing separate I-wave components using short interval intracortical facilitation

Each assessment had to be replicable across different muscle groups and different motor tasks, tested in healthy human subjects.

Objective 2: Improve and customise wearable device protocols

As a second objective, this project aimed to develop an effective protocol using the wearable electronic device to enhance and shape RST output in healthy human subjects. The best combination of the following parameters to induce plastic changes in upper limb muscles were explored:

- Location of the electrical stimulus
- Inter-stimulus interval
- Stimulation frequency

Objective 3: Translate paradigms to SCI subjects, obtaining functional and electrophysiological evidence for beneficial plasticity

Once the optimal stimulus parameters were determined, the protocol was translated into SCI subjects. In addition to electrophysiological assessments, measures of upper limb function were used to determine evidence of beneficial plasticity.

The study was designed as a randomised, prospective and parallel group trial. The study was conducted in the Neurokinex Hemel centre, a non-profit community gym for motor rehabilitation. Subjects were assessed at week 0, 4 and 8. For 4 weeks subjects were instructed to use the wearable device at home for at least 4h a day.

Specific objectives for this trial were:

1. To assess the compliance (how long subjects use the device each day) using the device clock data.
2. To assess the adverse event profile among participants using our intervention device.
3. To compare the range, speed and accuracy of upper limb movement using a planar reaching task with Polhemus motion tracking system, before and after intervention in both groups.
4. To compare the maximum voluntary contraction force of elbow flexion and extension before and after intervention in both groups.
5. To compare the auditory startle response (StartReact paradigm) of triceps before and after intervention in both groups. This assay will examine the change of reticulospinal tract activity by the intervention (if any).

6. To compare auditory startle response (startle + TMS paradigm) of triceps before and after intervention in both groups. This assay will examine the change of reticulospinal tract activity by the intervention (if any).
7. To compare motor evoked potentials by transcranial magnetic stimulation (TMS with 2 different coil orientations) before and after intervention in both groups. This assay will examine the change of corticospinal tract activity by the intervention (if any).
8. To compare the scores in the Capabilities of Upper Extremity Questionnaire before and after intervention in both groups.

CHAPTER II – EFFECTS OF COIL ORIENTATION ON MOTOR-EVOKED POTENTIALS IN PROXIMAL AND DISTAL UPPER LIMB MUSCLES IN HUMANS WITH CHRONIC SPINAL CORD INJURY

The data described in this chapter was collected by Dr Hang Jin Jo, a postdoctoral associate at the Shirley Ryan AbilityLab in Chicago, and I. I collected the data for 13 SCI participants and 25 control subjects and Dr Jo collected the data for 4 SCI participants and 9 control subjects. I performed all data analysis.

Abstract

Most rehabilitation-based approaches that are aimed at promoting recovery after SCI probably depend largely on the recruitment of descending motor pathways. However, the extent to which corticospinal transmission is altered after SCI remains poorly understood, with proximal muscles often recovering better compared to more distal muscles. In this study, we used transcranial magnetic stimulation (TMS) to investigate these changes in the biceps brachii muscle, and compared them to results found in distal hand muscles provided by Jo et al. (2018). In participants with chronic cervical spinal cord injury, we used TMS to elicit motor-evoked potentials using posterior-anterior (PA) and anterior-posterior (AP) induced currents in the brain and compared them to MEPs evoked by direct activation of corticospinal axons using lateral-medial (LM) currents. In contrast to results from distal hand muscles, we found that MEP latencies in biceps were not significantly delayed in SCI compared to healthy control subjects in either coil orientations. However, latencies of MEP responses elicited by PA and AP stimulation relative to responses elicited by LM stimulation were shorter in SCI compared to control subjects, in line with MEP latency differences observed in distal hand muscles. Overall we did not find any significant differences when comparing MEP latency changes after SCI between the two muscles.

Introduction

After spinal cord injury (SCI), extensive anatomical and electrophysiological changes occur in the corticospinal tract (CST). SCI leads to motor and sensory impairments resulting in disabilities that can seriously diminish the quality of life (Middleton et al., 2007). The large plastic capacity of the CST for reorganization may contribute to functional recovery after SCI and most rehabilitation-based approaches that are aimed at promoting recovery after SCI probably depend largely on the recruitment of descending motor pathways including the CST.

One way to study changes in corticospinal transmission non-invasively after SCI is to use transcranial magnetic stimulation (TMS). TMS stimulates cells within the motor cortex both directly and indirectly (trans-synaptically), leading to multiple descending volleys to the spinal cord (Patton and Amassian, 1954, Rothwell et al., 1991). The earliest wave (D-wave) is thought to be due to direct activation of the corticospinal neuron, while later waves (I1, I2 and I3 waves) have a longer latency and are generated by indirect, transsynaptic activation of the corticospinal neuron (Terao and Ugawa, 2002, Di Lazzaro et al., 2012). A single pulse of TMS will elicit a motor evoked potential (MEP) that can be recorded from surface electromyographic (EMG) electrodes.

Several studies suggest that different neural elements in the cortex can be activated preferentially by changing the direction of induced currents (Werhahn et al., 1994, Sakai et al., 1997, Ni et al., 2011). By holding a figure-of-eight TMS coil in different orientations, activation can be biased toward different I waves (Sakai et al., 1997, Ziemann and Rothwell, 2000). The early I1-wave is preferentially recruited with a posterior-anterior (PA) current and elicits MEPs with the highest amplitude and lowest activation threshold (Mills et al., 1992, Brasilneto et al., 1992, Davey et al., 1994, Sakai et al., 1997, Chen et al., 2003). A coil orientation that induces an anterior-posterior (AP) current produces MEPs that have a longer latency (late I3-wave) and a higher motor threshold (Sakai et al., 1997, Di Lazzaro et al., 2001, Jung et al., 2012). Sufficiently high TMS intensities can also generate D-waves, which have a latency that corresponds to MEPs elicited via electrical stimulation, and are preferentially recruited through lateral-medial (LM) currents (Di Lazzaro et al., 2008).

Corticospinal responses elicited by TMS over the primary motor cortex have different characteristics in humans with SCI compared to uninjured controls. Previous studies found that MEPs have delayed latencies, decreased amplitude and higher thresholds in individuals

with SCI compared to controls (Ellaway et al., 2007, Perez, 2012). Importantly, while these differences are found in responses to both PA and AP stimulation, AP responses and late I-waves appear more affected after injury (Jo et al., 2018, Cirillo et al., 2016). Jo et al. (2018) found that in humans with tetraplegia, MEPs elicited in intrinsic finger muscles by PA and AP stimulation relative to those elicited by LM stimulation had a shorter latency compared with control subjects. Notably, the largest difference was present in MEPs elicited by AP currents, suggesting that changes in corticospinal transmission after SCI are more pronounced in neural structures activated by AP currents.

The study by Jo et al. (2018) looked at the first dorsal interosseous muscle; distal muscles are known to make a more limited recovery compared to proximal muscles after injury (Pestronk and Drachman, 1988, Colebatch and Gandevia, 1989). This fits with the assumption that monosynaptic CST projections are most pronounced for distal finger muscles (Porter and Lemon, 1993, Lawrence and Kuypers, 1968a), while proximal muscles receive more extensive projections from subcortical pathways (Kuypers, 1981b, Holstege and Kuypers, 1982, Holstege and Kuypers, 1987, Jones and Yang, 1985, Martin et al., 1985) and thus may have a bigger substrate for recovery after CST injury. However, an increasing number of anatomical and physiological studies in animals show that subcortical pathways, like the reticulospinal tract (RST), directly innervate muscles which control the digits (Riddle et al., 2009, Riddle and Baker, 2010, Soteropoulos et al., 2012). In fact, excitatory RST connections are as common and as strong in hand motoneuron groups as in forearm or upper arm motoneurons (Riddle et al., 2009). Also, Jo et al. (2018) report the biggest changes in 1DI responses to AP stimulation, which may reflect more indirect cortico-muscular transmission than responses to PA currents (Cirillo and Perez, 2015, Federico and Perez, 2017).

Overall, the extent to which corticospinal transmission is affected after SCI remains poorly understood. The research by Jo et al. (2018) highlights the changes seen in distal finger muscles; in this study we aimed to explore how these changes might affect a proximal upper arm muscle. We hypothesise that the biceps muscle demonstrates better recovery of motor function and comparatively less affected corticospinal transmission relative to the 1DI muscle, but that the recruitment of different neural elements is altered to a similar extent.

Methods

Subjects

Seventeen subjects with SCI (mean ± SD age = 43.0 ± 17.5 years, 4 females) and 34 age-matched, right-handed control subjects (mean ± SD age = 42.8 ± 15.7 years, 19 females) participated in the present study. All 17 SCI subjects and 15 control subjects were tested in the Shirley Ryan AbilityLab in Chicago and 19 control subjects were tested at Newcastle University. All subjects provided their written informed consent prior to participation, which was approved by the local ethics committee at the University of Newcastle and the local ethics committee at Northwestern University, in accordance with the guidelines established in the Declaration of Helsinki. The study was not registered in a database. Individuals with SCI had a chronic (≥1 year) cervical injury (C3–C7), see Table 2.1.

SCI subjects	Age (y)	Sex	Injury level	Time since injury (y)	ASIA
1	21	m	C4	2	A
2	47	m	C4-C7	12	D
3	46	f	C6	13	B
4	49	m	C5-C7	1	D
5	23	m	C6	1	C
6	56	m	C5-C6	36	A
7	26	f	C5-C7	4	D
8	40	m	C3-4	1	D
9	65	m	C5-C6	30	C
10	20	f	C5-6	1	C
11	68	m	C5	6	C
12	59	f	C4-5	36	D
13	45	m	C5-6	7	D
14	21	m	C6	1	D
15	71	m	C3	12	D
16	54	m	C4	3	D
17	20	m	C4	4	D

Table 2.1: *List of spinal cord injury participants*. M, male; F, female; C, cervical. ASIA, American Spinal Injury Association Impairment Scale.

Experimental procedures

Subjects were seated with the right arm flexed at the elbow by 90° (Figure 2.1A). At the beginning of experiments, subjects performed two brief MVCs for 3–5 s into biceps contraction separated by 30 s. MVC was measured by calculating the highest mean rectified electromyographic (EMG) activity found in the biceps muscle during the MVC burst. EMG activity from the biceps muscle was displayed continuously on a computer screen to ensure that physiological measurements were acquired at 5% of MVC across conditions.

EMG recordings

EMG was recorded from the right biceps muscle through surface electrodes (Cleartrace ECG electrodes, Conmed Corporation, New York, USA or Kendall H59P electrodes, Covidien, Mansfield, Massachusetts USA) secured on the skin over the muscle belly. EMG signals were amplified, filtered (band-width 30-2000 Hz), converted to digital data with a sampling rate of 5kHz (CED Micro 1401 with Spike2 software, Cambridge Electronic Design, Cambridge, UK) and stored on a computer for off-line analysis.

M-Max

The size of the maximal M-wave (M-max) was measured by stimulating the musculocutaneous nerve using a DS7A stimulator (1 ms duration; Digitimer Ltd, Welwyn Garden City, UK). The stimulation electrode was placed over the Erb's point that is located on the supraclavicular fossa and sternocleidomastoid muscle (Simmons, 2013). The stimulation current to obtain maximal M-wave was set such that two stimulations were given at maximal stimulator output (90 - 100 mA). The maximal amplitude of M-wave was determined as the mean peak-to-peak amplitude of the two maximal stimuli.

TMS

Transcranial magnetic stimuli were applied using a figure-of-eight coil through a Magstim 200 magnetic stimulator (Magstim, Whitland, UK) or a DuoMAG MP (Deymed Diagnostic, Hronov, Czech Republic) with a monophasic current waveform.

The three coil orientations tested were (Fig. 2.1B): (i) a figure-of-eight coil held tangentially on the scalp at an angle of 45° to the midline with the handle pointing laterally and posteriorly [posterior-anterior (PA) induced current]; (ii) a figure-of-eight coil handle in reverse position around the intersection of coil windings by placing the coil 180° to the position used for PA

currents [anterior-posterior (AP) induced current); and (iii) a figure-of-eight coil with the handle held leftwards 90° from the mid-sagittal line [lateral-medial (LM) induced current].

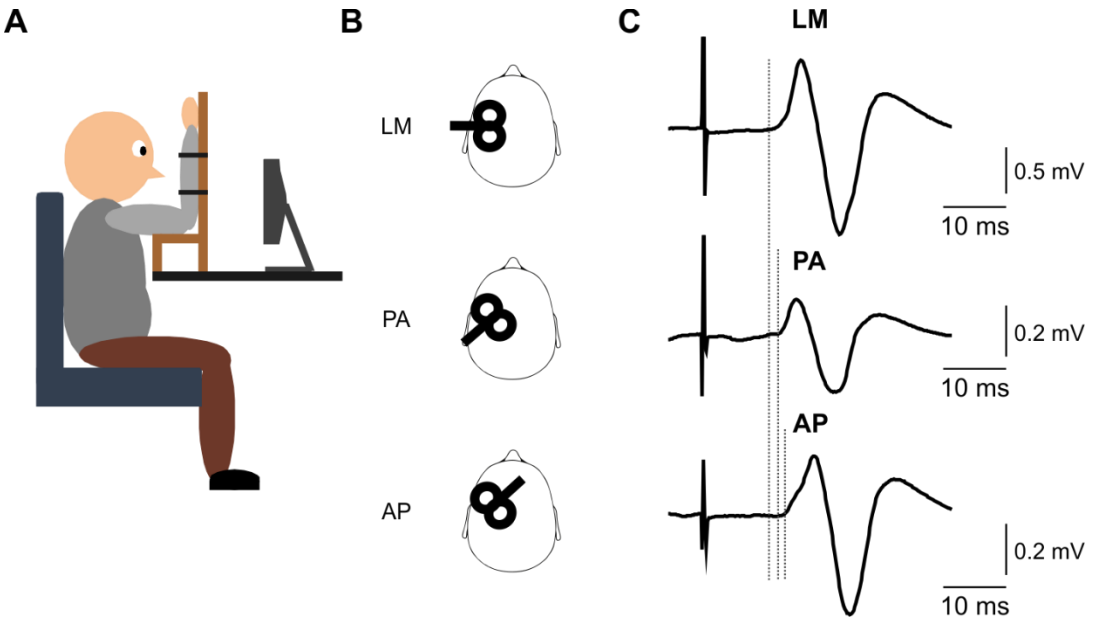

Figure 2.1: *Setup and TMS.* **(A)** Schematic of setup and arm posture during testing. Participants were asked to make a biceps contraction by pulling against the straps (black). Participants maintained a small contraction at 5% MVC throughout the experiment. **(B)** Schematic of the three different coil orientations used to elicit MEPs. **(C)** Traces show the average of 20 MEPs in the biceps tested with the TMS coil in the LM, PA and AP orientation in a control subject. Dotted lines mark the onset latencies. Note that latencies of MEPs elicited by AP and PA currents were longer compared to LM and AP was longer compared to PA latencies.

Measurements were performed during 5% MVC in all subjects. We determined the optimal position for eliciting a motor evoked potential (MEP) in the biceps muscle (hotspot) by moving the coil, with the handle pointing backwards and 45° away from the midline, in small steps along the arm representation of M1. The hotspot was defined as the region where the largest MEP in the biceps muscle could be evoked with the minimum intensity (Rothwell et al., 1999). The hotspot was determined with PA currents because the direction of the current does not significantly influence the position on the hotspot (Sakai et al., 1997, Arai et al., 2005).

A Polaris Vicra camera (Northern Digital Inc., Waterloo, Ontario, Canada) tracked both coil and head position, allowing the site of stimulation to be marked using the Brainsight neuronavigation system (Rogue Research Inc., Montréal, Quebec, Canada). This ensured a stable coil location throughout the experiment.

The coil was held manually by the experimenter. The different coil orientations were tested in a randomized order. TMS measurements included active (AMT) motor threshold and MEP onset latency as tested for each coil orientation.

MEPs

Active motor threshold (AMT) was defined as the stimulator intensity sufficient to elicit a MEP with amplitude >200 μV in at least 5 out of 10 consecutive stimuli, in the biceps contralateral to the stimulus with an active contraction of 5% maximal voluntary contraction (MVC). MEPs were tested during 5% of MVC using TMS intensities of 150% of the AMT for LM and 110% of the AMT for the PA and AP coil orientations (Hamada et al., 2013). A higher stimulus intensity was used for LM to ensure that corticospinal neurons were directly stimulated (D-wave) at this coil orientation. MEP onset latency was measured for individual trials in each subject and condition. The MEP latency was defined as the time point where rectified EMG signals exceeded 5 SD of the mean background EMG, measured 0-100 ms before the stimulus artefact. The latency of MEPs elicited by PA and AP directed currents was compared with the LM current to calculate the difference in latencies between PA-LM and AP-LM as a measure of activation of PA and AP-sensitive inputs, respectively. AP and PA MEP latencies were also compared. Single TMS pulses were delivered at 0.2Hz and 20 MEPs were recorded in each coil orientation. In a subset of participants (n = 7), 20 MEPs per coil orientation were additionally recorded from the first dorsal interosseous (1DI) muscle.

Statistical analysis

Data were analyzed using custom scripts written in the MATLAB environment (R2017a, MathWorks). Statistical tests were performed using MATLAB and IBM SPSS Statistics for Windows, version 24 (IBM Corp., Armonk, N.Y., USA).

Two-way ANOVAs were performed to determine the effect of GROUP (controls and SCI) and COIL ORIENTATION (LM, PA, AP) on AMT and MEP latency.

A two-way ANOVA was conducted to determine the effect of GROUP (controls and SCI) and MUSCLE (biceps and 1DI) on MEP latency differences.

Independent t-test were used to compare groups post hoc. Paired t-tests were used to compare within each group. Where necessary, the procedure introduced by Benjamini and Hochberg (1995) to correct for multiple comparisons was used. In the text, uncorrected P values are given, but statements of whether a test was significant or not describe the result after correction.

The significance level was set at $p < 0.05$. Descriptive statistics are presented as mean ± standard error.

Results

MVC, M-Max & AMT

Figure 2.2 shows the mean MVC and M-Max for the SCI and the control group.

There was no difference between the size of the maximal voluntary contractions across the two groups (Fig. 2.2A; controls = 0.5 ± 0.3 mV, SCI = 0.6 ± 0.4 mV; $t(47) = 0.793$, $p = 0.432$). Chronic spinal cord injury survivors also showed no significantly different size in maximal M-wave in the biceps (Fig. 2.2B; controls = 10.9 ± 5.9 mV, SCI = 12.6 ± 8.8 mV; $t(47) = 1.200$, $p = 0.236$).

Mean active motor thresholds for the different coil orientations are shown in Figure 2.2C. A two-way ANOVA showed no effect of GROUP ($F(1,49) = 0.572$, $p = 0.453$), but a significant effect of COIL ORIENTATION ($F(2,98) = 147.508$, $p < 0.001$) and their interaction ($F(2,98) = 12.441$, $p < 0.001$) on the active motor threshold. *Post hoc* tests revealed that AMT was lower for PA than for LM (controls = 43.6 ± 8.4 % and 49.1 ± 8.4 %, $t(33) = 9.525$, $p < 0.001$; SCI = 42.5 ± 6.2 % and 47.8 ± 6.6 %, $t(16) = 7.120$, $p < 0.001$) and AP (controls = 56.9 ± 11.6 %, $t(33) = -9.503$, $p < 0.001$; SCI = 64.9 ± 11.5 %, $t(16) = -9.950$, $p < 0.001$) and lower for LM than for AP (controls $t(33) = -5.767$, $p < 0.001$; SCI $t(16) = -7.570$, $p < 0.001$).

AMT was not significantly different for the SCI group compared to the controls (LM $t(49) = -0.577$, $p = 0.566$; PA $t(49) = -0.474$, $p = 0.637$; AP $t(49) = 2.329$, $p = 0.024$, not significant after correcting for multiple comparisons).

In order to make sure our results were not heavily influenced by the level of lesion in our SCI participants, we also compared the 7 subjects that had a C4 lesion or higher with 10 subjects

that had a C5 lesion or lower. There was no difference between these two groups for either MVC (C4 or higher = 0.6 ± 0.5 mV, C5 or lower = 0.6 ± 0.4 mV, t(15) = 0.068, p = 0.947), maximal M-wave (C4 or higher = 14.2 ± 1.0 mV, C5 or lower = 11.4 ± 8.3 mV, t(15) = 0.620, p = 0.545), or any of the active motor thresholds (PA: C4 or higher = 39.3 ± 5.5 %, C5 or lower = 44.8 ± 5.8 %, t(15) = -1.964, p = 0.068; AP: C4 or higher = 61.6 ± 8.6 %, C5 or lower = 67.1 ± 13.1 %, t(15) = -0.921, p = 0.371; LM: C4 or higher = 43.4 ± 4.9 %, C5 or lower = 50.8 ± 6.1 %, t(15) = -2.663, p = 0.018, not significant after correcting for multiple comparisons).

MEP latencies

Representative traces for MEPs elicited in the biceps muscle with the different coil orientations from one subject are shown in Figure 2.1C. Figure 2.3A shows the mean measured MEP latencies for the two groups in the biceps muscle. Data for the 1DI muscle (Fig. 2.3B) is taken from Jo et al. (2018), and was provided by the authors for comparison.

For the biceps muscle (Fig. 2.3A), a two-way ANOVA was conducted that examined the effect of GROUP and COIL ORIENTATION on MEP latency. There was no effect of GROUP ($F(1,49) = 0.525$, $p = 0.472$), but a significant effect of COIL ORIENTATION ($F(2,98) = 82.517$, $p < 0.001$) and their interaction ($F(2,98) = 4.591$, $p = 0.012$). *Post hoc* tests showed that in both groups, LM MEP latencies were shorter compared to the PA (controls $t(33) = -6.984$, $p < 0.001$; SCI $t(16) = -4.666$, $p < 0.001$) and AP (controls $t(33) = -10.822$, $p < 0.001$; SCI $t(16) = -7.842$, $p < 0.001$) and AP MEP latencies were longer than PA (controls $t(33) = -6.940$, $p < 0.001$; SCI $t(16) = -3.432$, $p = 0.003$).

MEP latencies for the biceps muscle were not significantly longer in any orientation for SCI compared to the control subjects (LM: controls = 11.8 ±1.2 ms, SCI = 12.3 ± 1.6 ms, $t(49) = 1.067$, $p = 0.291$; PA: controls = 13.6 ± 1.7 ms, SCI = 13.2 ± 1.4 ms, $t(49) = -0.914$, $p = 0.365$; AP: controls = 15.3 ± 1.8 ms, $t(49) = -1.611$, $p = 0.114$).

Notably, in the 1DI muscle (Fig. 2.3B), MEP latencies are significantly longer in all three coil orientations in SCI compared to controls (LM: controls = 21.5 ± 1.2 ms, SCI = 25.5 ± 3.3 ms, $t(32) = -4.789$, $p < 0.001$; PA: controls = 23.1 ± 1.3 ms, SCI = 26.4 ± 3.2 ms, $t(32) = -3.938$, $p < 0.001$; AP: controls = 24.7 ± 1.5 ms, SCI = 27.4 ± 3.3 ms, $t(32) = -3.182$, $p = 0.003$; data shared from Jo et al. (2018).

In a subset of our control participants (N=7 out of 34), we also measured MEPs in the 1DI muscle (blue bars in Fig. 2.3B). MEP latencies did not differ between our control group and

the control subjects measured by Jo et al. (2018) (LM: 21.6 ± 2.4 ms, t(23) = 0.251, p = 0.804; PA: 22.9 ± 2.3 ms, t(23) = -0.238, p = 0.814; AP: 24.9 ± 2.8 ms, t(23) = 0.260, p = 0.797).

Comparing SCI participants that had a C4 lesion or higher with subjects that had a C5 lesion or lower revealed no difference in MEP latencies (LM: C4 or higher = 11.8 ± 1.2 ms, C5 or lower = 12.6 ± 1.8 ms, t(15) = -1.016, p = 0.326; PA: C4 or higher = 13.0 ± 1.0 ms, C5 or lower = 13.4 ± 1.6 ms, t(15) = -0.17, p = 0.612; AP: C4 or higher = 13.5 ± 1.6 ms, C5 or lower = 15.1 ± 1.8 ms, t(15) = -1.883, p = 0.079) for the biceps muscle.

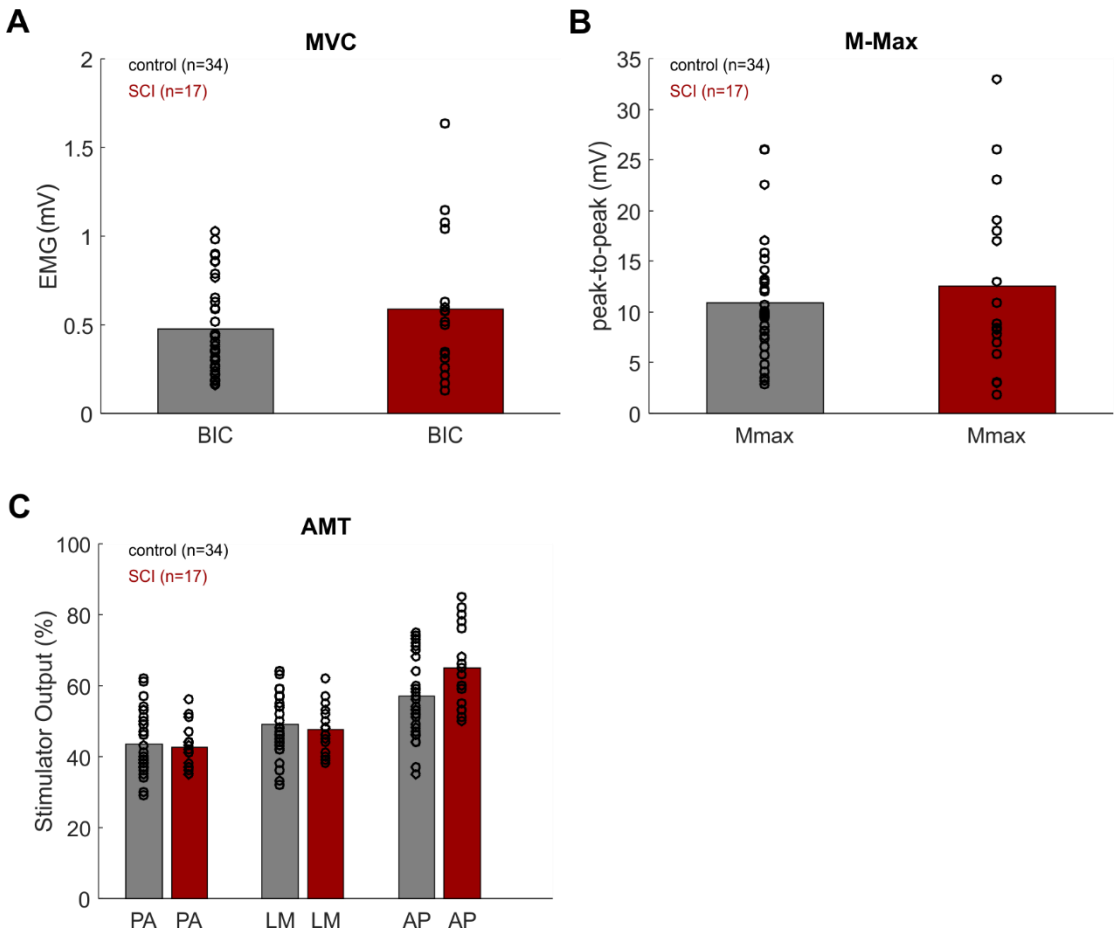

Figure 2.2: *Group results for MVC, M-Max and AMT.* **(A)** Group data for maximal voluntary contraction in biceps for the SCI (red) and control (grey) group. Bars show highest mean rectified EMG activity found in the muscle during the MVC burst. Circles represent individual subjects. **(B)** Group mean for peak-to-peak value of maximal M-wave in the biceps muscle. Circles represent individual subjects. **(C)** TMS stimulator output at active motor threshold across the different coil orientations and groups. Circles represent individual subjects.

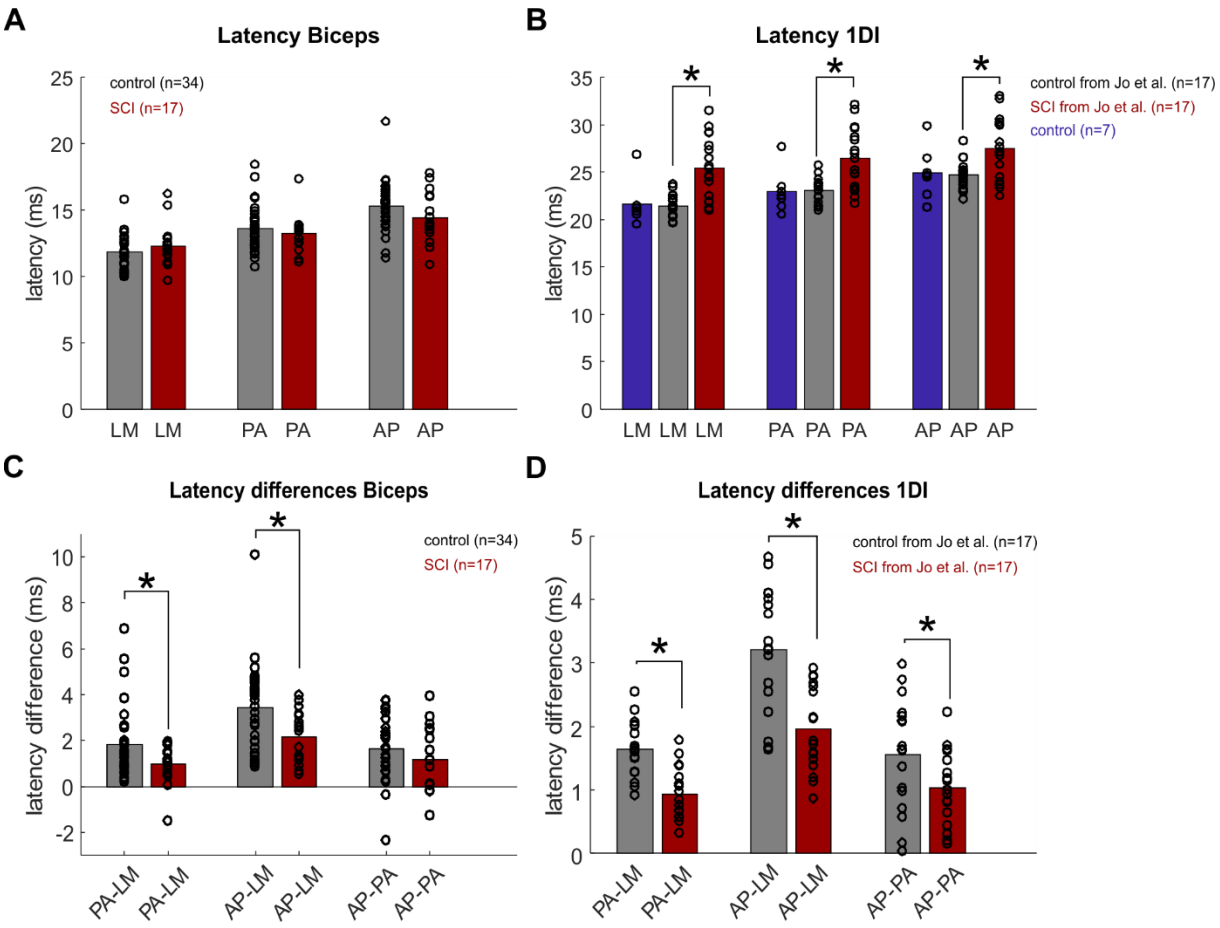

Figure 2.3: *MEP latencies.* **(A)** Group data showing the latencies of MEP evoked in the biceps muscle by TMS when the coil was oriented in LM, PA or AP direction for the SCI (red) and control (grey) group respectively. Circles represent individual subjects. **(B)** Group data showing the latencies of MEP evoked in the 1DI muscle by TMS when the coil was oriented in LM, PA or AP direction. Group data for SCI (red, n=17) and control (grey, n=17) were shared by Jo et al. (2018). Group data for control (blue, n=7) were measured in a subset of participants from the biceps study. Circles represent individual subjects. **(C)** Comparison of MEP latencies elicited with the coil in the LM, PA and AP orientation in the biceps muscle in SCI (red) and control (grey) subjects. Group data show PA-LM, AP-LM and AP-PA MEP latency differences. Circles represent individual subjects. **(D)** Comparison of MEP latencies elicited with the coil in the LM, PA and AP orientation in the 1DI muscle in SCI (red) and control (grey) subjects. Data shared by Jo et al. (2018). Circles represent individual subjects.

MEP latency differences across coil orientations

Figure 2.3C and 2.3D depicts the MEP latency differences (PA-LM, AP-LM & AP-PA) in biceps and 1DI muscle respectively. Data from the 1DI muscle were shared by the authors of Jo et al. (2018).

When looking at MEP latency differences in the biceps muscle, a two-way ANOVA demonstrated a significant effect of LATENCY DIFFERENCE ($F(2,98) = 21.140$, $p < 0.001$) and GROUP ($F(1,49) = 6.975$, $p = 0.011$), but not their interaction ($F(2,98) = 1.479$, $p = 0.233$). *Post hoc* tests revealed that the PA-LM difference was significantly reduced in SCI compared to control subjects ($t(49) = -2.149$, $p = 0.037$), similar to the PA-LM latency difference observed in the 1DI ($t(32) = 4.803$, $p < 0.001$; Fig. 2.3D). We also found a significantly reduced AP-LM latency difference in SCI compared to controls ($t(49) = -2.641$, $p = 0.011$), in line with previous observations in the 1DI ($t(32) = 4.295$, $p < 0.001$). AP-PA latency difference remained unchanged in SCI compared to controls ($t(49) = -1.079$, $p = 0.286$) in biceps, while there was a significant reduction in AP-PA latency difference after SCI in the 1DI ($t(32) = 2.075$, $p = 0.046$).

However, when comparing the latency differences across the two muscles, a three-way ANOVA with factors MUSCLE, GROUP and LATENCY DIFFERENCE showed no significant effect of MUSCLE ($F(1,81) = 0.473$, $p = 0.494$) or any of its interactions (MUSCLE*GROUP $F(1,81) = 0.007$, $p = 0.932$; MUSCLE*LATENCY DIFFERENCE $F(2,162) = 0.081$, $p = 0.922$) and there was no three-way interaction either ($F(2,162) = 0.069$, $p = 0.934$). There was a significant effect of GROUP ($F(1,81) = 16.197$, $p < 0.001$) and LATENCY DIFFERENCE ($F(1,162) = 49.479$, $p < 0.001$), as well as their interaction ($F(2,162) = 3.213$, $p = 0.043$).

Separate two-way ANOVA's with factors MUSCLE and GROUP on each latency difference confirmed that there was no effect of MUSCLE for any latency difference (PA-LM $F(1,81) = 0.184$, $p = 0.669$; AP-LM $F(1,81) = 0.473$, $p = 0.494$; AP-PA $F(1,81) = 0.178$, $p = 0.674$), or their interaction (PA-LM $F(1,81) = 0.084$, $p = 0.772$; AP-LM $F(1,81) = 0.007$, $p = 0.932$; AP-PA $F(1,81) = 0.027$, $p = 0.870$). There was an effect of GROUP for the PA-LM ($F(1,81)=10.305$, $p=0.002$) and the AP-LM ($F(1,81) = 16.197$, $p < 0.001$), but not for the AP-PA ($F(1,81) = 3.348$, $p = 0.071$) latency difference.

Comparing latency differences between the two muscles *post hoc*, revealed no significant differences between the SCI (PA-LM: biceps = 1.0 ± 0.8 ms, 1DI = 0.9 ± 0.4 ms, $t(32) = 0.147$, $p = 0.884$; AP-LM: biceps = 2.2 ± 1.1 ms, 1DI = 2.0 ± 0.7 ms, $t(32) = 0.598$, $p = 0.554$; AP-PA:

biceps = 1.2 ± 1.4 ms, 1DI = 1.0 ± 0.6 ms, t(32) = 0.420, p = 0.678), or control subjects (PA-LM: biceps = 1.8 ± 1.5 ms, 1DI = 1.6 ± 0.5 ms, t(49) = 0.464, p = 0.644; AP-LM: biceps = 3.5 ± 1.9 ms, 1DI = 3.2 ± 1.0 ms, t(49) = 0.506, p = 0.615; AP-PA: biceps = 1.6 ± 1.4 ms, 1DI = 1.6 ± 0.9 ms, t(49) = 0.188, p = 0.851) for biceps compared to 1DI.

The AP-LM latency difference was significantly smaller than the PA-LM difference in both muscles and in both the SCI (biceps t(16) = -3.432, p = 0.003; 1DI t(16) = -7.230, p < 0.001) and control subjects (biceps t(33) = -6.940, p < 0.001 ; 1DI t(16) = -7.307, p < 0.001).

In regards to the level of lesion, participants with C4 or higher lesions did not have significantly different latency differences in the biceps muscle compared to participants with C5 lesions or lower (PA-LM: C4 or higher = 1.2 ± 0.5 ms, C5 or lower = 0.8 ± 1.0 ms, t(15) = 1.018, p = 0.325; AP-LM: C4 or higher = 1.7 ± 1.4 ms, C5 or lower = 2.5 ± 1.1 ms, t(15) = -1.526, p = 0.148; AP-PA: C4 or higher = 0.6 ± 1.2 ms, C5 or lower = 1.7 ± 1.4 ms, t(15) = -1.917, p = 0.075).

Discussion

To investigate how changes in corticospinal transmission in humans after SCI may differ between distal and proximal upper limb muscles, we recorded MEPs from the biceps with the TMS coil in the LM, PA and AP orientation and compared it to data from Jo et al. (2018), who recorded MEPs from a distal intrinsic hand muscle.

We did not find significantly prolonged MEP latencies in the biceps in any of the coil orientations in SCI subjects compared with controls, contrary to the prolonged MEP latencies reported in the 1DI muscle after SCI (Jo et al., 2018). However, latencies of MEP responses elicited by PA and AP stimulation relative to responses elicited by LM stimulation were shorter in SCI compared to control subjects and the same pattern of MEP latency differences was observed in the 1DI muscle. We found no evidence that the changes in MEP latencies after SCI differed between the two muscles, suggesting that differences between MEPs elicited by distinct coil orientations are not fully preserved in humans with cervical SCI in both proximal and distal upper limb muscles.

TMS is an important non-invasive tool that allows measurement of several aspects of corticospinal function and can reveal impairments after SCI as well as reorganization of corticospinal pathways. A single pulse of TMS over the motor cortex leads to multiple

descending volleys (Patton and Amassian, 1954, Rothwell et al., 1991). These volleys differ in latency, activation threshold and most likely arise at least in part from different neural circuits (Di Lazzaro et al., 2012, Di Lazzaro et al., 2018, Di Lazzaro and Ziemann, 2013, Di Lazzaro and Rothwell, 2014). Experimental work using TMS has shown that it is possible to make inferences about the physiology of these different volleys from EMG recordings. Also, by using specific coil orientations to induce currents with different directions, it may be possible to preferentially activate different neural elements in the cortex (Werhahn et al., 1994, Sakai et al., 1997, Ni et al., 2011).

The earliest wave (D-wave) reflects the direct activation of the corticospinal neuron near the initial segment and is preferentially recruited through LM currents (Di Lazzaro et al., 2008). A PA current will preferentially recruit early I-waves (I1, I2). An AP orientation produces preferentially longer latency late indirect waves (I3) (Sakai et al., 1997, Di Lazzaro et al., 2001, Jung et al., 2012). I3 waves might involve contributions from multiple brain areas (Groppa et al., 2012, Volz et al., 2015) and therefore may reflect more indirect cortico-muscular transmissions (Cirillo and Perez, 2015, Federico and Perez, 2017).

Multiple studies have shown that TMS elicited MEPs have different characteristics in humans with SCI compared to healthy controls. The majority of research reports a higher threshold, a decreased amplitude and delayed latencies of MEPs following TMS stimulation. However, it is important to note that these studies have recorded MEPs from intrinsic hand muscles (Davey et al., 1998, Davey et al., 1999, Curt et al., 1998, Roy et al., 2011, Smith et al., 2000, Bunday and Perez, 2012), lower limb muscles (Brouwer et al., 1992, Alexeeva et al., 1998, Barthelemy et al., 2010, Roy et al., 2011), thoracic and erector spinae muscles (Ellaway et al., 2004, Ellaway et al., 2007), inspiratory and expiratory muscles (Lissens and Vanderstraeten, 1996), or paravertebral muscles (Cariga et al., 2002). Here we recorded from biceps brachii muscle, a proximal upper limb muscle, in people with chronic cervical spinal cord injury.

An important pathological process after SCI is the chronic and progressive demyelination of long motor axons in the white matter (Griffiths and Mcculloch, 1983, Bunge et al., 1993, Totoiu and Keirstead, 2005). Changes in MEP latencies can therefore provide an estimate of the impairment and in fact MEP recordings correlate with the outcome of ambulatory capacity and hand function in patients with SCI to a similar extent as performing the American Spinal Injury Association (ASIA) neurological examination (Curt et al., 1998).

Differences in study design, stimulation parameters and participants with varying post-injury time make it difficult to compare MEP latencies across published research. Nevertheless, the evidence suggests that delays in MEP latency after SCI range from 2 to 10 ms depending on which muscle group was used for testing.

In order to have a more direct comparison between proximal and distal upper limb muscles, we closely followed methodological parameters of Jo et al. (2018). Unlike MEP latencies recorded from the 1DI muscle, which showed a significant delay in all three coil orientations (PA, AP, LM; Figure 2.3B), MEP latencies were not significantly different in biceps brachii muscle after SCI in any of the coil orientations (Figure 2.3A). This is consistent with results found by Curt et al. (1998), which concluded that approximately 80% of the MEPs in biceps were normal, whereas 90% of MEPs in ADM were pathologic. However, their experiments included a mix of acute and chronic SCI patients and used just one coil position. A recent study reported a prolonged latency of MEP-max (with the coil held in PA orientation) and MEPs elicited by cervicomedullary stimulation (CMEPs) in both triceps and biceps (Sangari and Perez, 2020).

Cervical spinal cord injury leads to a wide variety and diverse range of severity in impairments. Motor function will depend on the specific type, location and extent of the injury as well as time since injury and the individual potential for recovery. It is therefore not surprising that studies including such a variable patient group might end up with differing results. Apart from not finding a significant delay in MEP latency in the biceps following TMS stimulation, there also were no significant differences in generated EMG during maximal voluntary contractions or amplitudes of maximal M-waves in SCI compared to healthy controls (Figure 2.2A & 2.2B). Most of the aforementioned studies (recording from lower limb muscles or hand muscles) using TMS have reported that active motor thresholds are increased after SCI, possibly as a result of reduced numbers of corticospinal axons reaching the pool of motoneurons (Smith et al., 2000). We did not find a significantly increased AMT in the biceps for the SCI group compared to controls (Figure 2.2C).

The spinal cord lesions in this study ranged from C3 to C6, which begs the question whether or not innervation to the biceps muscle was even affected in all participants. However, when comparing the group of SCI participants with a C4 lesion or higher with the group of participants with a C5 lesion or lower, we did not find any differing results for MVC, M-max, AMT or MEP latencies. This would imply that the change in latency differences observed after

SCI is not so much dependent on where the lesion is and rather reflects a general effect of SCI on the motor system and cortex.

In order to ascertain that our results for the two muscles did not diverge due to differences in data collection or analysis, we recorded MEPs from the 1DI muscle in a subset of our control participants (7 out of 34). MEP latencies did not differ between our control group and the control subjects measured by Jo et al. (2018), suggesting that methodological differences between the two studies were not influencing our results (Figure 2.3B).

A crucial finding of Jo et al. (2018) was that in addition to prolonged MEP latencies in all coil orientations, MEPs elicited by PA and AP stimulation had a shorter latency relative to LM stimulation in SCI compared with control subjects (Figure 2.3D). This latency difference was largest in MEPs elicited by AP currents. Our results revealed the same pattern (Figure 2.3C), with the latency differences between AP and LM elicited MEPs also being significantly smaller than between PA and LM elicited MEPs. This indicates that the same preferential effect on AP responses after SCI seen in the 1DI muscle is also present in the more proximal biceps brachii.

The fact that AP induced responses are the most impacted after SCI could be explained if late I3 waves involve contributions from multiple brain areas, and functional connectivity between cortical regions decreases after injury (Min et al., 2015, Rao et al., 2016). Alternatively, MEPs elicited by AP currents may be modulated by afferent input to a larger extent than MEPs elicited by PA currents (Hannah and Rothwell, 2017); afferent input is altered after SCI (Ozdemir and Perez, 2018).

Delayed latencies, decreased amplitudes and higher thresholds are all consistent with the view that corticospinal drive is impaired in SCI individuals (Calancie et al., 1999, Thomas et al., 1997). The biceps muscle often suffers overall less impairment compared to the 1DI muscle, but this does not necessary mean there is less CST damage. While proximal muscles are indeed known to make a better recovery after injury (Pestronk and Drachman, 1988, Colebatch and Gandevia, 1989), this could also be because they are benefitting more from the reorganization of corticospinal pathways. CST innervation is thought to play a greater role in distal muscles (Porter and Lemon, 1993, Lawrence and Kuypers, 1968a), while proximal muscles receive more extensive projections from subcortical pathways (Kuypers, 1981b, Holstege and Kuypers, 1982, Holstege and Kuypers, 1987, Jones and Yang, 1985, Martin et al., 1985), which might provide them with a bigger substrate for recovery after CST injury.

Overall our results suggest that the same MEP latency differences can be observed in both the biceps and distal 1DI muscle and these differences decrease significantly after SCI. In line with the results by Jo et al. (2018), neural structures activated by AP currents appear to be the most impacted, leading to a drastic shortening of AP elicited MEP latencies in relation to LM elicited MEP latencies, despite little apparent motor impairment in the biceps muscle of this SCI group.

CHAPTER III – PAIRING TRANSCRANIAL MAGNETIC STIMULATION AND LOUD SOUNDS PRODUCES PLASTIC CHANGES IN MOTOR OUTPUT

The data described in this chapter was collected by me, Siong Jason Ting, a summer student from NU Malaysia who I supervised for a two month project and Marco Raditya, an MRes student who I supervised for 6 months. All data collection was done under my supervision. I designed the plasticity protocol and performed all data analysis. Data from the experiment in monkeys was provided by Dr Annie Poll and Prof Stuart Baker.

Abstract

Most current methods for neuromodulation target the cortex. Approaches for inducing plasticity in sub-cortical motor pathways such as the reticulospinal tract could help to boost recovery after damage (e.g. stroke). In this study, we paired loud acoustic stimulation (LAS) with transcranial magnetic stimulation (TMS) over the motor cortex in healthy humans. LAS activates the reticular formation; TMS activates descending systems, including corticoreticular fibers. Two hundred paired stimuli were used, with 50 ms interstimulus interval at which LAS suppresses TMS responses. Before and after stimulus pairing, responses in the contralateral biceps muscle to TMS alone were measured. Ten and 20 minutes after stimulus pairing ended, TMS responses were enhanced, indicating the induction of long-term potentiation. No long-term changes were seen in control experiments which used 200 unpaired TMS or LAS, indicating the importance of associative stimulation. Following paired stimulation, no changes were seen in responses to direct corticospinal stimulation at the level of the medulla, or in the extent of reaction time shortening by a loud sound (StartReact effect), suggesting that plasticity did not occur in corticospinal or reticulospinal synapses. Direct measurements in monkeys undergoing a similar paired protocol revealed no enhancement of corticospinal volleys after the paired stimulation, suggesting no changes occurred in intracortical connections. The most likely substrate for the plastic changes, consistent with all of our measurements, is an increase in the efficacy of corticoreticular connections. This new protocol may find utility, as it seems to target different motor circuits compared to other available paradigms.

Introduction

The primary motor cortex and its corticospinal outputs forms the major neural control system for generation of voluntary movements in primates such as humans (Porter and Lemon, 1993). However, sub-cortical circuits such as the brainstem and spinal cord also play an important role. This may become of special importance following damage to the cortex, such as after stroke, when sub-cortical systems can compensate and thereby mediate some functional recovery (Zaaimi et al., 2012, Zaaimi et al., 2018, Tohyama et al., 2017).

Various neural stimulation approaches have been developed to induce synaptic plasticity in the motor system (e.g. Stefan et al., 2000, Ridding and Uy, 2003, Huang et al., 2005, Nitsche and Paulus, 2000, Foysal and Baker, 2020); these could provide a way to boost connections in surviving circuits and thereby enhance recovery in patients recovering from damage. However, to date such approaches have not entered routine clinical practice, as they provide inconsistent benefits (Rothwell, 2016). Importantly, most previous protocols to induce plasticity by stimulation targeted the motor cortex and corticospinal tract. New methods capable of generating long-term changes in a more diverse range of motor pathways might give better options to improve recovery, possibly by allowing individualized treatment based on the specific deficits.

In this laboratory, we recently devised one such protocol, which paired loud auditory clicks with weak electrical stimuli given to a muscle (Foysal et al., 2016). Loud clicks are known to activate reticulospinal cells (Fisher et al., 2012), probably via both cochlear (Irvine and Jackson, 1983) and vestibular (Peterson and Abzug, 1975, Rosengren et al., 2010) afferents, and the reticular formation also receives powerful somatosensory inputs (Leiras et al., 2010). Long-term potentiation or depression of motor output could be generated depending on whether synaptic inputs from the muscle stimulation arrived at the brainstem before or after action potentials generated by the click, in accordance with the principles of spike-timing dependent plasticity (Markram et al., 1997). We subsequently found changes in a variety of non-invasive measures consistent with a sub-cortical substrate for plasticity in this protocol (Germann and Baker, 2021), and showed that applying such paired stimuli to stroke patients could produce significant improvement in hand function (Choudhury et al., 2020).

One alternative promising stimulus to target reticulospinal systems is a loud auditory stimulus (LAS), capable of evoking the startle reflex. Such stimuli are typically 500-1000 Hz tone bursts

lasting around 50 ms; this contrasts with much briefer clicks (0.1 ms) which do not elicit startle. The neural substrate for the startle reflex involves the nucleus reticularis pontis caudalis (Leitner et al., 1980, Davis et al., 1982, Brown et al., 1991) and its reticulospinal projection (Delwaide and Schepens, 1995). LAS can also dramatically shorten voluntary reaction times, a phenomenon known as the StartReact effect. This may reflect involuntary release of a subcortically stored motor program (Valls-Sole et al., 1999a, Rothwell, 2006, Valls-Sole et al., 2008, Carlsen et al., 2004a), and has been deployed by many authors as a measure of the size of reticulospinal inputs to a given motoneuron pool (Choudhury et al., 2019, Baker and Perez, 2016, Sangari and Perez, 2019, Carlsen et al., 2009, Honeycutt et al., 2013).

Another approach which efficiently stimulates the reticulospinal tract is to activate the motor cortex with transcranial magnetic stimulation (TMS). This is capable of stimulating corticoreticular projections (Fisher et al., 2012) which can activate reticulospinal cells trans-synaptically both ipsilateral and contralateral to the stimulated hemisphere (Fisher et al., 2021). Many corticoreticular projections are collaterals of corticospinal axons (Keizer and Kuypers, 1989).

We hypothesise that consistent pairing of LAS with TMS will lead to plastic changes in motor output in healthy human volunteers, by modulating pathways distinct from the corticospinal tract. The protocol produced an enhanced motor output in healthy human volunteers, although the details of the changes differed from those seen following our previous approach involving clicks and peripheral stimuli. Results in monkey also suggested that the new method may be targeting a different set of synapses, and could be of benefit in different circumstances, or be used to augment changes produced by pre-existing protocols.

Methods

Participants

In total, 75 right-handed, healthy volunteers (18-35 years old, 51 females) participated in the study (16 participants, 11 females in Experiment 1; 15 participants, 12 females in Experiment 2; 16 participants, 11 females in Experiment 3; 15 participants, 10 females in Experiment 4 and 15 participants, 8 females in Experiment 5). Some participants took part in several experiments, in which case each session was separated by at least seven days. All subjects gave written informed consent to the experimental procedures, which were approved by the

local ethics committee of the Newcastle University Faculty of Medical Sciences. The study was performed in accordance with the guidelines established in the Declaration of Helsinki, except that the study was not pre-registered in a database.

Electromyography (EMG) recordings

EMG was recorded from the right biceps muscle through surface electrodes (Kendall H59P, Covidien, Mansfield, Massachusetts USA) secured on the skin over the muscle belly. EMG signals were amplified and filtered (band-width 30-2000 Hz) with a bioamplifier (D360 8-Channel Patient Amplifier, Digitimer, Welwyn Garden City, UK) and then converted to digital data with a sampling rate of 5kHz (CED Micro 1401 with Spike2 software, Cambridge Electronic Design, Cambridge, UK) and stored on a computer for off-line analysis.

Transcranial magnetic stimulation

Transcranial magnetic stimuli were applied using a figure-of-eight coil through a Magstim 200 magnetic stimulator (Magstim, Whitland, UK) with a monophasic current waveform. We determined the optimal position for eliciting a motor evoked potential (MEP) in the biceps muscle (hotspot) by moving the coil, with the handle pointing backwards and 45° away from the midline, in small steps along the arm representation of M1. The hotspot was defined as the region where the largest MEP in the biceps muscle could be evoked with the minimum intensity (Rothwell et al., 1999). In all experiments, the magnetic coil was held to induce electrical currents that flowed perpendicular to the presumed line of the central sulcus in a posterior—anterior direction. Active motor threshold (AMT) was defined as the minimal stimulus intensity needed to produce a visible MEP in at least 5 out of 10 consecutive trials in the tonically activated biceps. A TMS intensity of 130% AMT was used to collect all MEPs. To ensure a stable coil position during the experiment, the site of stimulation was marked in a Brainsight neuronavigation system (Rogue Research Inc., Montréal, Canada) which allowed online navigation. A Polaris Vicra camera (Northern Digital Inc., Canada) was used to track the coil.

Experimental paradigm (Experiments 1-3)

Figure 3.1 illustrates the experimental paradigm. Subjects were first seated with both arms relaxed and their forearms resting on their lap. Subjects were then asked to perform a biceps curl by pushing with their right arm up against a table in front of them, while keeping their left arm relaxed. Visual feedback of rectified and smoothed EMG activity from the biceps muscle

was provided to the subjects, involving a series of colored bars on a computer screen which illuminated in sequence as stronger contractions were made. This system was first calibrated to the subject's individual maximum voluntary contraction (MVC); all subsequent TMS measurements were made at 130% AMT, while the subject aimed for a consistent background contraction level, which was set between 5-10% of MVC for a given subject.

Baseline. 20 MEPs were recorded while subjects performed the controlled isometric biceps contraction. TMS pulses were applied with an inter-stimulus interval of 10-12.5 s. After baseline, subjects rested for 15 s.

Intervention. In total, subjects received 200 stimuli. The inter-trial interval varied between 10-12.5 s so that the timing of stimulation was unpredictable. Stimuli were given while subjects performed the controlled isometric biceps contraction. To avoid fatigue, subjects received 20 blocks of 10 stimuli, with 15 s breaks in-between each block.

For **Experiment 1**, subjects received 200 stimuli pairs. A loud acoustic stimulus (500 Hz, 120 dB) was presented 50 ms prior to the TMS pulse through two audio speakers located on a table ~100cm in front of the subject. For **Experiment 2**, subjects received 200 loud acoustic stimuli without any TMS. For **Experiment 3**, subjects received 200 TMS pulses, without any loud acoustic stimuli.

Assessments. Identical to the baseline, 20 MEPs were recorded while subjects performed a controlled isometric biceps contraction. TMS pulses were applied with an inter-trial interval of 10-12.5 s. This assessment was repeated 4 times in total; immediately after the intervention (0 min) and starting 10, 20 and 30 minutes after the end of the intervention.

Cervicomedullary Junction Stimulation (Experiment 4)

As a way of controlling for spinal excitability, we also measured cervicomedullary motor evoked potentials (CMEP) in the biceps brachii, as they are thought predominantly to reflect CST responses unaffected by changes in cortical excitability (McNeil et al., 2013). CMEPs were elicited via electrical stimulation of the corticospinal tract at brainstem level. Adhesive surface electrodes (Neuroline 720 00-S/25, Ambu, Copenhagen, Denmark) were fixed to the skin over the mastoid processes and current was passed between them (0.1 ms duration, 80–200 mA; model DS7AH, Digitimer Ltd, Welwyn Garden City, UK) with the cathode on the left side. The stimulation intensity was adjusted to elicit a CMEP amplitude of 1mV with an active isometric contraction of 5-10% MVC. 20 CMEPs were recorded before and 10 minutes after the

intervention. The intervention consisted of the same 200 stimuli pairs as in Experiment 1 (Fig. 3.1B).

StartReact (Experiment 5)

The StartReact response was examined using a previously tested paradigm (Baker and Perez, 2017). During testing, subjects held their right arm relaxed, with their forearm supinated and resting on their lap. Subjects were asked to observe a red light-emitting diode (LED) located ~100cm in front of them. When the LED was illuminated, participants were asked to flex their forearm up as fast as possible. Visual reaction time (VRT) was measured as the time from cue to onset of the EMG burst in the biceps muscle after the LED presentation. In some trials, the LED was presented with either a quiet acoustic stimulus (80dB, 500Hz, 50ms) or a startling acoustic stimulus (120 dB, 500 Hz, 50 ms). Subjects were presented with five consecutive LAS, without performing the task, to familiarize them with the startling cue. The time delay between the presentation of the quiet acoustic stimulus and the onset of the EMG response was referred as the visual-auditory reaction time (VART), whereas the time between the LAS and the EMG onset was defined as the visual-startle reaction time (VSRT).

StartReact responses were recorded before and 10 minutes after the intervention (Fig. 3.1C). The intervention consisted of the same 200 stimuli pairs as in Experiment 1. In each task, 20 responses were recorded in each condition (VRT, VART, and VSRT) in a pseudorandomized order with an inter-trial-interval between 5-6 s.

Data analysis

Data were analyzed using MATLAB (R2017a, MathWorks). EMG traces were full-wave rectified and then averaged. MEP amplitude was measured as the area under the curve (AUC) of this average, with onset and offset latencies chosen interactively by the experimenter for each subject. AUC was normalized to the baseline measurement made before the intervention, by expressing it as a percentage ([assessment MEP × 100]/baseline MEP).

All statistics were performed using IBM SPSS Statistics for Windows, version 24 (IBM Corp., Armonk, N.Y., USA)

Sphericity was tested with Mauchly's test of sphericity. When sphericity could not be assumed, the Greenhouse-Geisser correction statistic was used.

For Experiment 1, 2, and 3, one-way repeated measures ANOVAs were performed to determine the effect of TIME (before, during and 0 min, 10 min, 20 min and 30 min after intervention) on MEP AUC. For Experiment 4, a one-way repeated measures ANOVA was performed to determine the effect of TIME (before and after) on CMEP AUC.

For Experiment 5, a two-way repeated measures ANOVA was performed to determine the effect of SOUND (VRT, VART and VSRT) and TIME (before and after intervention) on reaction time. An automated program identified the reaction time, defined as the time point where mean rectified EMG signals exceeded 7 SD of the mean EMG measured 200 ms before each stimulus presentation; every trial was inspected visually, and erroneous activity onset times (caused, for example, by electrical noise artefacts) were manually corrected.

Paired t-tests were used to compare individual datapoints *post hoc* and reported with effect size Cohen's *d*. The Benjamini-Hochberg procedure was used to correct for multiple comparisons (Benjamini and Hochberg, 1995). The significance level was set at $p < 0.05$ and group data are presented as mean ± SD in the text.

Overall, 15 subjects were included in the final analysis for each Experiment 1-5. One subject was excluded from Experiment 1 and one from Experiment 3, because their change in MEP size fell greater than 3 SD outside the group mean.

Additional Study in Monkey

The indirect measurements made in humans were supplemented with data from two macaque monkeys, in which direct recordings of volleys from the spinal cord were possible.

All animal experiments were conducted under authority of appropriate licenses from the UK Home Office and were approved by the Animal Welfare and Ethical Review Board of Newcastle University. Two adult female macaques (monkey O: weight 7.75 kg, age 6 years 9 months; monkey V: weight 7.64 kg, age 7 years) were trained on a variety of grasp tasks for another, unrelated study, and were then surgically implanted with a titanium headpiece to allow head fixation. The headpiece incorporated chambers which allowed access to craniotomies over right M1 and the bilateral reticular formation. In the same surgery, EMG electrodes were implanted in hand and forearm muscles on the left side, and the wires tunneled subcutaneously to a connector on the head. A subsequent brief surgery implanted electrodes for stimulation in the pyramidal tract (PT) at the medulla, as we have previously reported (Baker et al., 1999). Single unit recordings were made during task performance for the main

study, lasting 8 months in monkey V, and 15 months in monkey O. A further surgery then implanted a recording chamber over the cervical enlargement of the spinal cord, involving fusing vertebrae from C4-T2 (Perlmutter et al., 1998, Williams et al., 2010, Riddle and Baker, 2010), after which neural recordings of spinal activity during task performance were made. All surgical implants were performed with aseptic technique and under full general anesthesia (sedation with 10 mg/kg ketamine IM; maintenance with sevoflurane (1.9-2.6%) in 100% O_2 with continuous IV infusion of alfentanil, 0.4 µg/kg/hour). Monitoring during surgery included pulse oximetry, capnography, non-invasive blood pressure, heart rate, core and peripheral temperature. Intravenous fluids were given (infusion rate including drug infusions 5-10 ml/kg/hour). The airway was protected with a tracheal catheter, and positive pressure ventilation used. A continuous IV infusion of methylprednisolone (5.4 mg/kg/hour) reduced edema. The animal was kept warm with a thermostatically-controlled heating blanket, and also a supply of warm air. Post-operative analgesics (buprenorphine 20-30 µg/kg, meloxicam, 0.2 mg/kg), dexamethasone (0.25 mg/kg) and prophylactic antibiotics (monkey V: 12.5 mg/kg Synulox SC; monkey O: 2 x 50 mg Synulox orally) were given.

For the present study, measurements were made once from each monkey in the conscious state, when all parts of the main experiment in that animal had been completed. Because both animals had metal headpieces, and the head fixation device in our primate chairs uses large metal blocks, it was not feasible to use TMS to activate the motor cortex. Fortunately, the dural surface over M1 was exposed in a recording chamber already in these animals, allowing us instead to stimulate epidurally. Cathodal stimulation of the cortical surface produces similar descending volleys to TMS (Patton and Amassian, 1954, Rosenthal et al., 1967, Edgley et al., 1990). In monkey V, at the conclusion of recordings from the M1 chamber, a fine wire (75 µm stainless steel, insulated with Teflon, catalog number FE6215, Advent Research Materials, Oxford, UK) was bared for a few millimeters at its tip, and this tip was placed on the dura overlying M1 within the recording chamber. The chamber was then sealed with dental acrylic, allowing M1 to be stimulated subsequently simply by connecting to the implanted wire. In monkey O, the chamber was opened and a silver ball electrode was temporarily placed on the dura to allow M1 stimulation. On the day of the study, the animal entered the primate chair, and the head and spinal chamber were stabilized. An electrode with 32 contacts (0.1 mm inter-contact spacing, U probe, Plexon Inc, Dallas, TX, USA) was penetrated through the spinal dura targeting the lateral funiculus. Stimulation through the M1 electrode was then carried

out (monkey O, 10mA, biphasic pulses, 0.2 ms per phase, cathodal stimulus first; monkey V, 10 mA, 0.4ms cathodal pulse; both with Model 2100 isolated stimulator, AM Systems Inc, Sequim, WA, USA). Clear D and I wave volleys were visible on the spinal recordings.

A block of stimuli was given to assess EMG and spinal responses; this formed a standardized assessment which was repeated throughout the study. In monkey O, a block comprised 20 stimuli to M1 at a minimum inter-stimulus of 10 s. In monkey V, a block comprised 50 stimuli to M1, and 50 stimuli to the chronically implanted PT electrode (train of two 500μA stimuli, biphasic pulses, 0.1 ms per phase, 3 ms between stimuli in the train, also Model 2100 stimulator, AM Systems). Stimuli to M1 and the PT were alternated, with minimum inter-stimulus interval 2.5 s. Stimuli were only given if the rectified EMG remained lower than a pre-selected amplitude, chosen based on recording noise, for 200 ms; this ensured that the animal was always at rest when stimuli were delivered. The EMG used for this purpose was flexor digitorum superficialis (FDS) in monkey O, and first dorsal interosseous (1DI) in monkey V. There was a strong correlation between muscles, such that if one muscle was at rest, it was a good indicator that the monkey was sitting quietly.

Two assessment blocks were given, beginning 0 minutes and 5 minutes after the start of the experiment. The intervention started 10 minutes after the start of the study, in which M1 stimulation as above was paired with LAS. The LAS was generated using the same system and with the same input waveform as for the human subjects (50 ms duration, 500Hz, 120 dB SPL); M1 stimulation was given at the end of the sound. The inter-stimulus interval was 10 s; 200 paired stimuli were given. The activity level of the animal was not used to gate these stimuli, but in practice the monkey also sat quietly for this part. After the paired stimulation intervention, seven further blocks of assessment stimuli were given starting 0 to 30 minutes after the end of the intervention, in 5 minute steps.

The analysis of EMG responses proceeded as for the data from human subjects, with measurement of the AUC of averages of full-wave rectified signals. Clear responses were seen in both animals from the 1DI muscle; this reflects the location of the M1 stimulus over the hand representation, which had been the target of our earlier experiments in these animals. Results from 1DI are therefore presented here. Averages of the spinal recordings were used to identify the profile of the D and I wave volleys with depth; good recordings were seen over the first half of the array, corresponding to the expected location of the dorsolateral funiculus. The probe contact with the largest volleys in the baseline measurements was used in all

subsequent analysis. Individual components of the response were identified based on their latency, as described in previous work (Edgley et al., 1990). The amplitude was measured from onset to peak, except for the D wave in monkey O, which was measured from peak to offset because the stimulus artifact prevented accurate visualization of the onset. Measures were expressed as a percentage of those in the baseline period; t tests were used to assess the significance of any change.

Results

Experiment 1: Effects of paired stimulation

In this group, subjects (N=15) received 200 stimuli pairs of a loud acoustic stimulus 50 ms prior to the TMS pulse. Figure 3.2A illustrates average traces of MEPs elicited by TMS in the biceps muscle from a representative subject. Note how MEP size is drastically suppressed during the intervention and then shows a small but consistent increase after.

Figure 3.3A shows the group data, with mean MEP AUC normalized to the baseline. Mauchly's test of sphericity indicated that the assumption of sphericity had not been violated ($\chi^2(14) = 11.893$, $p = 0.623$). A one-way repeated measures ANOVA showed that there was a significant change in MEP AUC over time, $F(5, 70) = 12.022$, $p < 0.001$, partial $\eta 2 = 0.462$. MEP AUC was significantly reduced during the intervention ($t(14) = -4.452$, $p = 0.001$, $d = -1.150$). MEP size then returned to baseline immediately after the intervention ($t(14) = 1.201$, $p = 0.250$, $d = 0.310$). However, both 10 and 20 minutes after receiving the paired stimulation, MEP AUC was significantly increased compared to baseline ($t(14) = 2.875$, $p = 0.012$, $d = 0.742$ and $t(14) = 3.562$, $p = 0.003$, $d = 0.920$). Importantly, this increase was seen in the majority of subjects (Figure 3.3A, right). Even 30 minutes after the intervention, the majority of participants still showed an increase in MEP AUC, but group means were not statistically significant ($t(14) = 1.847$, $p = 0.086$, $d = 0.477$).

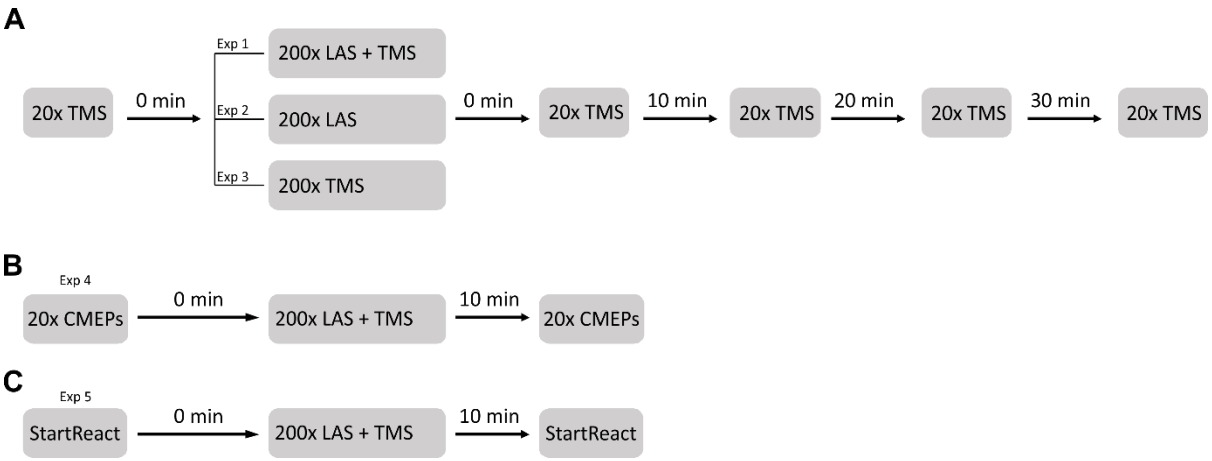

Figure 3.1: *Experimental paradigm.* **(A)** Experiment 1-3. Each group received 20 single pulse TMS before, immediately after and 10, 20 and 30 minutes after the intervention. The three groups received 3 different interventions, consisting of either paired stimulation of a loud acoustic stimulus (LAS) with TMS (Experiment 1), TMS alone (Experiment 2) or LAS alone (Experiment 3). **(B)** Experiment 4. 20 CMEPs were recorded immediately before and 10 minutes after the intervention. The intervention consisted of paired stimulation of a LAS with TMS (same as Experiment 1). **(C)** Experiment 5. Participants performed the StartReact assessment immediately before and 10 minutes after the intervention. The intervention consisted of paired stimulation of an acoustic startle sound with TMS (same as Experiment 1).

Experiment 2: Effects of loud acoustic stimulus alone

As a control experiment, subjects (N=15) received 200 LAS without any TMS. Figure 3.2B illustrates average traces of MEPs elicited by TMS in the biceps muscle from a representative subject. There was no MEP to illustrate during the intervention, as subjects did not receive any TMS. Participants were however still instructed to maintain a controlled isometric contraction, equal to Experiment 1.

Average MEP AUC across the group are shown in Figure 3.3B. The assumption of sphericity was violated, as assessed by Mauchly's test of sphericity ($\chi^2(14) = 27.499$, $p = 0.001$). Therefore, a Greenhouse-Geisser correction was applied ($\varepsilon = 0.648$).

There was no significant change in MEP AUC across time points, as shown by a one-way repeated measures ANOVA ($F(1.938, 27.139) = 0.617$, $p = 0.542$, partial $\eta 2 = 0.042$). Furthermore, there was no clear majority of subjects showing either an increase or decrease in MEP size (Figure 3.3B, right). We can therefore conclude that the effects observed during Experiment 1 are not likely simply to be due to LAS.

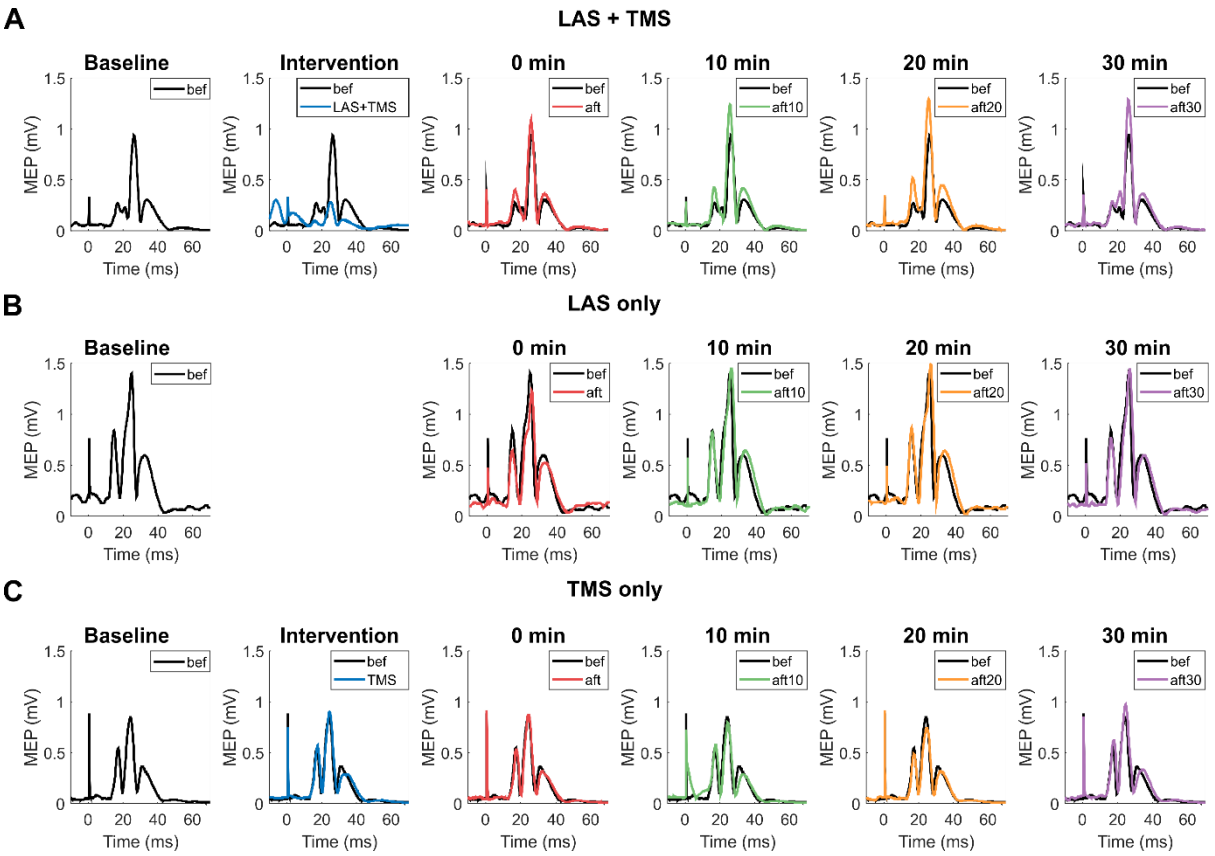

Figure 3.2: *Single subject examples.* Average traces of MEPs elicited by TMS in the biceps muscle from a representative subject for Experiment 1 **(A)**, Experiment 2 **(B)** and Experiment 3 **(C)**. Waveforms represent the average of 20 sweeps of rectified EMG, except for waveforms during the intervention (blue traces), which represent the average of 200 sweeps. Traces for each timepoint (colored traces) are overlaid with baseline average (black trace) for comparison.

Experiment 3: Effects of transcranial magnetic stimulation alone

In a second control experiment, subjects (N=15) received 200 single pulse TMS, without any LAS. Figure 3.2C illustrates average traces of MEPs elicited by TMS in the biceps muscle from a representative subject

Average MEP AUC across the group are shown in Figure 3.3C. The assumption of sphericity was met, as assessed by Mauchly's test of sphericity ($\chi^2(14) = 13.392$, $p = 0.505$). A one-way repeated measures ANOA showed no significant changes in MEP AUC across time ($F(5, 70) = 1.545$, $p = 0.187$, partial $\eta 2 = 0.099$). There also was no majority of participants showing either increase or decrease in MEP AUC, but rather a similar proportion of each across the group. It is therefore unlikely that the effects seen in Experiment 1 are due to prolonged TMS.

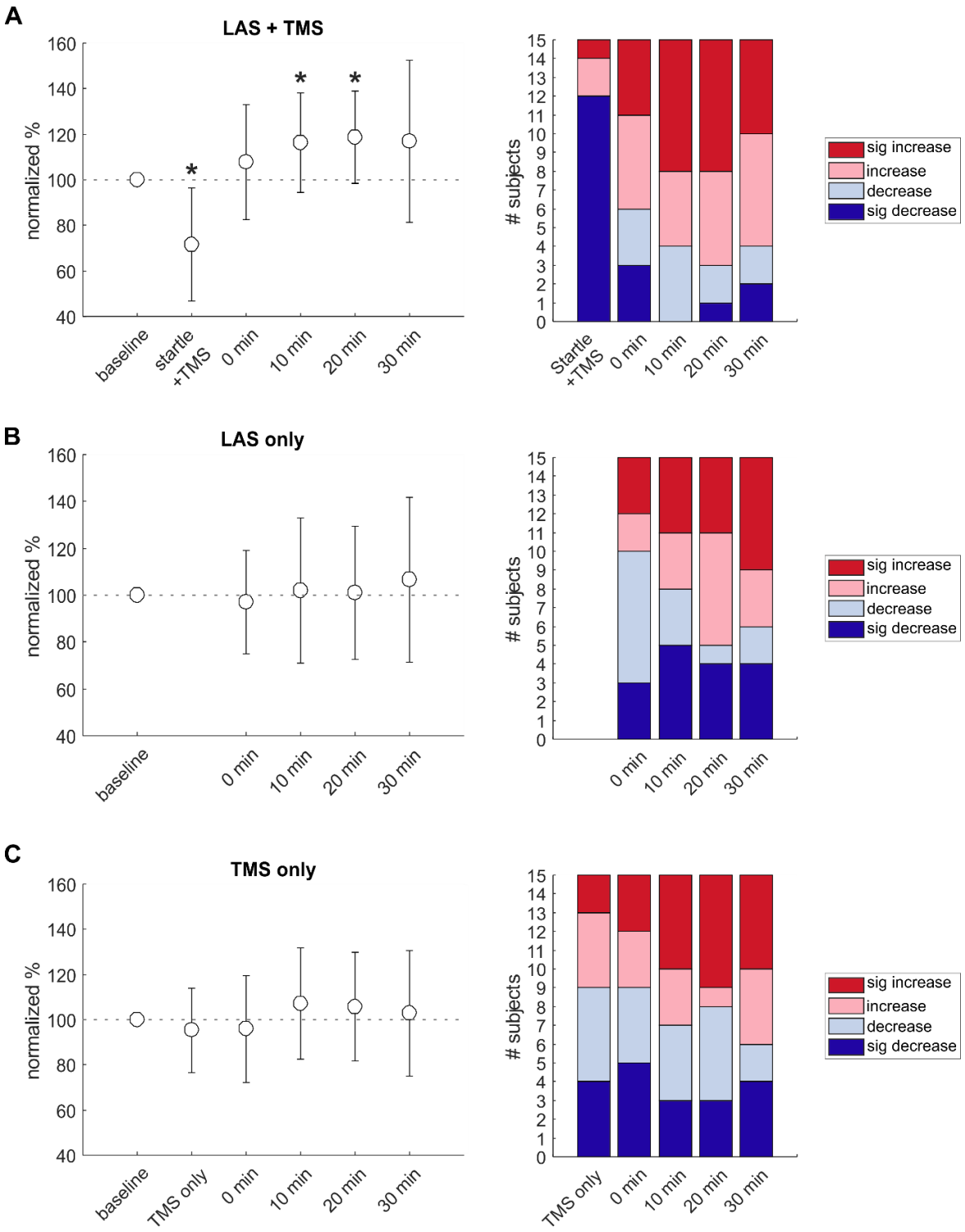

Figure 3.3: *Group data.* Group results for Experiment 1 **(A)** Experiment 2 **(B)** and Experiment 3 **(C)** *Left:* Mean MEP area-under-curve for each timepoint during the experiment, normalized to the baseline. Asterisks indicate significance ($p<0.05$). Error bars indicate standard deviations. *Right:* Number of subjects showing either a significant increase (red), non-significant increase (pink), non-significant decrease (grey) or significant decrease (blue) in MEP AUC compared to baseline.

Experiment 4: CMEPs

To test for changes in spinal excitability, CMEPs were measured before and after the intervention (LAS paired with TMS, as in Experiment 1). Figure 3.4 shows the group data (N = 15), with mean MEP AUC normalized to the baseline. There was no significant change in CMEP AUC after the intervention, as shown by a one-way repeated measures ANOVA ($F(1,14) = 1.905$, $p = 0.189$, partial $\eta 2 = 0.120$). Similar numbers of individual subjects showed an increase or a decrease in CMEP AUC after the intervention.

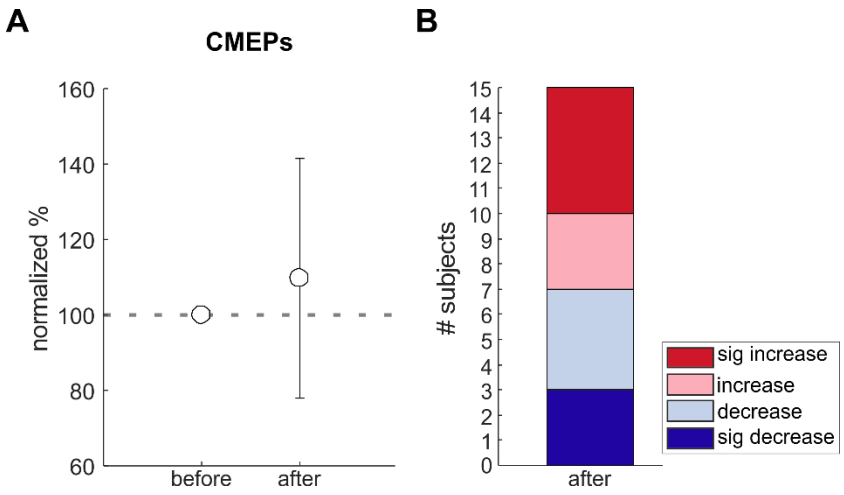

Figure 3.4: *CMEPs group results.* **(A)** Mean MEP area-under-curve normalized to the baseline. **(B)** Number of subjects (N=15) showing either a significant increase (red), non-significant increase (pink), non-significant decrease (grey) or significant decrease (blue) in MEP AUC compared to baseline.

Experiment 5: StartReact

Figure 3.5A illustrates the mean reaction times before and 10 minutes after the intervention. Participants (N=15) received the same intervention (LAS paired with TMS) as in Experiment 1.

The assumption of sphericity was met, as assessed by Mauchly's test of sphericity ($\chi^2(2) = 4.237$, $p = 0.115$). A two-way repeated measures ANOVA was performed to test the effects of SOUND (VRT, VART and VSRT) and TIME (before, after). There was no statistically significant two-way interaction between SOUND and TIME ($F(2,28) = 0.530$, $p = 0.595$) and no

significant main effect of TIME (F(1,14) = 4.080, p = 0.063). The main effect of SOUND showed a statistically significant difference in reaction time between trials (F(2,28) = 189.894, p < 0.001).

Post hoc testing showed that there was a significant *StartReact* effect (difference in VART vs. VSRT) before (t(14) = 4.530, p < 0.001, *d* = 1.053) and after (t(14) = 3.533, p = 0.003, *d* = 0.601) the intervention. However, *StartReact* before did not differ from *StartReact* after (t(14) = -0.670, p = 0.514; Figure 3.5B).

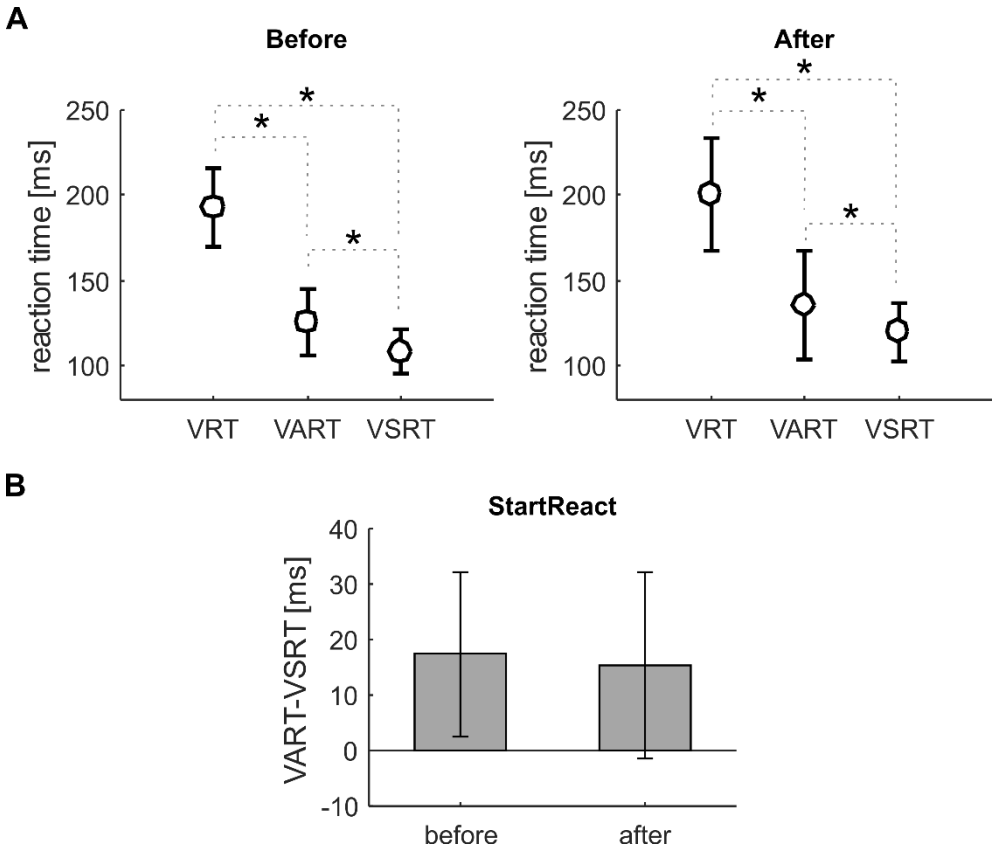

Figure 3.5: *StartReact group results.* **(A)** Mean visual reaction time (VRT), visual-auditory reaction time (VART) and visual-startle reaction time (VSRT) before (left) and 10 minutes after (right) the intervention. Asterisks indicate significant differences (p<0.05). Error bars indicate standard deviations. **(B)** StartReact effect (difference in VART vs. VSRT) before and after the intervention. Error bars indicate standard deviations.

Experiment in Monkey

Non-invasive measurements in human subjects necessarily allow only indirect conclusions about the pathways involved. In this study, we were fortunate to be able to test the paired stimulation protocol also in implanted macaque monkeys, where invasive recordings of spinal volleys could be measured alongside EMG. Figure 3.6 shows the results from these monkey experiments.

The core result observed in humans was largely replicated in both monkeys. Following pairing of M1 stimulation with loud sound, the EMG response of the 1DI muscle was elevated immediately and remained significantly higher than baseline for more than 15 minutes (Fig. 3.6A) in monkey O. In monkey V there was also a rise in the EMG response, although this was delayed after the stimulus pairing. The increases at 15 and 20 minutes after the intervention were significant at the individual level, but failed to pass the correction for multiple comparisons, so this should be considered a trend rather than a definitive effect (Fig. 3.6B). These increases were however not accompanied by comparable increases in the size of descending volleys at the spinal level. In monkey O, the D wave volley was initially suppressed, but recovered to its baseline amplitude by 15 minutes after the stimulus pairing. Both I1 and I2 volleys were significantly suppressed at all time points after the intervention; the I3 volley was also suppressed, although this did not develop immediately, but showed a significant reduction only after 10 minutes (Fig. 3.6C). In monkey V, both D and I waves were significantly reduced for almost all time points measured (Fig. 3.6D).

In monkey V, we also stimulated the PT directly during each assessment block. We would expect the extent of activation to remain constant, since this stimulation of the corticospinal tract in the medulla acts on axons distant from the initial segment, and hence is unaffected by cortical excitability. In fact, there was a steady decline in the size of this direct volley after the intervention (Fig. 3.6E). It is possible that this reflects a change in the recording conditions, for example a progressive accumulation of fluid around the spinal recording electrode which would shunt signals and reduce their amplitude. However, it was notable that the size of these (presumed artifactual) changes were comparable to those seen in the D wave from M1. The I waves from M1 showed an earlier and greater decrease than the D wave following PT stimulation, suggesting that there was a small genuine suppression of corticospinal output.

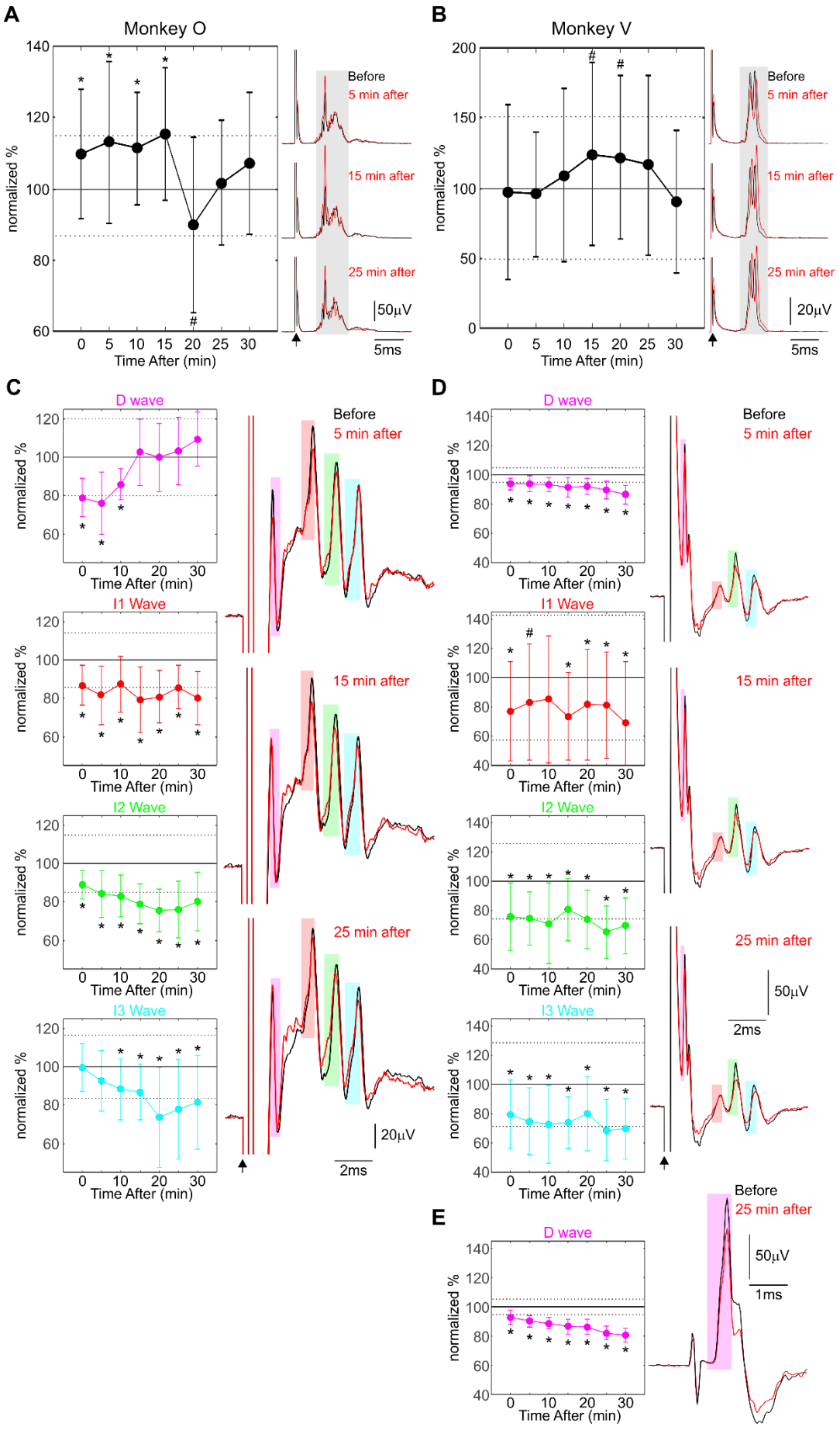

Figure 3.6. *Measurements in monkey.* **(A)** change in MEP in the 1DI muscle after M1

stimulation as a percentage of baseline, at different time points after paired M1-LAS stimulation, for monkey O. Example traces are illustrated on the right in red, with the baseline response superimposed on all in black for comparison. Grey shading indicates the region used to measure the MEP AUC. **(B)** as (A), but for monkey V. **(C)** changes in the amplitude of D, I1, I2 and I3 volleys measured in the spinal cord following M1 stimulation, at the same time points after paired M1-LAS stimulation as in (A), for monkey O. Example volleys are shown on the right in red, with the baseline measurement overlain in black for comparison. Colored shading highlights the regions used to measure the amplitude of each volley, with the same color used to plot the graphs on the left. **(D)** as (C), but for monkey V. **(E)** changed in D wave volley elicited by direct PT stimulation at the medulla, in monkey V, after paired M1-LAS stimulation. Plot on the right shows an example trace, from 25 minutes after paired stimulation (red), with the baseline overlain for comparison (black). Shaded region indicates the latencies over which the volley amplitude was measured. Note the different time base compared with (C,D). In all plots of responses compared to baseline, * indicates a significant change ($P<0.05$, t test) which passed the Benjamini-Hochberg correction for multiple comparisons; # indicates a change with $P<0.05$ which did not pass this correction, and hence must be considered a trend. Error bars indicate standard deviation; horizontal black lines mark 100% corresponding to the baseline, with the dotted lines indicating the standard deviation of this baseline measurement. Points are the average of 20 sweeps for monkey O, and 50 sweeps for monkey V, except for baseline measures which were compiled from 40 and 100 sweeps respectively.

None of the volley recordings, from either animal, were consistent with long-term potentiation of corticospinal output, suggesting that the increase in EMG responses likely had a sub-cortical origin.

Further insight came from examination of the EMG responses to the PT stimulation in monkey V, which are shown in Fig. 3.7. Measurement of the AUC for this response indicated a significant facilitation, which lasted until 30 minutes after the intervention (Fig. 3.7A). However, the averaged traces of the stimulus-evoked activity revealed more complexity. The earliest part of the response seemed to show little change, whereas after the intervention there was a substantial facilitation in the later response component (Fig. 3.7B). This was further quantified by measuring the AUC for each part separately. The early component did not change significantly after the intervention (Fig. 3.7C), but there were robust and strong increases in the later component (Fig. 3.7D).

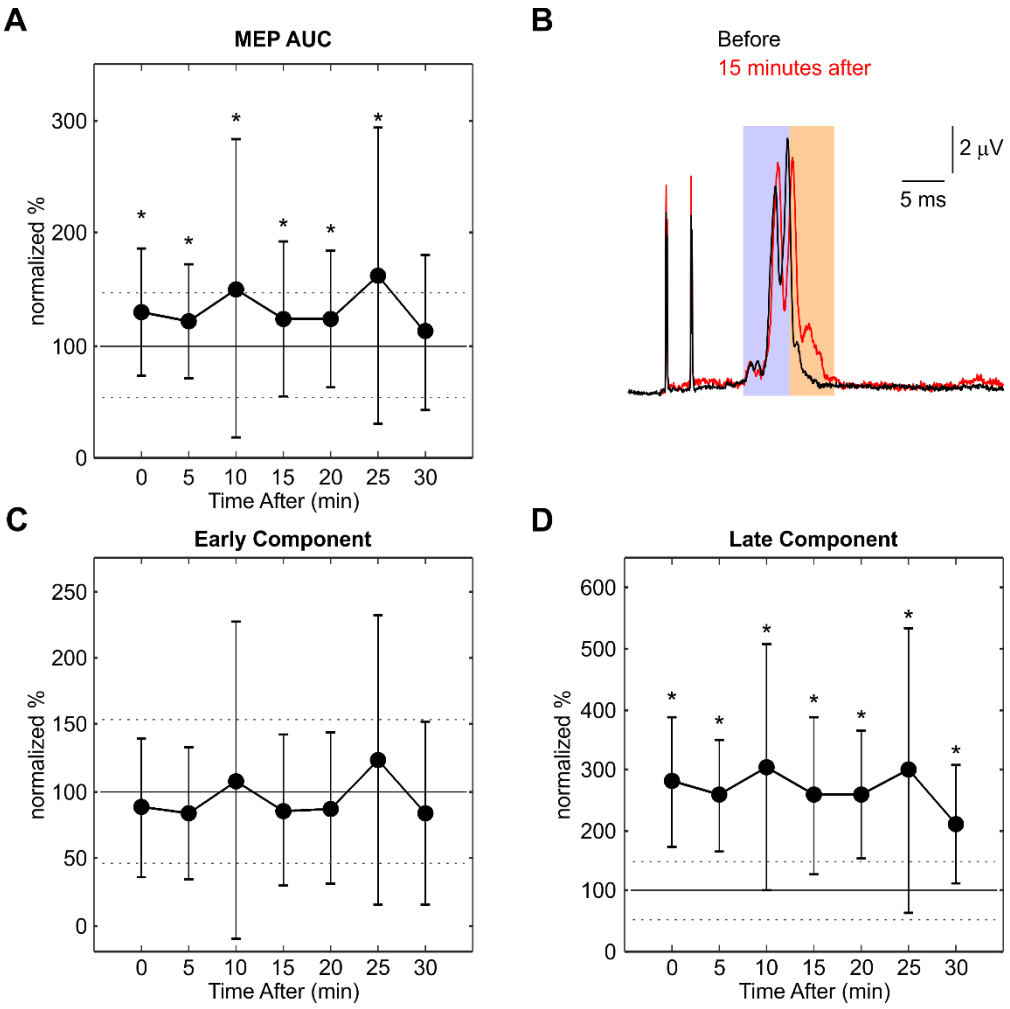

Figure 3.7. *MEP responses to direct PT stimulation in monkey V.* **(A)** change in AUC of MEP in the 1DI muscle as a percentage of baseline, as a function of time after paired M1-LAS stimulation. **(B)** example response, at 15 minute time point (red), with the baseline response overlain in black for comparison. **(C)** as (A), but for the early response component shaded purple in (B). **(D)** for the late component, shaded orange in (B). In (A,C,D), * indicates a significant change relative to baseline ($P<0.05$, t test corrected for multiple comparisons by the Benjamini-Hochberg procedure). Error bars indicate standard deviation; horizontal black lines mark 100% corresponding to the baseline, with the dotted lines indicating the standard deviation of this baseline measurement. Points are the average of 50 sweeps, except for baseline measures which were compiled from 100 sweeps.

In setting up for this experiment, we found that a single stimulus to the pyramidal tract produced only a weak response in the 1DI muscle with the monkey at rest, and therefore chose to deliver a train of two stimuli. It is well known that stimulus trains can enhance transmission over multiple synapses by temporal facilitation (Riddle et al., 2009). The finding in monkey that the earliest part of the muscle response to PT stimulation did not change after the intervention is comparable to the finding in humans with CMEPs, where only a single stimulus was used. The changes in the later, presumed oligosynaptic parts of the PT response agree with a sub-cortical basis for the plasticity.

Discussion

The current study demonstrated that repeated exposure to paired LAS and TMS generates a MEP facilitation which could last for at least 20 minutes after the stimulus pairing (Fig. 3.3A). This facilitation was not observed in either control group (Experiment 2 & 3; Fig. 3.3B & C), indicating that stimulus pairing was required. Interestingly, there was no increase in MEP amplitude immediately after the end of the pairing; it took time to develop; this was also seen in one of the monkeys (Fig. 3.6B). A similar delayed enhancement of responses has been reported using other plasticity protocols (Taylor and Martin, 2009), with some evidence that delay may depend on age (Fujiyama et al., 2014).

Timing of stimuli in a PAS protocol is critical for facilitating plastic change (Stefan et al., 2002, Mrachacz-Kersting et al., 2007, Murakami et al., 2008, Kumpulainen et al., 2012). Here we used a 50 ms ISI between the onset of the auditory stimulus and M1 stimulus. Paradoxically, we showed that MEPs were *suppressed* during paired stimulation (Fig. 3.3A), even though there was subsequent long-term *potentiation*. Loud sounds facilitate the H reflex at ISIs of 50 ms and above (Rossignol and Jones, 1976, Rudell and Eberle, 1985, Nakashima et al., 1994, Delwaide and Schepens, 1995), indicating an increase in motoneuronal excitability. The suppression of TMS-evoked MEPs at an interval of 50 ms, as reported previously by others and also observed here (Furubayashi et al., 2000, Tazoe and Perez, 2017, Kuhn et al., 2004) must therefore reflect a cortical suppression superimposed on a smaller spinal facilitation (Germann and Baker, 2021). The cortical suppression most likely results from activation of the reticular formation following the loud sound (Davis et al., 1982, Hammond, 1973, Leitner et

al., 1980, Fisher et al., 2012), and subsequent activation of cortical interneurons via reticulo-thalamic projections (Pare et al., 1988, Steriade et al., 1988).

Changes in MEP size may be influenced by effects at many possible levels of the motor system (see schematic of Figure 3.8). To identify the likely sites of plastic changes, we employed the same PAS protocol used in Experiment 1 to measure changes in CMEPs and the StartReact effect in humans, and also made direct measurements of descending volleys in monkey.

One limitation is that recordings from monkeys were made using different muscles (FDS, 1DI) compared to the biceps muscle in our experiments in humans. Ethically it is not possible to justify using two monkeys for just this study. The monkeys were already being used in separate experiments and had implanted EMG electrodes in hand and forearm, but not biceps, muscles. Despite this difference, we believe that the invasive recordings still add significantly to our interpretations, especially since the RST is known to project to motoneurons innervating both distal and proximal muscles in the upper limb (Davidson and Buford, 2004, Riddle et al., 2009, Davidson and Buford, 2006).

A single cortical stimulus evokes multiple descending volleys to the spinal cord: the initial direct (D) activation of the CST is followed by subsequent indirect (I) waves (Patton and Amassian, 1954, Rosenthal et al., 1967, Stoney et al., 1968, Jankowska et al., 1975). The size of both D and I waves is affected by the level of cortical excitability (Baker et al., 1995, Di Lazzaro et al., 1998b). By contrast, because stimulation at the cervicomedullary junction activates the corticospinal tract at the brainstem level (Ugawa et al., 1991, Maertens de Noordhout et al., 1992), the size of the descending volley should be unaffected by the state of the cortex. In the biceps muscle, this stimulation can evoke responses consistent with both monosynaptic (Fig. 3.8c) (Petersen et al., 2002) and oligosynaptic transmission (Fig. 3.8de) (Nakajima et al., 2017).

We found no change in CMEP amplitude after paired stimulation compared to baseline (Fig. 3.4). Although CMEPs were measured at only one time point (10 minutes after the intervention), this was a time at which MEPs were significantly facilitated in Experiment 1 (Fig. 3.3A). The lack of changes in CMEPs therefore suggests that the plastic changes in MEPs were not mediated at corticospinal synapses (Fig. 3.8cd). Consistent with this, there were no changes in the earliest component of EMG responses following PT stimulation in monkey (Fig. 3.7).

The reticulospinal tract is another possible site for the plasticity, especially since reticular formation (RF) neurons are known to be powerfully activated by loud sounds (Lingenhohl and Friauf, 1992) and play a pivotal role in the startle reflex (Davis et al., 1982). The RST makes both monosynaptic and disynaptic connections with upper limb motoneurons (Fig. 3.8ge and 3.8h (Riddle et al., 2009)). StartReact may reflect the involuntary release of a planned movement by the RST (Valls-Sole et al., 1999a, Rothwell, 2006, Baker and Perez, 2017), as the StartReact effect remains intact or is enhanced in patients with damaged CST (Honeycutt and Perreault, 2012, Nonnekes et al., 2014b, Choudhury et al., 2019).

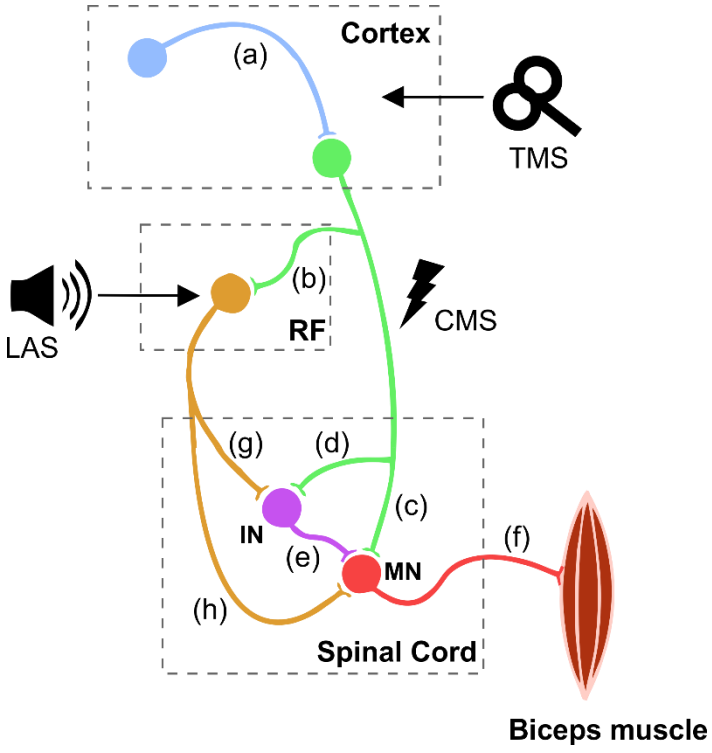

Figure 3.8: *Schematic showing simplified pathways*. RF, Reticular Formation. IN, spinal cord interneuron. MN, motoneuron. TMS, transcranial magnetic stimulation. CMS, cervicomedullary stimulation. LAS, loud acoustic stimulus. (a) Intracortical connections, (b) corticoreticular connections, (c) cortico-motoneuronal synapses, (d) corticospinal projections to interneurons, (e) interneuron projections to motoneurons, (f) motoneuron projection to muscle, (g) reticulospinal projections to interneurons, (h) reticulospinal projections to motoneurons.

In Experiment 5, we observed a notable StartReact effect (difference in VART vs. VSRT, Fig. 3.5A) both before and 10 minutes after paired associative stimulation. However, the size of this difference did not change between the two time points (Fig. 3.5B). If the plasticity increases in MEPs were underpinned by changes in reticulospinal connections (Fig. 3.8ge and 3.8h), we would expect to see a change in the StartReact effect, as we recently reported using a different plasticity protocol designed to affect the RST (Germann and Baker, 2021). Since such changes did not occur, we conclude the increased MEP size after paired stimulation was unlikely to be generated by modification of reticulospinal synapses.

A further way in which the MEP amplitude could show long-term changes is if there were increases in the excitability of either motoneurons or interneurons in the spinal cord, as this would lead to larger responses to the same synaptic input. However, such changes would also produce increases in CMEPs and the StartReact effect, which were not seen. They should also produce parallel changes in all parts of responses to PT stimulation in monkey, rather than the selective increase in late components which was seen. We therefore rule out post-synaptic excitability changes as contributing to the plasticity which we have observed.

One explanation for our findings in humans is that there was potentiation of intracortical connections (Fig. 3.8a), which would lead to increased I wave volleys following TMS. Indeed, many previous studies have used a situation where MEPs change, but CMEPs do not, to argue for a cortical basis for the observed effect. However, at the 50 ms inter-stimulus interval used, the cortex was suppressed, meaning that during the paired stimulation MEPs were actually reduced in amplitude (Fig. 3.2A, 3.3A), as previously reported by other investigators (Furubayashi et al., 2000, Tazoe and Perez, 2017, Kuhn et al., 2004). It seems unlikely that a conditioning stimulus which reduces cortical excitability should lead to long term potentiation of intracortical circuits, and indeed the direct measurements of volleys in monkey revealed long term depression (Fig. 3.6).

One remaining substrate for the observed plasticity, which could be consistent with our experimental findings, is the corticoreticular connection (Fig. 3.8b). It is known that M1 stimulation can powerfully activate corticoreticular fibers (Fisher et al., 2012, Fisher et al., 2021), which form an extensive divergent and convergent network linking both primary and pre-motor areas bilaterally to the reticular nuclei (Fisher et al., 2021, Fregosi et al., 2017, Darling et al., 2018). If the LAS increased the excitability of reticulospinal cells, they would be more likely to respond to corticoreticular inputs, generating reliable post-synaptic spiking just

after the corticoreticular pre-synaptic input, and thereby fulfilling the requirements for long-term potentiation by mechanisms of spike-timing dependent plasticity (Markram et al., 1997, Bi and Poo, 2001). We previously demonstrated that stimulation of the corticospinal tract can generate a reticulospinal volley by trans-synaptic activation of the reticular formation (Fisher et al., 2015); many corticoreticular axons are collaterals of corticospinal fibers (Keizer and Kuypers, 1989). Plastic changes at corticoreticular synapses would therefore lead to an increased reticulospinal output after M1 stimulation. It is known that in primate cervical spinal cord, both motoneurons (Riddle et al., 2009) and interneurons (Riddle and Baker, 2010) receive extensive convergence from corticospinal and reticulospinal tracts (as is shown schematically in Fig. 3.8). Enhanced reticulospinal inputs would therefore very likely lead to larger MEPs. The change in late, but not early, components of the MEP following PT stimulation in monkey is also consistent with this site for the plasticity, as is the lack of enhancement of corticospinal volleys.

Importantly it appears that the method described here acts on a different circuit from another paradigm which we recently introduced, also with the aim of targeting sub-cortical systems (Foysal et al., 2016, Germann and Baker, 2021). That paradigm paired loud auditory click sounds with electrical stimulation over a muscle (to activate low threshold afferents), and generated plastic changes in the StartReact effect, but not in MEPs elicited (as here) with the TMS coil oriented to induce current in a posterior-anterior direction. By contrast, with the present protocol, we generated changes in MEPs, but not in the StartReact effect. Stimulus-evoked plasticity is of great interest because it may allow the strengthening of residual motor pathways after damage (e.g. following stroke), and thereby boost functional recovery. Several approaches already exist to target the corticospinal system, but sub-cortical systems such as spinal cord interneurons and the reticulospinal tract might also play an important role in recovery (Mazevet et al., 2003, Tohyama et al., 2017, Zaaimi et al., 2012, Zaaimi et al., 2018). Exploiting these richly diverse systems to improve function will likely require an equally diverse range of non-invasive stimulation protocols.

CHAPTER IV – EVIDENCE FOR SUBCORTICAL PLASTICITY AFTER PAIRED STIMULATION FROM A WEARABLE DEVICE

The experiments described in this chapter were performed by me. They were supported by Prof Stuart Baker, who designed the wearable devices. I performed all data analysis.

Abstract

Existing non-invasive stimulation protocols can generate plasticity in the motor cortex and its corticospinal projections; techniques for inducing plasticity in sub-cortical circuits and alternative descending pathways such as the reticulospinal tract are less well developed. One possible approach developed by this laboratory pairs electrical muscle stimulation with auditory clicks, using a wearable device to deliver stimuli during normal daily activities. In this study, we applied a variety of electrophysiological assessments to male and female healthy human volunteers during a morning and evening laboratory visit. In the intervening time (~6 hours), subjects wore the stimulation device, receiving three different protocols, in which clicks and stimulation of the biceps muscle were paired at either low or high rate, or delivered at random. Paired stimulation: 1) increased the extent of reaction time shortening by a loud sound (the StartReact effect); 2) decreased the suppression of responses to transcranial magnetic brain stimulation (TMS) following a loud sound; 3) enhanced muscle responses elicited by a TMS coil oriented to induce anterior-posterior (AP) current, but not posterior-anterior (PA) current in the brain. These measurements have all been suggested to be sensitive to sub-cortical, possibly reticulospinal, activity. Changes were similar for either of the two paired stimulus rates tested, but absent after unpaired (control) stimulation. Taken together, these results suggest that pairing clicks and muscle stimulation for long periods does indeed induce plasticity in sub-cortical systems such as the reticulospinal tract.

Introduction

In primates such as humans, the corticospinal tract (CST) is the dominant descending pathway for motor control; other pathways play distinctive but lesser roles. The reticulospinal tract (RST) projects to motoneurons innervating both distal and proximal muscles in the upper limb (Davidson and Buford, 2004, Riddle et al., 2009, Davidson and Buford, 2006). After CST lesions, RST connections strengthen, partially forming the substrate for recovery (Zaaimi et al., 2012). The near-absence of a rubrospinal tract in humans (Nathan and Smith, 1955, Onodera and Hicks, 2010) means that the RST may be the only major intact descending motor pathway following CST damage. It would be beneficial to develop ways of modifying RST connections to enhance functional recovery.

Neuronal connections can be strengthened if a postsynaptic neuron is activated consistently after a presynaptic input (spike timing-dependent plasticity, STDP, Markram et al., 1997). Plasticity can be induced non-invasively by giving two appropriately-timed stimuli that converge on a common target circuit (e.g. Stefan et al., 2000, Ridding and Uy, 2003). Reticulospinal neurons receive extensive afferent (Leiras et al., 2010), auditory (Davis et al., 1982, Hammond, 1973, Leitner et al., 1980, Irvine and Jackson, 1983) and vestibular (Ladpli and Brodal, 1968, Peterson and Abzug, 1975) input. In monkey, loud auditory clicks produce robust RST activation (Fisher et al., 2012), probably via a mixture of auditory and vestibular pathways. We previously developed a wearable device to deliver clicks paired with electrical stimulation of the biceps muscle while a subject goes about their normal daily activities (Foysal et al., 2016). In healthy subjects, this led to plastic changes in the long-latency stretch reflex (LLSR). Potentiation or depression occurred depending on stimulus timing, consistent with STDP at the level of the brainstem. Applying this protocol in stroke survivors produced a small but significant improvement in upper limb function (Choudhury et al., 2020).

Unlike the CST, non-invasive methods to measure RST function in humans are limited. Two promising approaches use loud sound stimuli, which are of interest because they are known to elicit a startle response via the RST (Davis et al., 1982). Firstly, loud sounds can reduce the reaction time to a visual cue (the *StartReact* effect). This may reflect involuntary release of a planned movement by RST (Valls-Sole et al., 1999a, Rothwell, 2006, Baker and Perez, 2017), as the StartReact effect remains intact in patients with damaged CST (Honeycutt and Perreault, 2012, Nonnekes et al., 2014b, Choudhury et al., 2019).

Secondly, loud sounds can transiently modulate motor responses to transcranial magnetic stimulation (TMS) and transcranial electrical stimulation (Furubayashi et al., 2000). The different effects on these two stimulus modalities points to both a cortical inhibition and sub-cortical facilitation; the latter may have a reticulospinal component.

TMS stimulates cells within the motor cortex both directly and indirectly (trans-synaptically), leading to multiple descending volleys to the spinal cord (Patton and Amassian, 1954, Rothwell et al., 1991). TMS over the motor cortex can activate reticular neurons trans-synaptically (Fisher et al., 2012). Although all activation involves the corticospinal tract, the available evidence is that more indirect, subcortical pathways contribute to MEPs elicited following late I-waves (Cirillo and Perez, 2015, Cirillo et al., 2016, Long et al., 2017). Several studies suggest that different neural elements in the cortex can be activated preferentially by changing the direction of induced currents (Werhahn et al., 1994, Ni et al., 2011, Sakai et al., 1997). Responses to anterio-posterior (AP) current may reflect more indirect cortico-muscular transmission than posterior-anterior (PA) current (Cirillo and Perez, 2015, Federico and Perez, 2017). Comparison of these responses might allow isolation of sub-cortical effects. As a way of controlling for spinal excitability, cervicomedullary motor evoked potentials (CMEP) can be measured, as they are thought predominantly to reflect direct effects from the CST (McNeil et al., 2013).

Here, we tested these various assessments before and after a period of paired stimulation with the wearable device. If RST is the substrate for the induced plastic changes, then we predict each of these assessments to change in a manner consistent with this hypothesis. Namely increased RST outflow should lead to an increased StartReact effect, a reduction in MEP suppression in response to a loud sound and an increase in AP elicited MEP size due to subcortical elements being more readily recruited.

Methods

Subjects

In total, 65 healthy volunteers (48 females and 17 males; 18-35 years old, right-handed by self-report) participated in the study. Four subjects took part in two experiments, one subject took part in three experiments. If participants took part in several stimulation paradigms, each session was separated by at least seven days. All subjects gave written informed consent to

the experimental procedures, which was approved by the ethics committee of the Faculty of Medical Sciences at Newcastle University. The study was performed in accordance with the guidelines established in the Declaration of Helsinki, except that the study was not pre-registered in a database.

Experimental Design

In total, five experiments were carried out, which included various assessments (Table 4.1). The experimental paradigm (Figure 4.1A) required subjects to come to the laboratory at around 9am, where baseline assessments were carried out. They were then fitted with a wearable electronic device to deliver paired electrical and auditory stimuli, and the subject left and continued their normal daily activities. In the evening, the subject returned, the device was removed, and the assessments repeated. The order of the various assessments was randomized for a given subject, but kept the same for the morning and evening recordings in that person. The two assessment sessions were at least 6 hours apart. For a summary of experiments, assessments and participant numbers, see Table 4.1.

Experiment	Intervention	N	Sex (f)	Assessments
1	Paired	15	13	StartReact
				Loud sound + TMS
		12	10	Loud sound + CMEP
2	Double	14	9	StartReact
				Loud sound + TMS
		11	8	Loud sound + CMEP
3	Control	15	11	StartReact
				Loud sound + TMS
		10	6	Loud sound + CMEP
4	Paired	15	10	Coil orientations
5	Control	12	8	Coil orientations

Table 4.1: *Summary of experiments performed.* Five separate experiments (Experiment 1-5) were conducted with 3 different device protocols (Intervention: paired, double or control). In one experiment, several assessments could be performed on the same subjects. A sub-set of subjects participated in assessments involving CMEPs. A few subjects participated in more than one experiment (see Methods). Experiments were carried out in the following order across the study: Experiment 1, Experiment 3, Experiment 2, Experiment 4, Experiment 5.

Wearable Device

The wearable device (Figure 4.1B) was the same as used in our previous work (Choudhury et al., 2020). It comprised a plastic box containing an electrical stimulator and audio amplifier, powered by an internal battery which could be recharged via a standard microUSB port. The wearable device generated constant-current electrical stimulation to the right biceps muscle through surface electrodes (220 V compliance, 0.15 ms pulse width). A knob on the device allowed adjustment of the stimulus intensity, which was set to be just below the motor threshold (defined as a visible muscle twitch). Auditory stimuli were generated by delivering a 0.1 ms wide, 12 V square excitation pulse into a miniature earpiece; this produced a brief click with an intensity of 110 dB SPL. The earpiece was placed in the left ear (contralateral to the stimulation of the right biceps). Three different interventions were tested:

For the *paired stimulation group* (Figure 4.1C, top row), stimuli were delivered with an inter-trial interval of 1250 - 1750 ms (chosen at random from a uniform distribution); the delay between electrical stimulation and auditory click was 10 ms. This inter-stimulus interval was chosen so that the afferent volley should arrive at the brainstem just prior to RST cell activation by the click (as in our previous work, Foysal et al., 2016).

For the *double stimulation group* (Figure 4.1C, middle row), the stimulus frequency was doubled (interval randomly chosen 575 – 825 ms, uniform distribution), while the interval between biceps stimulus and click was kept at 10 ms as in the paired stimulation group. This allowed us to test whether increasing the stimulus rate could enhance the size of plastic changes.

For the *control stimulation group* (Figure 4.1C, bottom row), the click and shock occurred independently at random. The time between successive clicks, and between successive biceps stimuli, followed the same distribution as in the paired stimulation group.

Participants were not told which group they were in. However, the experimenter was not blinded to the intervention.

Based on calculations given in Foysal et al. (2016) and Rosengren et al. (2010), the clicks produced by the device exposed the subjects to sound intensities of 68 dB L_{Aeq} for the paired stimulation group, and 71 dB L_{Aeq} for the double stimulation group (assuming device usage for at most 8 hours). This is well below accepted hearing safety limits for noise exposure of 85 dB

L_{Aeq} (The Stationery Office, 2005); the device could potentially be used every day at these levels without concern.

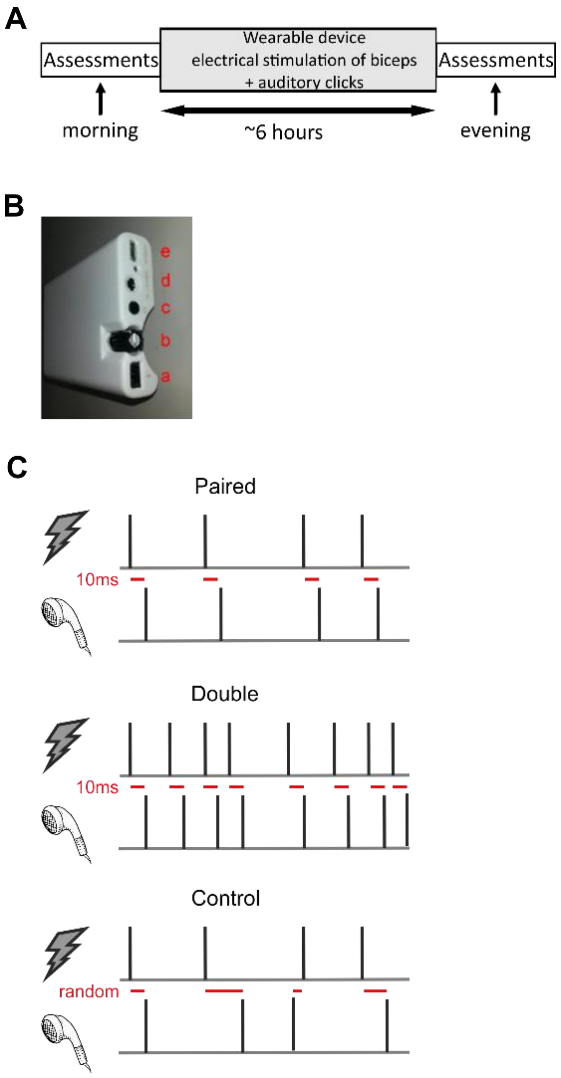

Figure 4.1: *Wearable device and schematic diagram showing the different stimulus conditions.* **(A)** General experimental protocol. **(B)** Photograph of the wearable device; a, stimulus output port; b, stimulus intensity adjustment; c, audio output; d, on/charge switch; e, microUSB charge connection. **(C)** The three different stimulus conditions implemented by the wearable device. *Top:* paired stimulation group, with 10 ms interstimulus interval between clicks and biceps electrical stimuli. *Middle:* double stimulation group, with 10 ms interstimulus interval, but double the stimulation frequency as the other groups. *Bottom:* unpaired control stimulation group, with random interstimulus intervals.

Electromyography (EMG) recordings

EMG was recorded through surface electrodes (disposable Kendall H59P Electrodes, Covidien, Mansfield, Massachusetts, USA) secured on the skin over the belly of the biceps or the right first dorsal interosseous (1DI) muscle. Because the electrodes over the right biceps muscle were used for both EMG recording and for wearable stimulation, they were kept in place for the whole day, ensuring consistency between the morning and evening sessions. For the right 1DI and the left biceps, the location was marked after the morning session with a UV fluorescent marker pen, allowing fresh electrodes to be replaced in the same location in the evening. EMG signals were amplified and filtered (30-2000 Hz, gain 1000) with a bioamplifier (D360 Amplifier, Digitimer, Welwyn Garden City, UK), digitized at a sampling rate of 5kHz (CED Micro 1401 with Spike2 software, Cambridge Electronic Design, Cambridge, UK) and stored on a computer for off-line analysis. Where necessary for a given assessment (see below), the level of biceps EMG activity was displayed continuously on a computer screen via series of colored bars, allowing subjects to maintain a constant isometric contraction.

Transcranial Magnetic Stimulation (TMS)

Transcranial magnetic stimuli were applied using a figure-of-eight coil through a Magstim 200^2 magnetic stimulator (Magstim, Whitland, UK) with a monophasic current waveform. We determined the optimal position for eliciting a motor evoked potential (MEP) in the biceps muscle (hotspot) by moving the coil, with the handle pointing backward and 45° from the midline, in small steps along the arm representation of M1. The hotspot was defined as the region where the largest MEP in the biceps muscle could be evoked with the minimum intensity (Rothwell et al., 1999). Unless stated otherwise, the magnetic coil was held in this orientation over the left hemisphere for subsequent measurements, to induce currents in the brain that flowed perpendicular to the presumed line of the central sulcus in a posterior—anterior (PA) direction. Active motor threshold (AMT) was defined as the stimulator intensity sufficient to elicit a MEP with amplitude >200 µV in at least 5 out of 10 consecutive stimuli, in the biceps contralateral to the stimulus with an active contraction of 10-20% maximal voluntary contraction (MVC).

A Polaris Vicra camera (Northern Digital Inc., Waterloo, Ontario, Canada) tracked both coil and head position, allowing the site of stimulation to be marked using the Brainsight neuronavigation system (Rogue Research Inc., Montréal, Quebec, Canada). This ensured a

stable coil location throughout the experiment, and allowed us to return to the same site in the evening as had been used earlier in the day.

Cervicomedullary Junction Stimulation

CMEPs were elicited via electrical stimulation of the corticospinal tract at brainstem level. Adhesive surface electrodes (Neuroline 720 00-S/25, Ambu, Copenhagen, Denmark) were fixed to the skin over the mastoid processes and current was passed between them (0.1 ms duration, 80–200 mA; model DS7AH, Digitimer Ltd, Welwyn Garden City, UK) with the cathode on the left side. The stimulation intensity was adjusted to elicit a CMEP amplitude of 1mV with an active contraction of 10-20% MVC.

Assessment: StartReact

StartReact was examined using a previously tested paradigm (Baker and Perez, 2017) which measures reaction time from EMG in response to a visual cue (visual reaction time, VRT), a visual plus quiet auditory cue (visual-auditory reaction time, VART), and a visual plus loud auditory cue (visual-startle reaction time, VSRT). The acceleration of reaction time between VART and VSRT is believed to involve the rapid involuntary release of the pre-prepared movement, and to reflect the action of the RST (Valls-Sole et al., 1999a, Rothwell, 2006, Baker and Perez, 2017, Carlsen et al., 2004b, Smith et al., 2019). Some previous studies on StartReact have measured startle responses from the sternocleidomastoid (SCM) muscle, and excluded reaction times measured when this muscle was not activated (Valls-Sole et al., 1999a, Honeycutt et al., 2013, Carlsen et al., 2004b). We and others have previously found that SCM activity is unreliable (Honeycutt et al., 2013, Dean and Baker, 2017, Baker and Perez, 2017), and can be generated both in response to startling and non-startling cues. In this study, we therefore simply included all reaction times measured from the relevant cue, as in our previous publications (Dean and Baker, 2017, Baker and Perez, 2017, Choudhury et al., 2019).

Subjects sat with the right forearm supinated and placed on the table top, and the hand loosely placed around a horizontal handle. A green light-emitting diode (LED) was located ~1 m in front of the subject. Subjects were instructed to grip the handle and push upwards as quickly as possible after the LED illuminated. EMG was recorded from both the 1DI and biceps muscles, and reaction time measured as the time from cue to onset of the EMG burst. Three types of trial were randomly interleaved (20 repeats per condition; inter-trial interval 5-6 s; Figure 4.2A): LED illumination alone (VRT), LED paired with a quiet sound (80dB, 500Hz, 50ms,

VART), LED paired with a loud sound (500 Hz, 50 ms, 120 dB, VSRT). Subjects were initially presented with five consecutive loud sounds, without performing the task, to allow familiarization.

Data were analyzed trial-by-trial using a custom MATLAB program which identified the reaction time as the point where the rectified EMG exceeded the mean + 7 SD of the baseline measured 0-200 ms prior to the stimulus. Every trial was inspected visually, and erroneous activity onset times (caused, for example, by electrical noise artefacts) were manually corrected. This yielded a reaction time distribution for each condition (see Fig. 4.2B).

Assessment: Loud Sound with MEP or cMEP

A paradigm similar to previous studies (Tazoe and Perez, 2017, Furubayashi et al., 2000) was used (Figure 4.2C). Loud (500 Hz, 120 dB SPL) sound stimuli were given 50 ms before a TMS pulse over M1; this elicits a smaller MEP than the same TMS pulse given alone, which is believed to reflect cortical inhibitory processes. Similar sound stimuli were also given 80 ms before electrical stimulation of the cervicomedullary junction; this causes a facilitation of the cMEP compared to that elicited by electrical stimulation alone, which likely arises from subcortical circuits. The two intervals used were selected as these gave the largest suppression and facilitation respectively in a previous detailed examination of these effects (Furubayashi et al., 2000). Sounds were given through two audio speakers located on a table ~1 m in front of the subject. The sound ended at the time of the test stimulus. To avoid stimulus predictability, the inter-trial interval was chosen randomly between 20.5 and 23 s (uniform distribution). At the beginning of the study, five consecutive loud sounds were presented to habituate the startle reflex. During testing, subjects sat with the arm resting on their leg under a table top, and pushed up against the table at 10-20% of MVC. The level of biceps EMG activity was displayed continuously on a computer screen via a series of colored bars, allowing subjects to maintain a constant isometric contraction, which was kept the same across sessions for that subject. The test stimulus intensity was adjusted to elicit a peak-to-peak MEP of 1 mV in the right biceps muscle. Ten test MEPs and 10 conditioned MEPs were measured in each condition, in randomized order. As expected from previous work, at the tested interval of 50ms MEPs were typically suppressed, whereas with the 80ms interval CMEPs were facilitated (see examples in Fig. 4.2D). Some of the CMEP traces showed a small early component (see Fig. 4.2D, small 'shoulder' at the onset of the CMEP responses), with an onset latency which may be consistent with direct stimulation of the spinal motor roots (McNeil et

al., 2013). However, this was small compared to the later component which arose from corticospinal stimulation and trans-synaptic activation of motoneurons. A direct root response would not be expected to modulate (as is the case for the response shown in Fig. 4.2D), so that the presence of this small component would not have materially affected our results.

CMEPs can be uncomfortable for the subject, and several participants withdrew from this part of the study; numbers participating in both CMEP and MEP assessments are given in Table 4.1.

Assessment: MEPs with Different Coil Orientations

By holding a figure-of-eight TMS coil in different orientations, activation can be biased towards different indirect (I) waves (Ziemann and Rothwell, 2000, Sakai et al., 1997). With the coil tangential to the scalp, at an angle of 45° to the midline with the handle pointing laterally and posteriorly, a posterior-anterior (PA) current is induced in the brain, which mainly recruits early I waves. By contrast, in the reverse orientation (handle pointing medial and anterior; anterior-posterior (AP) induced current), predominantly late I waves are recruited. Here, we measured MEPs with different coil orientations to compare changes in direct versus indirect corticospinal pathways. We assessed changes bilaterally, as the cortico-reticulospinal system is known to be bilaterally organized: RST axons project to both sides of the spinal cord (Davidson et al., 2007, Peterson et al., 1975, Davidson and Buford, 2006), and cells within the reticular formation can be stimulated by TMS to M1 over either ipsilateral or contralateral hemispheres (Fisher et al., 2012).

MEPs in the contralateral biceps muscle were measured from both hemispheres in two different coil orientations (Figure 4.2E). As for the measurements of MEPs described above, the figure-of-eight coil was first held to induce a posterior-anterior (PA) current in the brain. The optimal scalp position was located with this orientation, and marked in the Brainsight neuronavigation software. This site was then used for stimulation to induce an anterior-posterior (AP) current in the brain, by rotating the coil so that the handle faced anterior and medial, as the current direction does not significantly influence the position of the hotspot (Arai et al., 2005, Sakai et al., 1997). Within each subject, we randomized the order of hemispheres tested (left vs right), and for each side the order of coil orientations (PA vs AP); the same order was used for the morning and evening assessments. Stimulus intensity was set to 1.1x active motor threshold **(**four separate thresholds were measured, one for each hemisphere and coil orientation), while subjects contracted to 10% MVC. The level of biceps

EMG activity was displayed continuously on a computer screen via a series of colored bars. 20 MEPs were recorded (5 s interstimulus interval) while subjects maintained a constant isometric contraction of 10% MVC. As expected from previous work, the MEP onset latency was slightly later for AP vs PA orientation (see example traces from one subject in Figure 4.2F).

Data Analysis

Data were analyzed using custom scripts written in the MATLAB environment (R2017a, MathWorks). Statistical tests were performed using MATLAB and IBM SPSS Statistics for Windows, version 24 (IBM Corp., Armonk, N.Y., USA).

EMG traces were full-wave rectified and then averaged. MEP amplitude was measured as the area under the curve of this average. Where MEPs were conditioned by loud sound, the amplitude of the conditioned MEP was expressed as a percentage of the unconditioned MEP. The StartReact effect was measured as the difference between the mean VART and VSRT.

For each experiment, individual paired t-tests were used to compare the measurements after wearable device stimulation to the measurements at baseline. In order to compare stimulation groups, one-way analysis of variance (ANOVAs) were performed on the differences (after – before wearable device intervention) for each measurement. Independent t-test were used to compare groups post hoc. Where necessary, the procedure introduced by (Benjamini and Hochberg, 1995) to correct for multiple comparisons was used. Cohen's *d* was used to measure effect size. Monte Carlo methods were performed to determine if the number of subjects showing a certain change were more than expected by chance based on a binomial distribution.

For the assessment which conditioned MEPs with loud sound, a one sample t-test was performed for each group to compare the normalized conditioned MEP amplitude against 100%, to evaluate the effect of conditioning at baseline.

The significance level was set at $p < 0.05$. Descriptive statistics are presented as mean ± standard deviation.

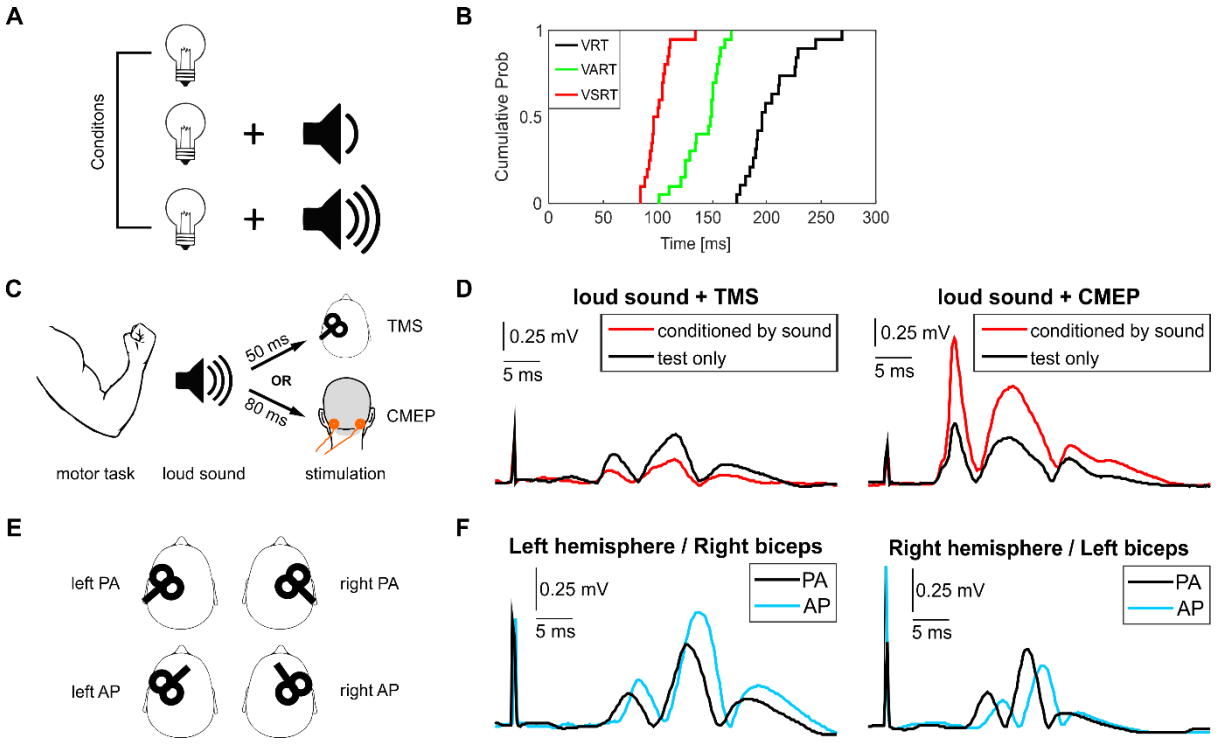

Figure 4.2: *Experimental setup and single subject example for the different assessments.* **(A)** The three conditions tested for the StartReact assessment; visual reaction time (VRT), visual-auditory reaction time (VART) and visual-startle reaction time (VSRT). **(B)** Cumulative distribution of EMG onset times for all trials of a single subject at baseline. **(C)** Setup for the two loud sound assessments. For the loud sound + TMS assessment, sound was delivered 50 ms before TMS pulse. For the loud sound + CMEP assessment, sound was delivered 80 ms before stimulation. **(D)** Average rectified EMG traces at baseline of a single subject for conditioned (red) and unconditioned (black) MEPs for the two assessments. **(E)** Setup for the assessment of MEPs using different coil orientations and lateralities. Stimulation over the left hemisphere elicited MEPs in the right biceps, which received wearable device stimulation; right hemisphere stimulation elicited MEPs in the left biceps, which did not receive wearable device stimulation. **(F)** Average rectified EMG traces at baseline of a single subject for MEPs elicited with PA (black) or AP (blue) coil orientation at baseline from each hemisphere.

Results

StartReact

Figure 4.3 presents results for the StartReact assessment, for both the biceps and 1DI muscles.

In biceps, there was a significantly larger StartReact effect after paired ($p= 0.004$) and double ($p<0.001$) stimulation, but no difference after unpaired ($p= 0.760$) stimulation (Fig. 4.3Aa). The difference in the StartReact effect after wearable device stimulation compared to baseline (Fig. 4.3Ab) was significantly different for the three stimulation groups ($F(2,41)=5.233$, $p=0.009$, partial $\eta2=0.203$). Post hoc t-tests revealed that the paired and the double stimulation groups showed a significantly bigger difference in the StartReact effect compared to the control group (paired group $t(28)=-2.445$, $p=0.021$, $d= -0.893$; double group $t(27)=-3.160$, $p=0.004$, $d=-1.175$), but that there was no difference between the paired and the double stimulation group ($t(27)=0.673$, $p=0.507$).

The analysis presented so far shows average effects across all subjects tested, which is appropriate for statistical analysis. However, it is known that many plasticity protocols have variable effects across subjects (Cheeran et al., 2008, Wiethoff et al., 2014). Similar to our previous publications (Foysal and Baker, 2019, Foysal et al., 2016), Figure 4.3Ac presents the fraction of subjects in which the StartReact effect increased or decreased, with the aim of providing information about the consistency of the effect. There was an increase in the StartReact effect in more subjects than expected by chance for the paired (13/15; $p<0.001$, binomial test) and the double (12/14; $p=0.001$) but not the control (7/15; $p=0.992$) groups (Fig. 4.3Ac).

To respond to the cues, participants had to tighten their grip around the handle and push up against it. It was therefore possible to record a response in the 1DI muscle, as well as in biceps. Figure 4.3B shows results for StartReact measured in this muscle, which is of interest as it did not receive any wearable device stimulation. There was no significant increase in the StartReact effect in any of the groups after wearable device stimulation (paired group $p=0.179$; double group $p=0.364$; control group $p= 0.681$; Fig. 4.3Ba), and no effect of stimulation group on StartReact difference (Fig. 4.3Bb, $F(2,41)=0.729$, $p=0.489$, partial $\eta2=0.034$). However a majority of subjects did show an increased StartReact effect after paired (10/15) and double (11/14) stimulation, but not unpaired (7/15) stimulation (Fig.

4.3Bc). This was significantly higher than chance only for the double stimulation group (p=0.012), but not for the paired (p=0.110) or the control (p=0.598) group.

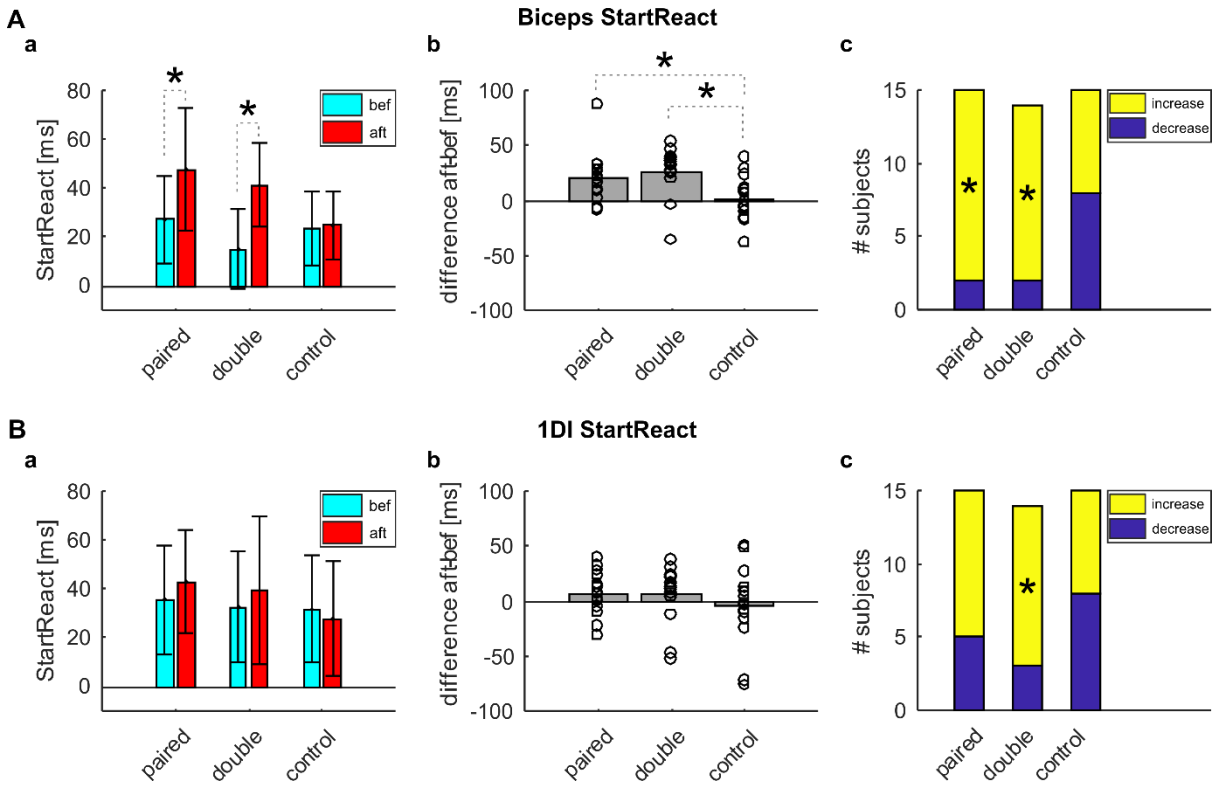

Figure 4.3: *Group results for the StartReact assessment.* **(A)** Results for the biceps muscle (paired n=15; double n=14; control n=15). *a:* StartReact effect (difference between VART and VSRT) before (cyan) and after (red) wearable device stimulation. Coloured bars represent group means; error bars indicate standard deviations. Asterisks indicate significant differences. *b:* Difference in StartReact effect between before and after wearable device stimulation. A positive difference indicates a more pronounced StartReact effect after wearable device stimulation. Bars represent group means; circles show single subject values. *c:* Number of subjects showing an increase (yellow) or decrease (blue) in StartReact after wearable device stimulation. Asterisks indicate proportions significantly different from the 50% expected by chance. **(B)** Results for the 1DI muscle, in the same format as (A).

MEPs Conditioned by Loud Sounds

Figure 4.4A shows the results when MEPs elicited by TMS were conditioned by a loud sound beginning 50 ms before the magnetic stimulus. As expected from previous studies (Furubayashi et al., 2000, Tazoe and Perez, 2017), at baseline MEPs were significantly suppressed in all three groups (cyan bars below grey 100% line in Fig. 4.4Aa; one sample t-test paired group p=0.001; double group p<0.001; control group p=0.004). For both the paired and the double stimulation group, conditioned MEPs were significantly less suppressed after wearable device stimulation (red bars compared with cyan bars; paired group p=0.009; double group p<0.001). On the other hand, the control stimulation group, which received unpaired stimuli, did not show any significant difference after wearing the device (p=0.993).

Figure 4.4Ab plots the difference in MEP amplitude after compared to before the wearable device intervention for each group; a positive difference here indicates less suppression of the conditioned MEP after wearable device stimulation. A one-way ANOVA showed that the three stimulation groups differed significantly ($F(2,41)=4.044$, $p=0.025$, partial $\eta^2=0.165$). Post hoc t-tests confirmed there was a significantly bigger difference in the double stimulation group compared to the control stimulation group ($t(27)=2.708$, $p=0.012$, $d=1.006$). There was also a larger difference in the paired stimulation group compared to the control, however this just failed to reach significance ($t(28)=2.227$, $p=0.034$, $d=0.815$; threshold for significance $p<0.033$ using Benjamini-Hochberg correction for multiple comparisons). There was no significant difference between the paired and the double stimulation group ($t(27)=-0.128$, $p=0.899$). Significantly more participants showed MEP increases than the 50% expected by chance after paired (11/15; p=0.035, binomial test) and double (13/14; p<0.001) stimulation, but not after unpaired stimulation (8/15; p=0.604) (Fig. 4.4Ac).

Figure 4.4B presents results for conditioning of CMEPs with loud sounds, in the same format as Figure 4.4A. CMEPs were facilitated by a loud sound at 80 ms interval at baseline in all groups (cyan bars above grey 100% line, Fig. 4.4Ba). This facilitation was significant for the paired and control groups, but not the double stimulation group (p=0.024, 0.018 and 0.157 respectively). There was no significant difference after wearable device stimulation compared to baseline in any of the groups (Fig. 4.4Ba, paired group p=0.690; double group p=0.718; control group p=0.476) and the groups did not differ significantly from each other ($F(2,30)=0.423$, $p=0.659$, partial $\eta2=0.027$, Fig. 4.4Bb).

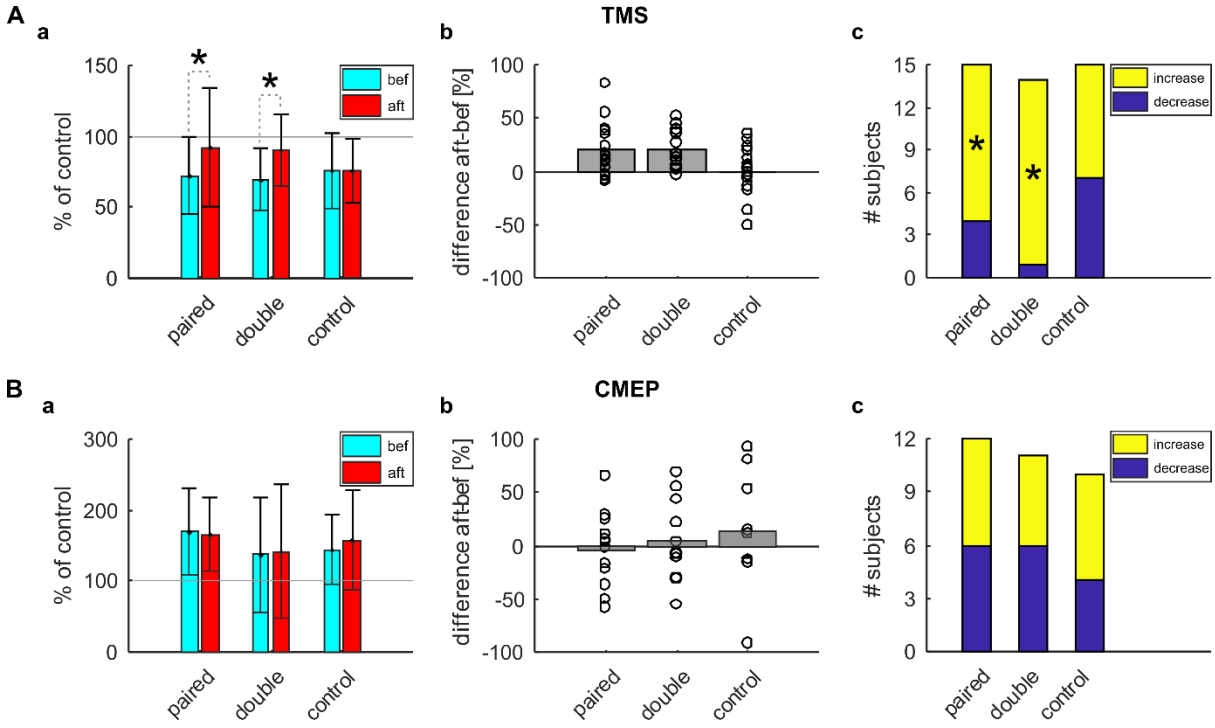

Figure 4.4: *Group results for the conditioning MEPs with loud sounds.* **(A)** Group results for the loud sound + TMS assessment at 50 ms interval (paired n=15; double n=14; control n=15). *a:* Conditioned MEP amplitude normalized to unconditioned amplitude, before (cyan) and after (red) wearable device stimulation for the three different stimulation groups. Coloured bars represent group means; error bars indicate standard deviations across subjects**.** Asterisks indicate significant differences. *b:* Difference in normalized MEP amplitude between before and after wearable device stimulation. A positive difference indicates less suppression of the conditioned MEP after wearable device stimulation. Bars represent group means; circles show single subject values. *c:* Number of subjects showing an increase (yellow) or decrease (blue) in conditioned MEP amplitude after wearable device stimulation. Asterisks indicate proportions significantly different from the 50% expected by chance. **(B)** Group results for the loud sound + Cervicomedullary MEPs (CMEP) assessment at 80 ms interval (paired n=12; double n=11; control n=10). Layout is the same as for (A).

The number of participants showing a positive or negative difference was approximately equal in all groups and not significantly higher than the 50% expected by chance for any group (Fig. 4.4Bc, paired group p=0.783; double group p=0.990; control group p=0.336). Overall our results indicate that there was no change in conditioned CMEP amplitude after any of the wearable device stimulation paradigms.

MEPs Measured Bilaterally with Different Coil Orientations

Figure 4.5 shows the group results for the four combinations of coil orientation and laterality tested.

When the coil was held in the PA orientation over the left hemisphere (contralateral to the arm stimulated by the wearable device), there was no change in MEP size in the contralateral biceps after wearable device stimulation (paired group p=0.572; control group p=0.724, Fig. 4.5Aa) and changes for the two stimulation groups were not significantly different ($F(1,25)=0.909$, p=0.350, partial ($\eta 2$)=0.035, Fig. 4.5Ab). The number of subjects with increased MEPs was no different from the distribution expected by chance (paired group 9/15, p=0.307; control group 4/12, p=0.152; Fig. 4.5Ac).

In marked contrast, when the coil was held in the AP position, there was a significant increase in MEP amplitude after paired (p= 0.006), but not after control (p=0.925) stimulation (Fig. 4.5Ba). The difference in MEP amplitude after wearable device stimulation was significantly greater in the paired group ($F(1,25)=8.585$, p=0.007, partial ($\eta 2$)=0.256; Fig. 4.5Bb). Significantly more subjects showed an increase in MEP amplitude than expected by chance after paired (13/15; p=0.006) but not after control (6/12; p=0.765) stimulation (Fig. 4.5Bc).

Figure 4.5C presents results from PA TMS applied over the right hemisphere (ipsilateral to the stimulated arm) and MEPs measured in the contralateral biceps, which had not received wearable device stimulation. There was no change in MEP size in the left biceps in either group (paired group p= 0.338; control group p= 0.596, Fig. 4.5Ca) and the two stimulation groups did not differ from each other ($F(1,25)=0.263$, p=0.612, partial ($\eta 2$)=0.010, Fig. 4.5Cb). The number of participants showing an increase or decrease in MEP amplitude was approximately equal in both groups (paired group 8/15, p=0.293; control group 5/12, p=0.370, Fig. 4.5Cc).

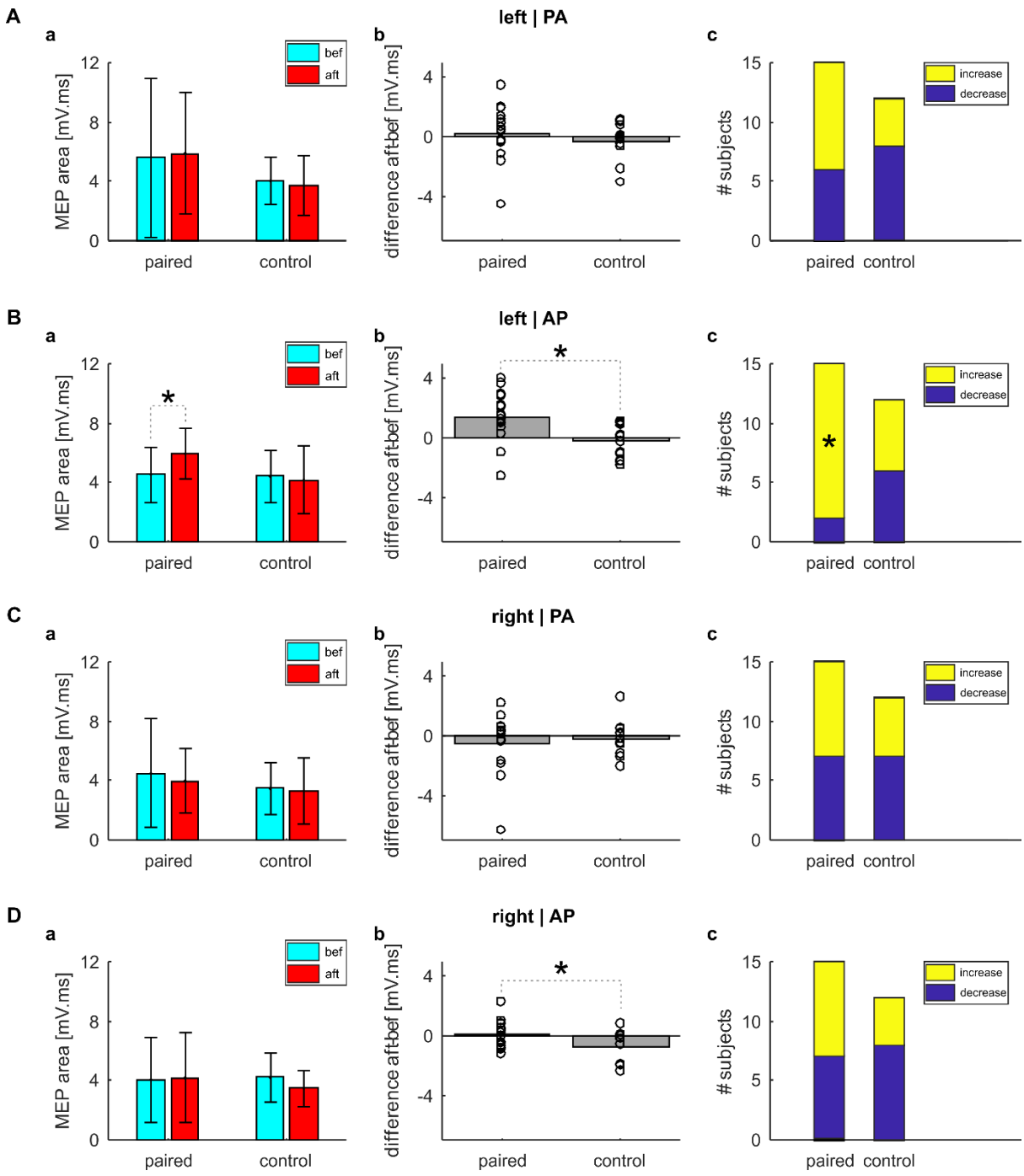

Figure 4.5: *Group results for the coil orientations assessment.* **(A)** Results when holding the coil in posterior-anterior (PA) orientation and stimulating over the left motor cortex. *a:* MEP amplitude before (cyan) and after (red) wearable device stimulation for the two different stimulation groups (paired n=15; control n=12). Coloured bars represent group means; error bars indicate standard deviations**.** Asterisks indicate significant differences. *b:* Difference in MEP amplitudes between before and after wearable device stimulation. A positive difference indicates an increase in MEP size after wearable device stimulation. Bars represent group means; circles show single subject values. *c:* Number of subjects showing an increase (yellow) or decrease (blue) in MEP amplitude after wearable device stimulation. Asterisks indicate proportions significantly different from the 50% expected by chance. **(B)** Results for an

anterior-posterior (AP) coil orientation stimulating over the left motor cortex. **(C)** Results for a posterior-anterior (PA) coil orientation stimulating over the right motor cortex. **(D)** Results for an anterior-posterior (AP) coil orientation stimulating over the right motor cortex.

When TMS was applied in the AP orientation over the right hemisphere (Fig. 4.5D), there was no change in MEP size for the paired group ($p=0.647$), or after unpaired stimulation (control group $p=0.029$; threshold for significance $p<0.025$ using Benjamini-Hochberg correction for multiple comparisons; Fig. 4.5Da). A one-way ANOVA showed that MEP amplitude decreased slightly but significantly more after unpaired stimulation compared to after paired stimulation ($F(1,25)=5.061$, $p=0.034$, partial ($\eta 2$)$=0.168$, Fig. 4.5Db). However, the number of subjects showing a decrease in MEP size was not significantly higher than chance for either group (paired 7/15, $p=0.299$; control 8/12, $p=0.148$, Fig. 4.5Dc).

Discussion

Converging Evidence for Sub-cortical Plasticity

After wearable device paired stimulation at either of the two rates tested, the StartReact effect increased. Importantly, this change only occurred in the biceps muscle which had been stimulated by the wearable device; there was no change in the unstimulated 1DI muscle. This appears to follow the plasticity principle of specificity (Barrionuevo and Brown, 1983). StartReact reflects the involuntary release of a planned movement, and several studies suggest that the size of this effect is a measure of RST outflow (Valls-Sole et al., 1999a, Rothwell, 2006, Baker and Perez, 2017, Carlsen et al., 2004b, Smith et al., 2019). The changes seen in StartReact are thus consistent with a strengthening of RST output to the biceps motor nucleus after wearable device stimulation.

A single TMS pulse evokes multiple descending volleys to the spinal cord: an initial direct (D) followed by subsequent indirect (I) waves (Patton and Amassian, 1954, Rosenthal et al., 1967, Stoney et al., 1968, Jankowska et al., 1975). I-waves are further classified as early (I1, I2) and late (I3 etc.) (Patton and Amassian, 1954, Rothwell et al., 1991). TMS can preferentially recruit different descending waves in humans by changing the direction of the current induced in the brain (Sakai et al., 1997, Ziemann and Rothwell, 2000). PA-directed current predominantly

recruits early, whereas AP current predominantly recruits late I-waves (Day et al., 1989, Sakai et al., 1997, Di Lazzaro et al., 2001, Ni et al., 2011). Several studies in humans suggest that subcortical pathways contribute to muscle responses to late I-waves (Cirillo and Perez, 2015, Cirillo et al., 2016, Long et al., 2017). In monkey, repetitive stimulation of the corticospinal tract generates a supernumerary extra volley in the RST (Fisher et al., 2015); the repetitive corticospinal activation produced by successive I waves could have a similar effect.

We considered first MEPs elicited in the biceps muscle which had received wearable device stimulation, after TMS over the contralateral hemisphere. After wearable device stimulation, the MEP amplitude following TMS with PA oriented current was unchanged. Such MEPs are likely to originate from early I waves, and activate motoneurons predominantly via monosynaptic corticomotoneuronal connections. This result therefore argues that there were no changes in either the strength of corticospinal connections, or changes in cortical excitability. By contrast, MEP amplitude after TMS using AP oriented current was significantly increased following paired stimulation. This could arise from selective changes in intracortical circuits generating late I waves, but equally could occur following subcortical plasticity, for example increased efficacy of cortico-reticular or reticulospinal connections. This would lead to enhanced activation of the biceps motor nucleus.

The RST makes bilateral projections to the spinal cord (Davidson et al., 2007, Peterson et al., 1975, Davidson and Buford, 2006), and the reticular nuclei receive inputs from both contralateral and ipsilateral hemispheres (Fregosi et al., 2017, Darling et al., 2018). We were therefore interested to assess changes contralateral to the arm which had received wearable device stimulation. We found no significant changes in MEPs following paired stimulation for either of the tested coil orientations. Control stimulation may have caused a small decrease in MEPs from the right hemisphere relative to paired stimulation, although this effect was weak. It may represent a slight non-specific effect of the stimulation. In our previous study, delivering biceps stimulation after clicks induced a reduction in the R1 component of the stretch reflex, which is likely to reflect mainly spinal processes (Foysal et al., 2016).

When testing the effect of conditioning MEPs or CMEPs with loud sound, multiple overlapping processes are likely to contribute to the net response facilitation or suppression which is observed. Loud sounds facilitate the H reflex at intervals larger than 50 ms (Rossignol and Jones, 1976, Rudell and Eberle, 1985, Nakashima et al., 1994, Delwaide and Schepens, 1995), indicating an increase in motoneuronal excitability. The suppression of TMS-evoked MEPs

seen at the 50 ms interval (Furubayashi et al., 2000, Tazoe and Perez, 2017, Kuhn et al., 2004) must therefore reflect a cortical suppression superimposed on a smaller spinal facilitation. The cortical suppression most likely results from stimulation of the reticular formation by the loud sound (Davis et al., 1982, Hammond, 1973, Leitner et al., 1980, Fisher et al., 2012), and activation of cortical interneurons via reticulo-thalamic projections (Pare et al., 1988, Steriade et al., 1988). Stimulation at the cervicomedullary junction activates the corticospinal tract at the brainstem level (Ugawa et al., 1991), and hence the size of the descending volley should be unaffected by cortical excitability. In the biceps muscle, this stimulation can evoke responses consistent with both monosynaptic (Petersen et al., 2002) and oligosynaptic transmission (Nakajima et al., 2017). At an 80ms interval, although CMEPs and H reflexes are facilitated, MEPs are not (Furubayashi et al., 2000, Tazoe and Perez, 2017), suggesting that the cortical suppression persists at this interval and is now equally balanced by spinal facilitation.

In this study, we found that the MEP suppression at the 50ms interval was reduced after paired wearable device stimulation, but that the CMEP facilitation at 80 ms was unchanged. This may reflect a decrease in cortical inhibition elicited by the loud sound. It is also possible that the reduced net suppression arose from an increase in spinal facilitation, which might arise from sub-cortical pathways, although then we might have expected to see an increase in the CMEP facilitation at 80 ms. Our results have strong similarity to the work of Tazoe and Perez (2017), who measured these effects in the contracting 1DI muscle while subjects performed different types of grasp. During a power grip MEP suppression was smaller, and CMEP facilitation the same as during an isolated index finger abduction. These authors argued that the reduced suppression was indicative of a smaller cortical contribution to the motoneuron drive during power grip, whereas the similarity of CMEP facilitation indicated no change in corticomotoneuronal synaptic efficacy or motoneuron excitability. Our results may similarly indicate a relative shift away from corticospinal drive to activate biceps after wearable device stimulation. However, it should be noted that we found no reduction in MEP amplitude elicited by PA TMS (Fig. 4.5A); by contrast, Tazoe and Perez (2017) did see a smaller MEP during a power grip than isolated finger abduction.

Previous work from this laboratory introduced the protocol of pairing auditory clicks with electrical muscle stimulation using a wearable device, and showed that it was capable of generating plastic changes in the LLSR (Foysal et al., 2016). The modality of paired stimuli, and their inter-stimulus interval, were originally chosen with the aim of targeting the RST. As the

LLSR in biceps likely has a subcortical component (Kimura et al., 2006, Kurtzer, 2014, Shemmell et al., 2009), we speculated that plasticity had indeed been generated subcortically, possibly in the RST. In the present study, we have extended the evidence in support of this conclusion. Paired device stimulation increased the StartReact effect, decreased the suppression of MEPs by loud sounds, and increased MEPs elicited by an AP coil orientation. All of these changes are consistent with plasticity in subcortical pathways, including the RST. By contrast, MEPs generated by the PA coil orientation were unaltered, suggesting that plasticity did not occur in the corticospinal tract. Non-invasive measures in humans are rarely completely unambiguous, but convergent results using multiple measurements build a more convincing case than any single finding. Whilst we still cannot exclude a contribution from other circuits, we believe that the weight of evidence points towards changes in subcortical circuits, particularly the RST, following paired device stimulation.

An important question is why repeated convergent activation of auditory/vestibular and afferent inputs at the brainstem should alter a wide range of sub-cortical response measures, many of which are likely to rely on synapses in the cortico-reticulospinal pathway, rather than those carrying sensory inputs to the brainstem. One possibility is that wearable device stimulation not only strengthened specific synapses related to the paired inputs, but also elevated brainstem excitability leading to a general increase in RST output. We have previously reported a similar situation during recovery from CST damage, where there are changes not only in selected RST connections to motoneurons (Zaaimi et al., 2012) but also increases in single cell activity within the reticular formation itself (Zaaimi et al., 2018).

Potential for Rehabilitation

Stimulus rate is an important parameter in protocols which induce plasticity, and the direction of effects (potentiation vs suppression) can even be altered by changing rate (Pitcher et al., 2003). Importantly, here we extended our previous work (Foysal et al., 2016) by testing a higher frequency of paired stimulation. This did not significantly increase the size of plastic changes, indicating that the original frequency was at or above the optimal level. Anecdotally, some subjects found the higher stimulus rate irritating, whereas the lower rate was well tolerated. The similar results are thus encouraging, as they suggest that there is no benefit to using the more unpleasant stimulation. In our recent clinical trial of this device in stroke

patients over a four week period (Choudhury et al., 2020), patients who chose to wear the device for longer each day showed greater functional gains. This suggests that greater plastic changes can be generated by longer periods of paired stimulation. In the present study subjects always wore the device for 6 hours; further work is needed to define what stimulation duration is optimal.

The device could easily be worn during standard therapist-led or self-directed rehabilitation to complement physical therapy programs. Increasing RST motor output might enable greater functional gains due to the availability of stronger connections to the muscle. We would expect optimal benefits when wearable stimulation is used concomitantly with a customized therapy regime.

Following extensive CST damage such as after stroke or spinal cord injury, the RST may be the only major descending motor pathway remaining and plays an important role in recovery (Zaaimi et al., 2012, Baker, 2011, Zaaimi et al., 2018). Prior studies usually attempted to boost functional recovery using neurostimulation targeted cortical changes, and often met with disappointing results (Rothwell, 2016). The ability to manipulate plasticity in a sub-cortical target may be capable of achieving gains not accessible by other means.

CHAPTER V – TESTING A NOVEL WEARABLE DEVICE FOR MOTOR RECOVERY OF ELBOW EXTENSOR TRICEPS BRACHII IN CHRONIC SPINAL CORD INJURY

The study with SCI participants described in this chapter was largely conducted at the NeuroKinex centre in Hemel Hempstead. The NeuroKinex team let me use their facilities for several months and helped me with recruiting. The data was collected by me and I performed all data analysis.

Abstract

After corticospinal tract damage from spinal cord injury (SCI), reticulospinal connections to motoneurons strengthen preferentially to flexor muscles, which could contribute to the poor recovery of extensors seen after SCI and stroke.

In this study, we paired electrical muscle stimulation with auditory clicks using a wearable device to deliver stimuli to the triceps muscle over a prolonged period of time. Healthy human volunteers wore the stimulation device for ~6 hours and a variety of electrophysiological assessments were used to measure changes in triceps motor output. In contrast to previous results in the biceps muscle, paired stimulation: 1) did not increase the StartReact effect; 2) did not decrease the suppression of responses to transcranial magnetic brain stimulation (TMS) following a loud sound; 3) did not enhance muscle responses elicited by a TMS coil oriented to induce anterior-posterior current.

In a second study, chronic cervical SCI survivors wore the stimulation device for ~4 hours every day for 4 weeks; this was compared to them not wearing the device for another 4 weeks. Functional and electrophysiological assessments were repeated at week 0, week 4 and week 8. We did not observe any significant changes in our assessments after paired stimulation. Functional measurements such as maximal force, as well as trajectories made during a planar reaching task, also remained unchanged.

Our results suggest that elbow flexors and extensors have a different potential for plasticity, perhaps due to a differential control of flexor and extensor motoneurons by corticospinal and reticulospinal pathways. However, it should be noted that both studies have a low number of participants.

Introduction

Damage to the corticospinal tract through spinal cord injury (SCI) often results in decreased voluntary control of muscles below the level of injury, or even full paralysis. The recovery of any remaining function following SCI is associated with plastic changes and extensive reorganization of neural pathways.

While extensive axonal regeneration in the central nervous system is absent, even the most severe SCIs often spare regions of white matter (Petersen et al., 2012, Angeli et al., 2014, Barthelemy et al., 2015, Kakulas, 1999) and surviving CST fibres in these bridges may contribute to recovery, for example through spontaneous sprouting (Rosenzweig et al., 2010).

Alternatively, other descending pathways may provide a route for motor command transmission. Monkeys show a remarkable recovery after CST lesions (Lawrence and Kuypers, 1968a, Lawrence and Kuypers, 1968b) and regain most of their gross locomotor functions, with motor outputs from the red nucleus strengthening (Belhaj-Saif and Cheney, 2000) to provide a substrate for recovery. However, the rubrospinal tract may be weak or non-existent in humans (Nathan and Smith, 1955, Onodera and Hicks, 2010), which could explain the stark difference in functional recovery after CST damage.

In the absence of a rubrospinal tract, humans may have to rely on medial brainstem pathways, including the reticulospinal tract (RST), after damage to the CST. While the RST is widely accepted to play a role in posture and gross motor function (Prentice and Drew, 2001, Schepens and Drew, 2004, Iwamoto et al., 1990, Isa and Sasaki, 2002), evidence supporting RST contribution to even distal limb function has accumulated in recent years. The RST innervates forearm and intrinsic hand muscles (Riddle et al., 2009), and many interneurons are under shared control of both CST and RST (Riddle and Baker, 2010). Also, reticular formation cells modulate their discharge during fine finger movements at least as much as corticospinal neurons in M1 (Soteropoulos et al., 2012).

While the CST has become the dominant pathway in primates, reticulospinal connections to motoneurons strengthen after CST lesions, partially restoring lost synaptic drive (Zaaimi et al., 2012). Increased inputs from both CST and RST could help recovery after SCI. Importantly, reticulospinal neurons may have a better response to plasticity protocols than corticospinal neurons (Vavrek et al., 2007, Zorner et al., 2014).

Non-invasive methods to modulate the RST in humans are limited, but exploiting the fact that reticulospinal neurons receive extensive afferent input (Leiras et al., 2010) and auditory stimuli excite reticular neurons (Irvine and Jackson, 1983, Fisher et al., 2012), we have previously built a portable device capable of delivering stimuli to the motor point of a muscle paired with an auditory click, which is able to induce plastic changes in motor output (Foysal et al., 2016, Germann and Baker, 2021). Using this device at home for 4 weeks produced significant improvements in upper limb function for stroke survivors (Choudhury et al., 2020), which were retained for at least 4 weeks after device stimulation ceased.

Elbow extensors show notoriously limited recovery compared to elbow flexor muscles in individuals with cervical SCI (Ditunno et al., 1992, Ditunno et al., 2000, Calancie et al., 2004, McKay et al., 2011). This asymmetrical recovery of function is also commonly seen after stroke, with survivors often exhibiting flexor spasm and extensor weakness (Twitchell, 1951, Cauraugh et al., 2000, Kamper et al., 2003).

Most cervical spinal cord injuries affect more than one spinal segment (Schaefer et al., 1989, Benavides et al., 2020), making it unlikely that CST projections to elbow extensors would be regularly more damaged compared to elbow flexors. The location of motoneurons that innervate these muscles also largely overlap (Schirmer et al., 2011).

The imbalanced recovery might be due to the differential control of flexor and extensor motoneurons by corticospinal and reticulospinal pathways (Sangari and Perez, 2020). Indeed, after CST lesion in monkeys, reticulospinal connections strengthen to forearm flexor and intrinsic hand muscles, but not to forearm extensors (Zaaimi et al., 2012). In a healthy state, the RST has been shown to preferentially facilitate ipsilateral flexors and contralateral extensors (Davidson and Buford, 2006).

Our previous work using the wearable device to modulate motor output (Foysal et al., 2016), most likely by inducing subcortical plasticity (Germann and Baker, 2021), targeted the elbow flexor biceps brachii and the same protocol was able to improve upper limb function in stroke (Choudhury et al., 2020) by targeting forearm extensor muscles. With this study, we wanted to investigate whether the same plasticity protocol could improve function of the elbow extensor triceps brachii in chronic cervical spinal cord injury survivors. We hypothesise that prolonged wearable device stimulation would lead to electrophysiological and potentially functional changes in the triceps muscle. However, as an extensor muscle triceps might be

more resistant to plastic changes than the previously targeted biceps muscle. Therefore we also repeated our previous study (Germann and Baker, 2021) in healthy participants, but targeting the triceps muscle to be able to compare plasticity responses between elbow extensors and flexors in a healthy state.

Methods

Single day study in healthy volunteers: Subjects

In total, 11 healthy volunteers (6 females and 5 males; 18–35 years old, right-handed by self-report) participated in the study. Four subjects took part in two experiments. If participants took part in several stimulation paradigms, each session was separated by at least 7 days. All subjects gave written informed consent to the experimental procedures, which was approved by the ethics committee of the Faculty of Medical Sciences at Newcastle University. The study was performed in accordance with the guidelines established in the Declaration of Helsinki, except that the study was not preregistered in a database.

Single day study in healthy volunteers: Experimental Paradigm

The single day study in healthy subjects followed the same paradigm as our previous study targeting the biceps muscle (Germann and Baker, 2021).This required subjects to come to the laboratory at around 9am, where baseline assessments were conducted. They were then fitted with a wearable electronic device to deliver paired electrical and auditory stimuli, and the subject left and continued their normal daily activities. In the evening, the subject returned, the device was removed, and the assessments repeated. The order of the various assessments was randomized for a given subject, but kept the same for the morning and evening recordings in that person. The two assessment sessions were at least 6 h apart.

For this study, conducted over one day, the following assessments were used at baseline and after wearing the device: StartReact, loud sound with MEP, MEPs with different coil orientations (see below).

Seven subjects wore the earpiece in the contralateral ear and 8 subjects wore the earpiece in the ipsilateral ear (relative to the stimulated right triceps).

SCI study: Subjects

Subjects needed to fit the following inclusion criteria in order to be eligible for the study: Male or female at least 18 years of age; chronic (>1 year) cervical (C2-C7) injury; detectable EMG activity in triceps; without upper limb fracture or subluxation/dislocation of joints within last 6 months; be able to follow study instructions; willing to provide written informed consent (if necessary through an independent witness should the subject be unable to write themselves due to their injury).

For participant flow diagram see Figure 5.3.

SCI study: Trial Design

This study was designed as an interventional randomised cross over trial (Figure 5.3). The trial was registered in the ISRCTN registry (ISRCTN15025040). After completing the baseline session (week 0) which included all our assessments, participants were randomized to one of two groups using custom MATLAB code. Group A was issued the device to be used at home for 4 weeks, returned for a second assessment session (week 4) and then stopped wearing the device and returned in another 4 weeks (week 8). Group B first did not wear the device and returned for a second session (week 4), when they were issued the device to use for the remaining 4 weeks (week 8). For the period spent using the device, participants were instructed to wear it for at least 4 hours (total usage) every day, in line with the previous study in stroke survivors (Choudhury et al., 2020). Due to the nature of the intervention and control (device vs no device), subjects and researchers were not blinded.

The device can be worn during all activities with the exception of showering and sleeping. Participants were carefully shown how to place the electrodes and given a detailed information pamphlet on how to use the device, as well as plenty of electrodes to last them for the month. Participants chose whether they wanted to stimulate the left or right triceps for the duration of the study (11 chose right arm, 4 chose left arm). Participants were free to choose the stimulated side, so any potential improvement would be of maximal benefit to them.

SCI study: Adverse Events

An Adverse Event (AE) were defined as any untoward medical event, including abnormal laboratory values, occurring during the use of the study device, but not necessarily causally related to it. Events with onset prior to start of study device use were not considered as

adverse events unless there was an increase in severity and/or frequency following institution of the study device.

Adverse events included symptoms complained of by the subject during follow up visits as well as any signs detected by the subject's physician or other health professional during routine medical appointments. Subjects were instructed to contact the investigator immediately in the event of any physical discomfort while on the study. If a diagnosis was available, it was noted as AE; if no diagnoses was available each sign and symptom was recorded as individual adverse events.

For each individual AE the nature of the event, duration, maximum intensity, any action taken on trial medication, possible relation to study drug and finally subject outcome were noted. Causality assessment were done using the World Health Organization-Uppsala Monitoring Centre (WHO-UMC) Causality Assessment Criteria. AE severity were graded as mild, moderate and severe.

No AE was reported during the study.

Electromyography (EMG) recordings

EMG was recorded through surface electrodes (disposable Kendall H59P Electrodes, Covidien, Mansfield, Massachusetts, USA) secured on the skin over the belly of the triceps, biceps and deltoid muscle.

For the one day study in healthy subjects, the electrodes over the right triceps muscle were used for both EMG recording and for wearable stimulation, so they were kept in place for the whole day, ensuring consistency between the morning and evening sessions. For the SCI study, electrodes had to be repositioned.

EMG signals were amplified and filtered (30-2000 Hz, gain 1000) with a bioamplifier (D360 Amplifier, Digitimer, Welwyn Garden City, UK), digitized at a sampling rate of 5kHz (CED Micro 1401 with Spike2 software, Cambridge Electronic Design, Cambridge, UK) and stored on a computer for off-line analysis. Where necessary for a given assessment (see below), the level of triceps EMG activity was displayed continuously on a computer screen via series of coloured bars, allowing subjects to maintain a constant isometric contraction. Physiological measurements were acquired at 10-20% of MVC across conditions. The exact level of MVC varied across participants, but was kept constant for all assessments of each participant.

Transcranial Magnetic Stimulation (TMS)

Transcranial magnetic stimuli were applied using a figure-of-eight coil through a Magstim 200[2] magnetic stimulator (Magstim, Whitland, UK) with a monophasic current waveform. We determined the optimal position for eliciting a motor evoked potential (MEP) in the triceps muscle (hotspot) by moving the coil, with the handle pointing backward and 45° from the midline, in small steps along the arm representation of M1. The hotspot was defined as the region where the largest MEP in the triceps muscle could be evoked with the minimum intensity (Rothwell et al., 1999). Unless stated otherwise, the magnetic coil was held in this orientation over the left hemisphere for subsequent measurements, to induce currents in the brain that flowed perpendicular to the presumed line of the central sulcus in a posterior—anterior (PA) direction.

Active motor threshold (AMT) was defined as the stimulator intensity sufficient to elicit a visible MEP in at least 5 out of 10 consecutive stimuli, in the triceps contralateral to the stimulus with an active contraction of 10-20% maximal voluntary contraction (MVC).

A Polaris Vicra camera (Northern Digital Inc., Waterloo, Ontario, Canada) tracked both coil and head position, allowing the site of stimulation to be marked using the Brainsight neuronavigation system (Rogue Research Inc., Montréal, Quebec, Canada). This ensured a stable coil location throughout the experiment, and allowed us to return to the same site in all sessions.

Assessment: StartReact

StartReact was examined using a previously reported paradigm (Baker and Perez, 2017, Germann and Baker, 2021), which measures reaction time from EMG in response to a visual cue (visual reaction time, VRT), a visual plus quiet auditory cue (visual-auditory reaction time, VART), and a visual plus loud auditory cue (visual-startle reaction time, VSRT). The acceleration of reaction time between VART and VSRT is believed to involve the rapid involuntary release of the pre-prepared movement, and to reflect the action of the RST (Valls-Sole et al., 1999a, Carlsen et al., 2004b, Rothwell, 2006, Baker and Perez, 2017, Smith et al., 2019). Some previous studies on StartReact have measured startle responses from the sternocleidomastoid (SCM) muscle, and excluded reaction times measured when this muscle was not activated (Valls-Sole et al., 1999a, Carlsen et al., 2004b, Honeycutt et al., 2013). We and others have previously found that SCM activity is unreliable (Honeycutt et al., 2013, Baker and Perez, 2017,

Dean and Baker, 2017), and can be generated both in response to startling and non-startling cues. In this study, we therefore simply included all reaction times measured from the relevant cue, as in our previous publications (Baker and Perez, 2017, Dean and Baker, 2017, Choudhury et al., 2019, Germann and Baker, 2021).

Subjects were seated with the arm flexed at the elbow by 90° and secured in an arm restraint.

A green light-emitting diode (LED) was located ~1 m in front of the subject. Subjects were instructed to push against the restraint (elbow extension) as quickly as possible after the LED illuminated. EMG was recorded from both the triceps and biceps muscles, and reaction time measured as the time from cue to onset of the EMG burst. Three types of trial were randomly interleaved (20 repeats per condition; inter-trial interval 5-6 s): LED illumination alone (VRT), LED paired with a quiet sound (80dB, 500Hz, 50ms, VART), LED paired with a loud sound (500 Hz, 50 ms, 120 dB, VSRT). Subjects were initially presented with five consecutive loud sounds, without performing the task, to allow familiarization and to habituate the overt startle reflex.

Data were analysed trial-by-trial using a custom MATLAB program which identified the reaction time as the point where the rectified EMG exceeded the mean + 7 SD of the baseline measured 0-200 ms prior to the stimulus. Every trial was inspected visually, and erroneous activity onset times (caused, for example, by electrical noise artefacts) were manually corrected. This yielded a reaction time distribution for each condition.

Assessment: loud sound with MEP

A paradigm similar to previous studies (Furubayashi et al., 2000, Tazoe and Perez, 2017, Germann and Baker, 2021) was used. Loud (500 Hz, 120 dB SPL) auditory stimuli (LAS) were given 50 ms before a TMS pulse over M1; this elicits a smaller MEP than the same TMS pulse given alone, which is believed to reflect cortical inhibitory processes. The interval used was selected as it gave the largest suppression in a previous detailed examination of these effects (Furubayashi et al., 2000). Sounds were given through two audio speakers located on a table ~1 m in front of the subject. The sound ended at the time of the test stimulus. To avoid stimulus predictability, the inter-trial interval was chosen randomly between 20.5 and 23 s (uniform distribution). At the beginning of the study, five consecutive loud sounds were presented to habituate the startle reflex. During testing subjects were seated with the arm flexed at the elbow by 90° and pushed against the restraint at 10-20% of MVC. The level of triceps EMG activity was displayed continuously on a computer screen via a series of colored

bars, allowing subjects to maintain a constant isometric contraction, which was kept the same across sessions for that subject. The test stimulus intensity was adjusted to be 130% of the AMT. Ten test MEPs and 10 conditioned MEPs were measured in each condition, in randomized order.

Assessment: MEPs with different coil orientations

By holding a figure-of-eight TMS coil in different orientations, activation can be biased towards different indirect (I) waves (Sakai et al., 1997, Ziemann and Rothwell, 2000). With the coil tangential to the scalp, at an angle of 45° to the midline with the handle pointing laterally and posteriorly, a posterior-anterior (PA) current is induced in the brain, which mainly recruits early I waves. By contrast, in the reverse orientation (handle pointing medial and anterior; anterior-posterior (AP) induced current), predominantly late I waves are recruited. Here, we measured MEPs with different coil orientations to compare changes in direct versus indirect corticospinal pathways.

MEPs in the triceps muscle were measured from the contralateral hemisphere in two different coil orientations. As for the measurements of MEPs described above, the figure-of-eight coil was first held to induce a posterior-anterior (PA) current in the brain. The optimal scalp position was located with this orientation, and marked in the Brainsight neuronavigation software. This site was then used for stimulation to induce an anterior-posterior (AP) current in the brain, by rotating the coil so that the handle faced anterior and medial, as the current direction does not significantly influence the position of the hotspot (Sakai et al., 1997, Arai et al., 2005). Within each subject, we randomized the order of coil orientations (PA vs AP); the same order was used for the baseline and all following assessments. Stimulus intensity was set to 1.1x active motor threshold (two separate thresholds were measured, one for each coil orientation). Subjects were seated with the arm flexed at the elbow by 90° and secured in a restraint.

The level of triceps EMG activity was displayed continuously on a computer screen via a series of colored bars. Twenty MEPs were recorded (5 s interstimulus interval) while subjects maintained a constant isometric contraction of 10%-20% MVC by pushing against the arm restraint.

Assessment: MVC & Force

Subjects performed three brief MVCs (3 s) for biceps and triceps each. Subjects were asked to perform maximal contractions by pushing or pulling against the arm restraint, for elbow extension or elbow flexion respectively. Each contraction was separated by 60 s. Force was measured with a dynamometer built into the arm restraint.

Assessment: planar reaching task

Participants sat at a custom built table (Figure 5.1) with their trunk secured to a high-backed chair. Table height was adjusted to bring shoulder, elbow and wrist close to the same horizontal plane. The reaching arm was supported on an air cushion sled that used continuous pressurized airflow to support the limb against gravity and allowed near frictionless movements. Participants were instructed to make 20 straight movements to visual targets (160 trials in total), projected using a two way mirror to appear in the same plane as a blue LED cursor (diameter 3 mm) attached to the sled.

The targets consisted of a start position at the centre and 8 targets of equal angular range around the central target, each with 1 cm radius. The targets were arranged at a distance 10 centimetres radially from the centre start position. One target at a time would light up green. The target turned red as soon as the cursor reached the target area. Participants had to hold the cursor inside the target for 800 - 1209.6 ms, before the centre target would light up green and participants returned to start position. Targets appeared in a pseudo-randomized order.

Arm position was tracked using a Polhemus Liberty^{TM} motion tracking system (Polhemus, Colchester, Vermont, USA) with a sensor built into the support sled.

Despite the arm support, two participants were unable to perform the required reaching movement and analysis is based on the remaining 13 participants.

Targets for participants who chose to use their left arm for the study were mirrored across the midline, so all trajectories could be analysed the same.

Trajectories of SCI participants were compared to data from 18 healthy volunteers performing the same task with their right arm (13 females and 5 males; 18-35 years old, right handed by self-report).

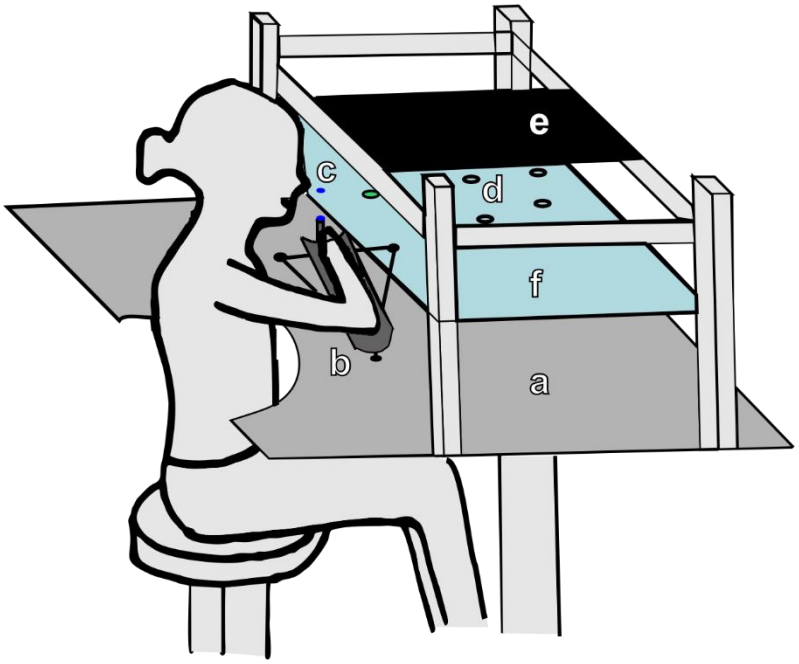

Figure 5.1: *Schematic representation of the planar reaching task*. a, smooth table surface. b, arm support air sled. c, LED cursor, positioned on top of the air sled. d, targets, projected to plane of the arm from e, LED lights panel via f, two-way mirror.

Assessment: CUE Questionnaire

The Capabilities of Upper Extremity (CUE) Questionnaire measures upper extremity functional limitations in individuals with tetraplegia (Marino et al., 1998). It is a 32-item questionnaire evaluating perceived difficulty completing actions using the right (15 items), left (15 items), or both (2 items) upper extremities. The participant gave each action a score from 0-4, with higher scores reflecting less limitation. Left and right arm function can be derived separately. Total score for both arms were totalled up and compared across sessions.

Intervention: Wearable Device

The wearable device was similar to that used in our previous work (Choudhury et al., 2020). It comprised a plastic box containing an electrical stimulator and audio amplifier, powered by an internal battery which could be recharged via a standard USB-C port. The wearable device generated constant-current electrical stimulation to the right biceps muscle through surface

electrodes (220 V compliance, 0.15 ms pulse width). A knob on the device allowed adjustment of the stimulus intensity, which was set to be just below the motor threshold (defined as a visible muscle twitch). Auditory stimuli were generated by delivering a 0.1 ms wide, 12 V square excitation pulse into a miniature earpiece; this produced a brief click with an intensity of 110 dB SPL.

Based on calculations provided by (Rosengren et al., 2010) and (Foysal et al., 2016), this intensity corresponds to an A-weighted intensity of 68 dB LA_{eq} when delivered at 0.66 Hz, and 71 DB LA_{eq} when delivered at 1.32 Hz; assuming device usage for at least 8 hours. This is well below the recommended safe limit for noise exposure of 85 dB LA_{eq} given by the UK's Control of Noise at Work Regulations (The Stationery Office, 2005). The device can therefore potentially be used every day for at least 8 hours at these levels without concern.

For the one day study in healthy subjects, seven subjects wore the earpiece in the contralateral ear and eight subjects wore the earpiece in the ipsilateral ear (relative to the stimulated right triceps). For the SCI study, the earpiece was always placed contralateral to the stimulated triceps muscle.

Stimuli were delivered with an inter-trial interval of 1250 - 1750 ms (chosen at random from a uniform distribution); the delay between electrical stimulation and auditory click was 10 ms. This inter-stimulus interval was chosen so that the afferent volley should arrive at the brainstem just prior to RST cell activation by the click.

The device logged to flash memory how many stimuli were given each time it was switched on, allowing the experimenter to check how often it had been used at the end of the four week usage period.

Data Analysis

Data were analysed using custom scripts written in the MATLAB environment (R2017a, MathWorks). Statistical tests were performed using MATLAB and IBM SPSS Statistics for Windows, version 24 (IBM Corp.).

EMG traces were full-wave rectified and then averaged. MEP amplitude was measured as the area under the curve of this average.

Where MEPs were conditioned by loud sound, the amplitude of the conditioned MEP was expressed as a percentage of the unconditioned MEP.

The StartReact effect was measured as the difference between the mean VART and VSRT.

For the assessment which conditioned MEPs with loud sound, a one sample t test was performed to compare the normalized conditioned MEP amplitude against 100%, to evaluate the effect of conditioning at baseline.

For each experiment, individual paired t tests were used to compare the measurements of each session to the measurements at baseline.

For the SCI study, the session preceding device usage was taken as the 'before' (week 0 for group A; week 4 for group B) and the session immediately after wearing the device was taken as the 'after' (week 4 for group A; week 8 for group B) for the 'device' condition. The same was done for the 'no device' condition; with the 'before' session being week 4 for group A and week 0 for group B and the 'after' session being week 8 for group A and week 4 for group B. Differences between before and after sessions were compared with paired t tests.

Where necessary, the procedure introduced by Benjamini and Hochberg (1995) to correct for multiple comparisons was used. Cohen's d was used to measure effect size.

To assess the overall movement quality during planar reaching, Mahalanobis distance squared (MDC^2) was calculated using functional principal component analysis, a generalization of traditional PCA (Cortes et al., 2017, Goldsmith and Kitago, 2016, Kitago et al., 2015). MDC^2 was derived from a comparison between reaching trajectories of SCI participants and trajectories from a group of healthy controls (N=18).

For the reaching task, two-way repeated measures ANOVAs were performed with factors time (before, after) and target (Target 1-8) on speed, distance and MDC^2 of trajectories.

Additionally, two-way repeated measures ANOVAs were performed with factors target (Target 1-8) and condition (device, none) on speed, distance and MDC^2 differences (after-before). Speed, distance and MDC^2 at baseline (week 0 for both group A and B) were also assessed with a repeated measures ANOVA with factor target (Target 1-8).

The significance level was set at $p < 0.05$. Descriptive statistics are presented as mean ± SD.

Binomial tests were performed to determine if the number of subjects showing a certain change were more than expected by chance based on a binomial distribution.

Results

Single day study in healthy volunteers

Figure 5.2 presents group results for the single day study in healthy volunteers, for the StartReact (Fig. 5.2A), LAS with TMS (Fig. 5.2B), MEPs elicited with AP coil orientation (Fig. 5.2C) and MEPs elicited with PA coil orientation (Fig. 5.2D) assessments. Seven participants wore the earpiece in the contralateral ear and eight in the ipsilateral ear. Both groups received electrical stimulation to the right triceps. Due to the low number of participants, results were also combined to a total N=15.

There was no significant difference in StartReact effect after wearable device stimulation ($p=0.628$ contralateral, $p=0.732$ ipsilateral, $p=0.538$ combined; Fig. 5.2Aa).

Figure 5.2B shows the results when MEPs elicited by TMS were conditioned by a loud sound beginning 50ms before the magnetic stimulus. Our previous study in the biceps muscle (Germann and Baker, 2021), showed significantly suppressed MEPs at baseline. For the triceps, the group wearing the earpiece contralaterally did show a significant MEP suppression (one sample t test $p<0.001$) at baseline (Fig. 5.2Ba), however for the group wearing the audio ipsilaterally, this suppression did not quite reach significance ($p=0.059$). When the groups were combined, MEPs were significantly suppressed at baseline ($p<0.001$) as expected from literature (Furubayashi et al., 2000, Tazoe and Perez, 2017).

There was no change in conditioned MEP suppression after wearable device stimulation ($p=0.340$ contralateral, $p=0.426$ ipsilateral, $p=0.939$ combined; Fig. 5.1Ba).

There was no change in MEP size in the triceps after wearable device stimulation, when the coil was held in the AP ($p=0.851$ contralateral, $p=0.111$ ipsilateral, $p=0.203$ combined; Fig. 5.2C) or PA ($p=0.160$ contralateral, $p=0.790$ ipsilateral, $p=0.494$ combined; Fig. 5.2D) orientation over the left hemisphere (contralateral to the arm stimulated by the wearable device).

Overall, there did not seem to be any changes in the triceps muscle after wearable device stimulation for a single day. These results are in stark contrast to our results in the biceps muscle (Germann and Baker, 2021), which used the same stimulation protocol and duration, but could be influenced by the much lower number of participants in the present study.

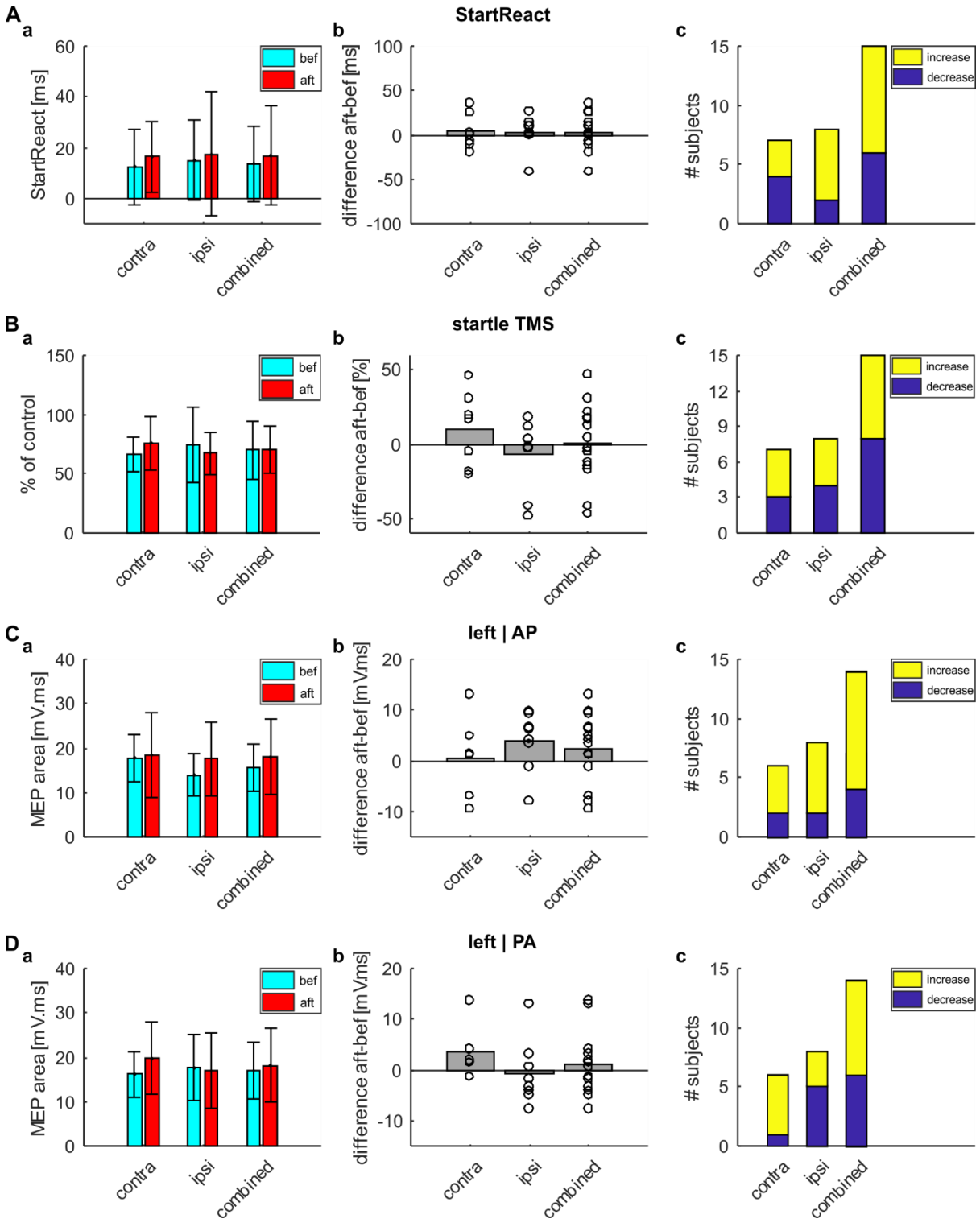

Figure 5.2: *Group results for the single day study in healthy triceps.* **(A)** Results for the StartReact assessment (contralateral audio N=7, ipsilateral audio N=8, both groups combined N = 15). Figure represents StartReact effect (difference between VART and VSRT). **a**, StartReact effect before (cyan) and after (red) wearable device stimulation. Colored bars represent group means; error bars indicate SDs. **b**, difference in StartReact effect between before and after wearable device stimulation. A positive difference indicates a more pronounced StartReact effect after wearable device stimulation. Bars represent group means; circles show single

subject values. **c**, Number of subjects showing an increase (yellow) or decrease (blue) in StartReact effect after wearable device stimulation.
(B) Results for the conditioned MEPs with loud sounds. Figure represents conditioned MEP amplitude normalized to unconditioned amplitude (as percentage of control). Layout is the same as for **(A)**.
(C), Results for the coil orientation assessment when stimulation with an AP coil orientation. Figure represents MEP amplitude as area under the curve. For one subject stimulation threshold was too high to detect AP MEPs, so subject was excluded for the coil orientation assessment (contralateral audio N=6, ipsilateral audio N=8, combined N=14). Layout is the same as for **(A)**.
(D), Results for the coil orientation assessment when stimulation with a PA coil orientation. Figure represents MEP amplitude as area under the curve. For one subject stimulation threshold was too high to detect AP MEPs, so subject was excluded for the coil orientation assessment (contralateral audio N = 6, ipsilateral audio N=8, combined N=14). Layout is the same as for **(A)**.

While there was no significant majority (as expected by chance based on a binomial distribution) of subjects showing a certain direction of change for any of the assessments (Fig. 5.2Ac, 5.2Bc, 5.2Cc, 5.2Dc), most subjects receiving the clicks ipsilaterally showed the expected effects; an increase in StartReact, attenuation of MEP suppression in response to LAS and facilitation of MEPs elicited with AP induced current. All of these measures had two clear outliers which could have a disproportionate impact on our results with such a small sample size.

SCI study

For our SCI trial, a total of 22 participants with chronic cervical spinal cord injury were recruited to the study (Table 5.1). All participants had to complete three sessions, each separated by approximately 4 weeks. Participant flow is depicted in Figure 5.3. Six participants dropped out during the course of the study, as they were unable to attend all three session appointments within an acceptable number of days of the target date (>8 days difference). One subject was excluded from group analysis, as their usage of the device was too low during the 4 weeks. Subsequent analysis is based on the remaining 15 participants (6 females, 9 males, 45.2 ± 14.0 years old; Table 5.1).

Of these 15 participants, 1 subject had to be excluded from the StartReact Assessment due to equipment failure during one session, 2 subjects were unable to perform the required reaching movements for the planar reaching task and had to be excluded for that task and in 2 subjects it was not possible to elicit MEPs with the AP coil orientation, so they had to be excluded for the coil orientation assessment.

Participant no.	Age (y)	Gender	Level	Injury (y)	Arm	Device usage (days)
1	35	F	C5 incomplete	2	R	28
2	32	F	C5-C6 incomplete	3	R	27
3	52	M	C3-C4 incomplete	6	R	28
4	67	M	C3-C4 incomplete	13	R	28
5	39	M	C5-C6 incomplete	17	R	28
6	62	M	C5-C6 complete	28	R	28
7	45	F	C4 incomplete	17	R	28
8	30	M	C4 complete	11	R	31
9	34	M	C4 complete	5	R	29
10	67	F	C3-C7 incomplete	4	R	28
11	60	F	C2-T2 incomplete	15	L	35
12	22	M	C5 incomplete	5	L	28
13	47	F	C4-C5 incomplete	3	L	28
14	39	M	C4-C5 incomplete	2	R	28
15	47	M	C6 complete	22	L	28
16	*34*	*M*	*C4-C5 incomplete*	*10*	*R*	*40*

Table 5.1: *SCI participants.* Participant number 16 was subsequently excluded from analysis due to low compliance.

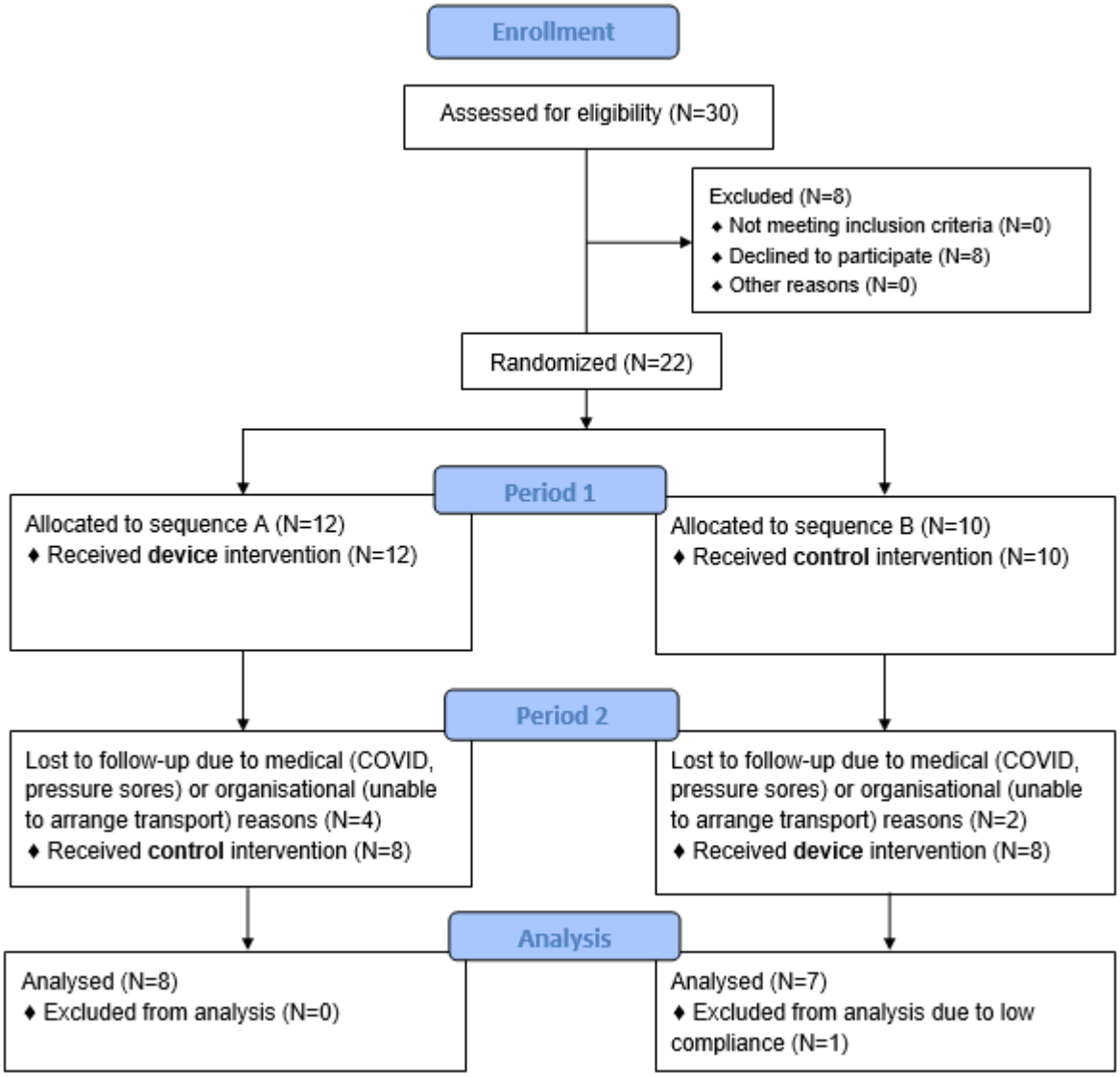

Figure 5.3: *Consort diagram.* Trial flow diagram for the SCI study. Participants were randomised into two groups (A,B), which both spent 4 weeks wearing the device and 4 weeks without wearing the device, but in opposite order. Subsequent analysis is based on the remaining 15 participants.

The device had an inbuilt flash memory which logged the number of paired stimuli given every time it was switched on. Participants were asked to use the device for a minimum of 4 hours a day, every day for 4 weeks (28 days). Based on the average stimulus frequency, this is equivalent to 268,800 paired stimuli. Figure 5.4 depicts each subject's total number of stimuli received over the course of 4 weeks, with the dotted line indicating this stimulus number. Only

three subjects exceeded the instructed minimum stimulus number, 12 subjects were below this level, but with a number judged acceptable. One subject had such a low compliance that they were subsequently excluded from group analysis.

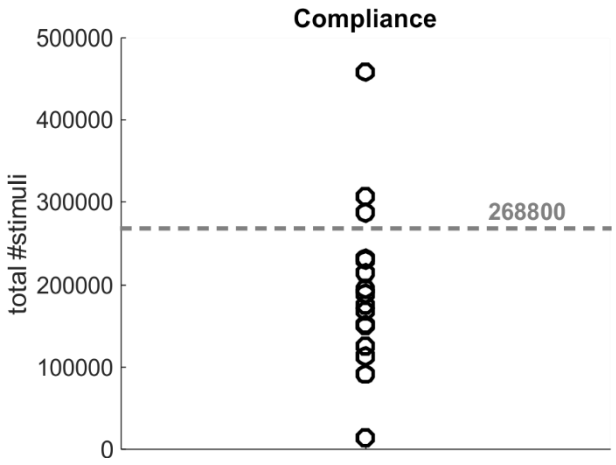

Figure 5.4: *Compliance of device usage in SCI participants.* The device recorded the number of stimuli given over the 4 week period. Grey dashed line represents total number of stimuli received if the device was used as instructed, with a minimum usage of 4 hours a day over the period of 4 weeks (28 days). Circles represent individual participants (N=16). One subject receiving a very low number of stimuli was subsequently excluded from analysis.

The total score achieved in the CUE questionnaire did not change between sessions (device p=0.133, none p=0.435; Fig. 5.5Aa) or between conditions (p=0.177; Fig. 5.5Ab). Maximal force generated during elbow flexion (device p=0.418, none p=0.507; Fig. 5.5B) or extension (device p=0.604, none p=0.617; Fig. 5.5C) also remained unchanged and the differences did not vary across conditions (flexion p=0.825, extension p=0.471; Fig. 5.5Bb, 5.5Cb). Since participants had to come back on different days, we also compared AMT between sessions, but found no significant changes in stimulation threshold with either PA coil orientation (device p=0.568, none p=0.354; Fig. 5.5D) or AP coil orientation (device p=0.630, none p=0.419; Fig. 5.5E).

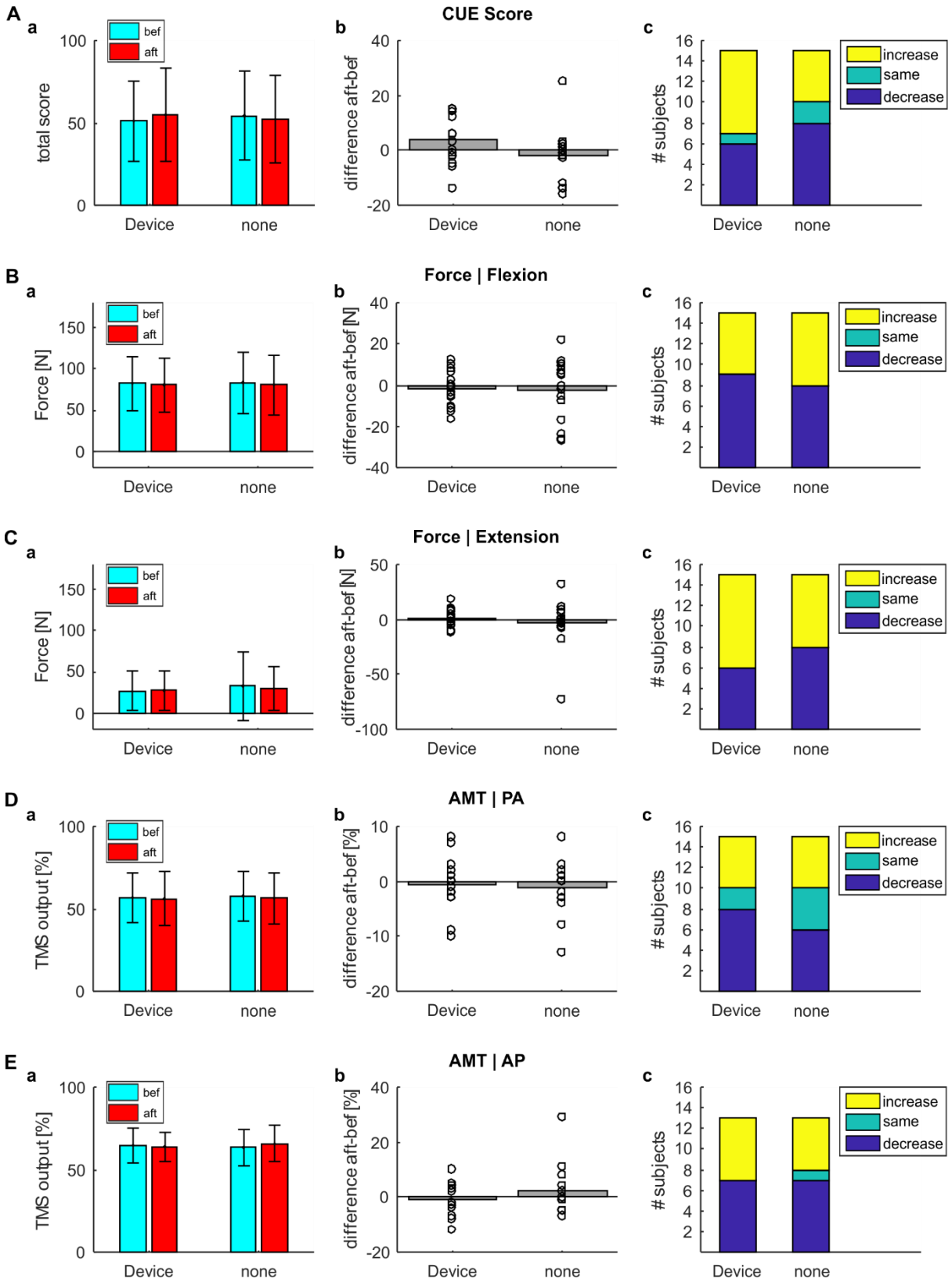

Figure 5.5: *Group results for the SCI study.*

(A), Results for the CUE questionnaire (N=15). Figure represents the total score achieved in the CUE questionnaire. **a**, Total CUE score before (cyan) and after (red) 4 weeks of wearing the device (device) or 4 weeks of not using the device (none). Colored bars represent group means; error bars indicate SDs. **b**, Difference in total CUE score between before and after using

the device or not. A positive difference indicates an increase in total score after 4 weeks. Bars represent group means; circles show single subject values. **c**, Number of subjects showing an increase (yellow) or decrease (blue) in total score after 4 weeks.
(B) Results for the maximal force produced during elbow flexion (N=15). Figure represents mean maximal force, measured with a force plate. Layout is the same as for **(A)**.
(C) Results for the maximal force produced during elbow extension (N=15). Figure represents mean maximal force, measured with a force plate. Layout is the same as for **(A)**.
(D), Results for the active motor threshold of MEPs elicited with PA coil orientation (N=15). Figure represents AMT. Layout is the same as for **(A)**.
(E) Results for the active motor threshold of MEPs elicited with AP coil orientation. For two subjects AMT was too high to detect AP MEPs (N=13). Figure represents AMT. Layout is the same as for **(A)**.

As with our healthy volunteers, there was no significant difference in StartReact effect after wearable device stimulation (device p=0.461, none p=0.476; Fig. 5.6A).

Figure 5.6B depicts group results for MEPs conditioned with loud sound. Notably, in these SCI subjects MEPs were not suppressed at baseline (device p=0.796, none p=0.4137; Fig. 5.6Ba), which is unexpected based on previous findings. MEP size remained unchanged across sessions (device p=0.382, none p=0.587) and did not differ between conditions (p=0.471; Fig. 5.6Bb).

Figure 5.6C illustrates average size of MEPs elicited with AP coil orientation normalized to the size of MEPs elicited with PA coil orientation. There was no apparent difference in MEP size between sessions (device p=0.246, none p=0.281; Fig. 5.6Ca) or between conditions (p=0.114; Fig. 5.6Cb). However, more subjects than expected by chance based on a binomial distribution showed an increase in MEP size elicited with AP compared to PA induced currents after wearable device stimulation (device p=0.022, none p=0.500).

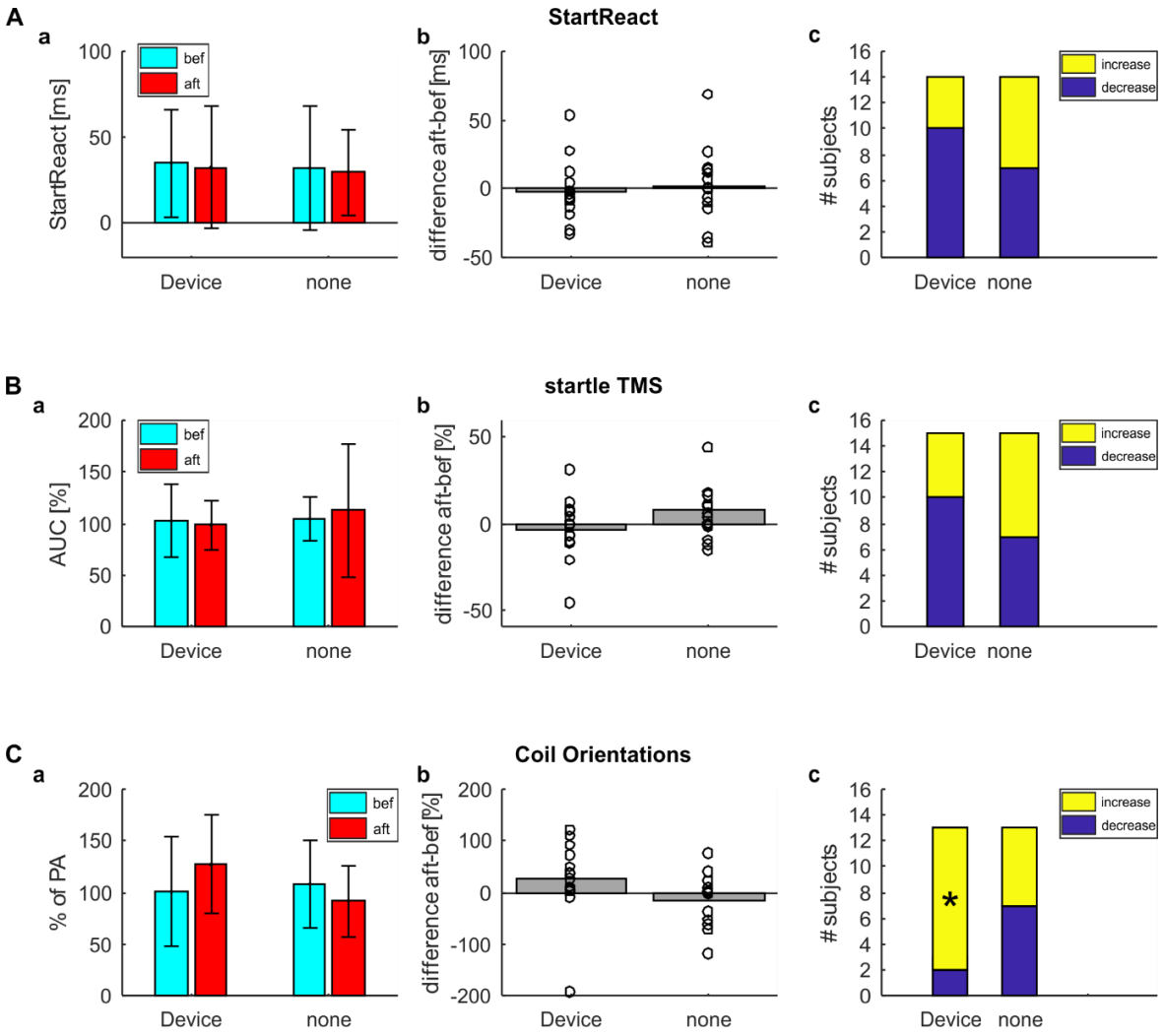

Figure 5.6: *Group results for StartReact, startle TMS and MEPs with different coil orientations.* **(A)** Results for the StartReact assessment. For one subject equipment failure prevented recordings, so subject had to be excluded for this assessment (N=14). Figure represents StartReact effect (difference between VART and VSRT). **a**, StartReact effect before (cyan) and after (red) wearing the device for 4 weeks (device) or 4 weeks of not using the device (none). Colored bars represent group means; error bars indicate SDs. **b**, Difference in StartReact effect between before and after using the device or not. A positive difference indicates a more pronounced StartReact effect after 4 weeks. Bars represent group means; circles show single subject values. **c**, Number of subjects showing an increase (yellow) or decrease (blue) in StartReact effect after 4 weeks. Asterisks indicate proportions significantly different from the 50% expected by chance. **(B)** Results for the conditioned MEPs with loud sounds (N=15). Figure represents conditioned MEP amplitude normalized to unconditioned amplitude (as percentage of control). Layout is the same as for **(A)**. **(C)** Results for the coil orientation assessment. For two subjects stimulation threshold was too high to detect AP MEPs, so subjects were excluded for the coil orientation assessment (N=13). Figure represents MEP amplitudes elicited by AP orientation normalized to MEP amplitudes elicited by PA orientation. Layout is the same as for **(A)**.

Group analysis of trajectories during the planar reaching task are shown in Figure 5.7. Targets are arranged radially according to where they were positioned during the task (for subjects using their right arm; targets were mirrored across the midline for subjects using their left arm), with target 7 being the closest to where subjects would sit at the table. Both maximal speed and distance from straight line were significantly modulated with target position (speed $F(7,84)=8.648$, $p<0.001$, $\eta2=0.419$; distance $F(7,84)=14.170$, $p<0.001$, $\eta2=0.541$; Figure 5.7Aa and 5.7Ba). There was a significant effect of *target* for both measures after 4 weeks of using the device (speed $F(7,84)=8.074$, $p<0.001$, $\eta2=0.402$; distance $F(7,84)=16.092$, $p<0.001$, $\eta2=0.573$) and 4 weeks of not using the device (speed $F(7,84)=8.205$, $p<0.001$, $\eta2=0.406$; distance $F(7,84)=17.644$, $p<0.001$, $\eta2=0.595$), but no effect of *time* (speed 'device' $F(1,12)=3.759$, $p=0.076$, $\eta2=0.239$; speed 'none' $F(1,12)=0.101$, $p=0.756$, $\eta2=0.008$; distance 'device' $F(1,12)=0.439$, $p=0.520$, $\eta2=0.035$; distance 'none' $F(7,84)=17.644$, $p<0.001$, $\eta2=0.595$) or their interaction (speed 'device' $F(7,84)=0.627$, $p=0.733$, $\eta2=0.050$; speed 'none' $F(7,84)=0.808$, $p=0.583$, $\eta2=0.063$; distance 'device' $F(7,84)=0.395$, $p=0.903$, $\eta2=0.032$; distance 'none' $F(7,84)=0.333$, $p=0.937$, $\eta2=0.027$).

Comparing the differences between sessions (Figure 5.7Ab and 5.7Bb) revealed no effect of *condition* (speed $F(1,12)=0.743$, $p=0.406$, $\eta2=0.058$; distance $F(1,12)=0.070$, $p=0.797$, $\eta2=0.006$), *target* (speed $F(7,84)=0.547$, $p=0.7961$, $\eta2=0.044$; distance $F(7,84)=0.462$, $p=0.859$, $\eta2=0.037$), or their interaction (speed $F(7,84)=0.751$, $p=0.629$, $\eta2=0.059$; distance $F(7,84)=0.340$, $p=0.933$, $\eta2=0.028$).

Trajectories were also evaluated using functional principal component analysis to compute Mahalanobis distance squared (MDC^2; Figure 5.7C) compared to trajectories from healthy volunteers (N=18). A mixed ANOVA with repeated measure *target* (1-8) and between-subject factor *group* (SCI, healthy) was used to analyse trajectories at baseline (Figure 5.7Ca). Mauchly's Test of Sphericity indicated that the assumption of sphericity had been violated ($\chi2(27) = 239.232$, $p < 0.001$) and therefore a Greenhouse-Geisser correction was used. Overall quality of trajectories from SCI participants differed significantly from healthy trajectories at baseline, with a main effect of group ($F(1,29)=15.686$, $p<0.001$, $\eta2=0.351$), target ($F(7,203)=3.518$, $p=0.043$, $\eta2=0.108$) and their interaction ($F(7,203)=3.518$, $p=0.0431$, $\eta2=0.108$).

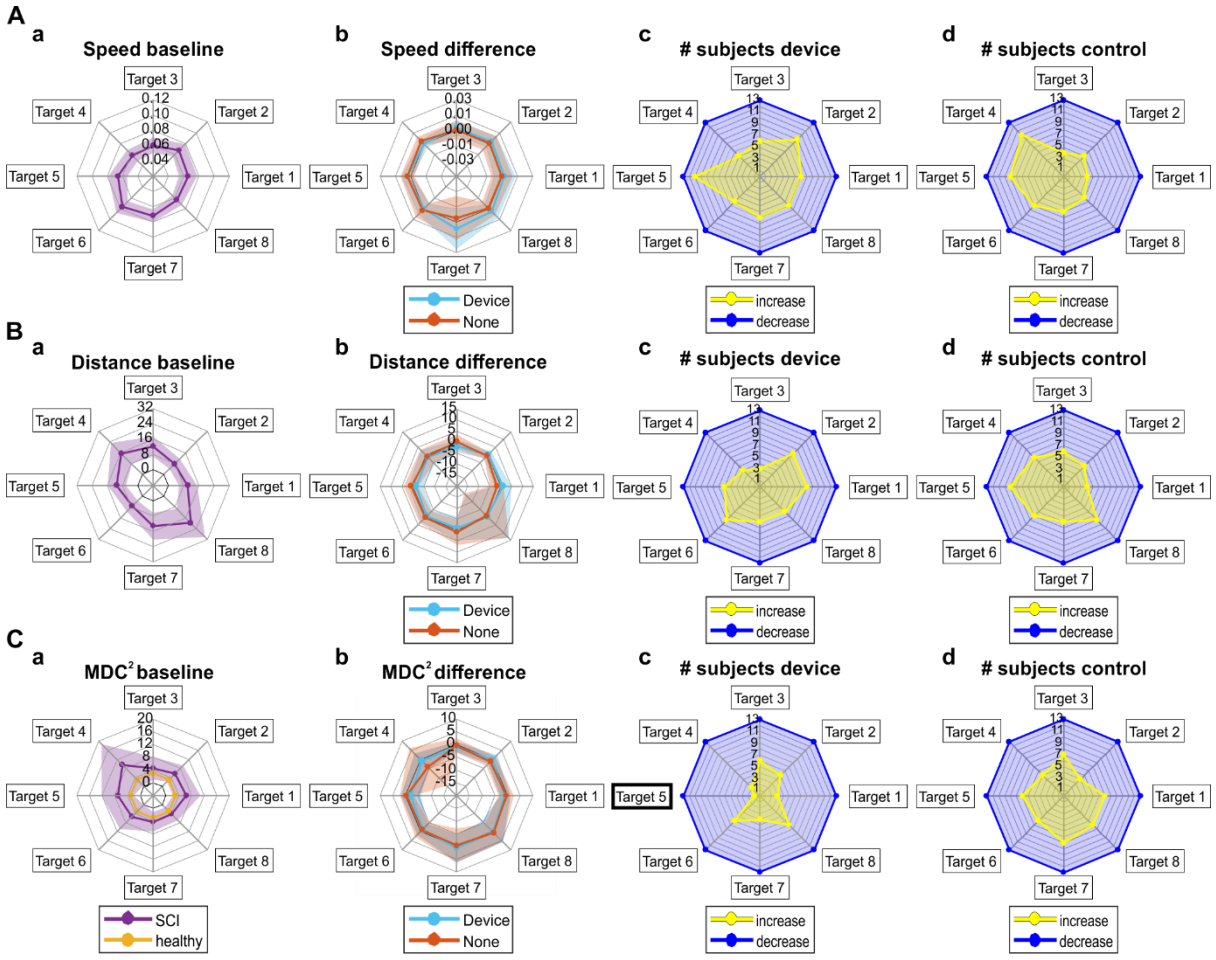

Figure 5.7: *Group results for the planar reaching task.* Two subjects were unable to perform the required reaching movements and group analysis is based on the remaining 13 participants.

(A) Maximal speed of trajectories achieved while reaching for each target (Target 1-8). **a**, Mean maximal speed of trajectories across SCI participants at baseline (N=13). Purple line represents mean values, shaded area represents standard deviation. **b**, Difference in maximal speed between before and after 4 weeks of using the device (light blue) or not (orange). **c**, Number of subjects showing an increase (yellow) or decrease (blue) in maximal speed after 4 weeks of using the device. **d**, Number of subjects showing an increase (yellow) or decrease (blue) in maximal speed after 4 weeks of not using the device.

(B) Maximal distance from straight line while reaching for each target (Target 1-8). Layout is the same as for **(A)**.

(C) Mahalanobis distance squared (MDC^2) of trajectories for each target (Target 1-8). MDC^2 was calculated by comparing trajectories from SCI participants (N=13) with trajectories from healthy controls (N=18) with functional PCA. **a**, Mean MDC^2 across SCI participants (purple) and healthy controls (amber). Layout is the same as for **(A)**. Bold label borders indicate proportions significantly different from the 50% expected by chance.

However, there was no effect of time (device F(1,12)=3.329, p=0.093, η2=0.217; none F(1,12)=2.005, p=0.182, η2=0.143), target (device F(7,84)=1.779, p=0.102, η2=0.129; none F(7,84)=2.138, p=0.048, η2=0.151), or their interaction (device F(7,84)=0.651, p=0.713, η2=0.051; none F(7,84)=1.009, p=0.431, η2=0.078) on MDC^2 across sessions. Similar to maximal speed and distance to straight line, there was no effect of condition (F(1,12)=0.091, p=0.768, η2=0.008), target (F(7,84)=1.803, p=0.097, η2=0.131), or their interaction (F(7,84)=0.521, p=0.817, η2=0.042) on MDC^2 when looking at the differences between sessions (Figure 5.7Cb).

Significantly more subjects than expected by chance showed a decrease in MDC^2 after wearable device stimulation for target 5 (device p=0.004, none p=0.710) and target 4 (device p=0.022, none p=0.290), although target 4 was not significant after correction for multiple comparisons.

Discussion

Single day study in healthy volunteers

Unlike our previous results with the device targeting the biceps muscle (Germann and Baker, 2021), pairing electrical stimulation to the triceps muscle with auditory clicks for 6 hours did not lead to changes in motor output.

In our previous study, auditory clicks were always delivered contralaterally to the target muscle. However, it has been shown that galvanic-evoked vestibulocollic reflexes project contralaterally to flexors and ipsilaterally to extensors (Watson and Colebatch, 1998b, Uchino et al., 1997). Auditory clicks of 100 dB are able to evoke vestibulospinal reflex responses with a similar latency as galvanic stimulation (Watson and Colebatch, 1998a). Therefore, when targeting the elbow extensor triceps brachii, auditory clicks might need to be delivered ipsilaterally. For comparison, half of our participants wore the earpiece in the contralateral ear and half in the ipsilateral ear. Due to the low number of participants we also combined the results (Figure 5.2).

Using the same plasticity protocol on the biceps significantly increased the StartReact effect, which remained unchanged after triceps stimulation (Figure 5.2A). Because the overt startle reflex is known to involve the reticulospinal tract (Davis et al., 1982), several studies suggest

that the size of this effect is a measure of RST outflow (Valls-Sole et al., 1999a, Rothwell, 2006, Baker and Perez, 2017, Carlsen et al., 2004b, Smith et al., 2019).

Similarly, paired wearable device stimulation of the biceps muscle was found significantly to reduce the MEP suppression in response to a loud sound at the 50ms interval (Germann and Baker, 2021), while triceps showed no change in MEP suppression (Figure 5.2B).

Multiple overlapping processes are likely to contribute to the net facilitation or suppression in the MEP response when conditioned with loud sound. Loud sounds facilitate the H reflex at intervals larger than 50 ms (Rossignol and Jones, 1976, Rudell and Eberle, 1985, Nakashima et al., 1994, Delwaide and Schepens, 1995), indicating an increase in motoneuronal excitability. The suppression of TMS-evoked MEPs seen at the 50 ms interval (Furubayashi et al., 2000, Tazoe and Perez, 2017, Kuhn et al., 2004) must therefore reflect a cortical suppression superimposed on a smaller spinal facilitation. The cortical suppression most likely results from stimulation of the reticular formation by the loud sound (Davis et al., 1982, Hammond, 1973, Leitner et al., 1980, Fisher et al., 2012), and activation of cortical interneurons via reticulo-thalamic projections (Pare et al., 1988, Steriade et al., 1988).

A reduction in net MEP suppression at the 50ms interval could therefore reflect a decrease in cortical inhibition elicited by the loud sound, or an increase in spinal facilitation. Either way, net MEP suppression remained unchanged after wearable device stimulation of the triceps (Figure 5.2B).

MEP amplitudes elicited by different coil orientations also did not change (Figure 5.2C, 5.2D). In contrast, our results in biceps muscle showed a significant increase in size of MEPs elicited by AP coil orientation (Germann and Baker, 2021).

TMS can preferentially recruit different descending waves in humans by changing the direction of the current induced in the brain (Ziemann and Rothwell, 2000, Sakai et al., 1997). PA-directed current predominantly recruits early, whereas AP current predominantly recruits late I-waves (Day et al., 1989, Di Lazzaro et al., 2001, Ni et al., 2011, Sakai et al., 1997).

MEPs elicited with PA coil orientation are likely to activate motoneurons predominantly via monosynaptic corticomotoneuronal connections and can be taken as a measure of cortical excitability. Meanwhile changes in MEP responses to AP currents could arise from changes in intracortical circuits generating late I waves, or following subcortical changes, for example increased efficacy of cortico-reticular or reticulospinal connections.

Increased amplitude in MEPs elicited by AP currents, increased StartReact effect and reduction in MEP suppression following LAS were all observed in biceps muscle after wearable device stimulation for 6 hours (Germann and Baker, 2021) and all point towards subcortical changes, such as enhanced RST output to the biceps motor nucleus. None of these measures showed any significant changes for the triceps muscle (Figure 5.2), but a (non-significant) majority of subjects receiving the clicks ipsilaterally did show these changes. A small number of outliers could have disproportionally affected our results due to the low number of participants.

A study by Foysal and Baker (2019) demonstrated that intrinsic hand and flexor muscle have a higher potential to show plasticity than extensors, which could explain the differences in our results. However, even though extensors might remain unaffected by our 6 hour protocol, prolonged stimulation over several weeks may be enough to induce plasticity.

SCI study

In addition to our electrophysiological measurements, we also had a range of functional measurements to assess motor function before and after wearable device stimulation in participants with chronic cervical SCI. There were no significant changes after 4 weeks of paired stimulation. This could be due to a number of factors.

Compliance was very variable between participants (Figure 5.4), with only three participants receiving more than the instructed minimum number of stimuli and 13 receiving fewer. Choudhury et al. (2020) demonstrated that the extent of functional gain in stroke patients was correlated with stimulus number. The smaller number of participants in our study, and even fewer participants reaching minimum compliance, could have affected our results.

Furthermore, we recruited participants with both complete and incomplete cervical SCI. This is because even when voluntary movement is completely absent in clinical evaluation, neurophysiological methods using surface electromyography are able to identify and quantify evidence of preserved translesional conduction in chronic clinically complete SCI subjects (McKay et al., 2004, McKay et al., 2011). However, each SCI lesion is highly individualized in regards to severity of impairment and which particular descending tracts are spared (Kakulas, 2004) and including a wider range of participants must invariably introduce more variability in the data. This considerable diversity in pathway interruption would also affect the amount of RST damage the study participants might have sustained.

The heterogeneity of the participants was mostly due to the lack of injury-specific inclusion criteria (see methods), as anyone with a cervical injury was allowed to participate. There was also very little clinical baseline data available, further contributing to the diverseness of the participants. It would be useful for future studies to thoroughly assess SCI participants, for example by using the ASIA scale, especially in regards to the target muscle. This would allow us to stratify participants and draw more accurate conclusions about the effect of the intervention.

A further limitation of our study design was the absence of both subject and outcome assessor blinding, due to the nature of the intervention and control condition (device vs no device). However, this appeared to have little impact on our results in this instance. For future studies, it would still be best to use independent electrical and auditory stimulation, similar to our control stimulation in the biceps study (Germann and Baker, 2021). This would allow for participants and assessor to remain blind throughout the study.

Similar to our single day study in healthy triceps, there was no change in StartReact effect after 4 weeks of paired stimulation in participants with SCI (Figure 5.6A). However, a recent study using extracellular recordings to investigate the StartReact mechanism in monkeys, showed a ceiling effect in StartReact increase (Tapia et al., submitted). Tapia et al.'s study demonstrated that loud sound only shortened reaction time if the majority (≥60%) of motoneuron drive came from the reticular formation, not M1. The extent of reaction time shortening increased as more drive came from the reticular formation, but StartReact effect did not grow further when more than 80% drive came from RST.

StartReact effect is increased after spinal cord injury and correlates with spasticity (Sangari and Perez, 2019), which might be a result from excessive RST activity (Brown, 1994). It is therefore conceivable that our SCI participants were already relying more heavily on the RST due to their injury and a further increase in StartReact effect just was not possible due to the existence of this ceiling effect.

Triceps showed no change in net MEP suppression when conditioned with loud sound both in healthy participants (Figure 5.2B) and after 4 weeks device usage in SCI (Figure 5.6B). Notably, there was no MEP suppression at baseline in SCI participants, which is unexpected based on existing literature (Furubayashi et al., 2000), and MEPs were significantly suppressed in healthy triceps (Figure 5.2Ba). Similar to our StartReact result, the absence of a net MEP

suppression at a 50ms interval could imply that SCI survivors are more reliant on pathways that are responsible for the spinal facilitation caused by the loud sound. This increased facilitation would therefore cancel out the cortical suppression evoked by the loud sound. In support of this, Sangari and Perez (2020) found that responses elicited by cervicomedullary stimulation (CMEPs) were facilitated by a loud sound at an 80ms interval after SCI to a similar extent as controls in triceps, and even exhibited more facilitation than controls in the biceps muscle. This would be in line with the idea that reticulospinal inputs are increased after injury to compensate for the loss of corticospinal axons (Pettersson et al., 2000, Zaaimi et al., 2012). The absence of a net MEP suppression at baseline in SCI (Figure 5.6Ba), therefore makes it impossible to detect an attenuation of MEP suppression after paired stimulation and only an overt facilitation would be quantifiable as an effect.

There was also no change in any of our TMS measures across sessions. Corticospinal responses elicited by TMS over the primary motor cortex have different characteristics after SCI, including delayed MEP latencies, decreased amplitude and higher thresholds (Ellaway et al., 2007, Perez, 2012) and AP responses appear more affected after injury (Jo et al., 2018, Cirillo et al., 2016). Active motor thresholds for both PA- and AP-induced currents were fairly consistent across sessions (Figure 5.5D & E) and MEP amplitudes elicited by the two coil orientations didn't change in relation to each other (Figure 5.6C).

The CUE questionnaire is designed to measure upper extremity functional limitations in individuals with tetraplegia. However, 12 out of 32 questions focus on hand and finger function, hardly something expected to change after our plasticity protocol. As a more functional measure, we assessed maximal force produced before and after wearing the device (Figure 5.5B & C), which remained unchanged in both biceps and triceps muscle.

In addition to strength, motor control is just as essential for skilled use of our muscles, but is harder to assess as most movements have significant antigravity strength requirements. In order to separate motor control of the upper limb from strength, we used a planar reaching task similar to previous studies in stroke (Cortes et al., 2017, Goldsmith and Kitago, 2016) that allowed us to compare kinematic measures across sessions and compare range, speed and accuracy of upper limb movements.

Both speed and distance from straight line appeared to be modulated by target position (Figure 5.7Aa and 5.7Ba), but did not change across sessions (Figure 5.7Ab and 5.7Bb). As a

global kinematic measure, Mahalanobis distance squared can be calculated using functional principal component analysis, a generalization of traditional PCA. MDC^2 is derived from a comparison between reaching trajectories of SCI participants and trajectories from healthy controls and is sensitive to changes in overall movement quality (Cortes et al., 2017, Goldsmith and Kitago, 2016, Kitago et al., 2015). MDC^2 was significantly different for our SCI participants compared to healthy trajectories (Figure 5.7Ca) and one target did show a significant change in MDC^2 in SCI participants after wearable device stimulation (Figure 5.7Cc).

Overall, we did not find the same electrophysiological changes in triceps after paired stimulation as we did in biceps (Germann and Baker, 2021), in healthy volunteers or after prolonged wearable device usage in chronic cervical SCI.

Although reticulospinal neurons may respond better to plasticity protocols than corticospinal neurons (Vavrek et al., 2007, Zorner et al., 2014), there is a hierarchy in the ability to induce plastic changes across muscle groups (Foysal and Baker, 2019), with extensor muscles showing a much lower potential for plasticity. In fact, the study by Foysal and Baker (2019) showed that even when extensor muscles were stimulated, outputs were enhanced to flexors but not extensors. However, this difference was only seen in protocols that require integration of sensory input, while the same level of plasticity was observed when using a rTMS protocol.

This might be because flexor and extensor muscles receive differential control from corticospinal and reticulospinal pathways. Through corticospinal connections, flexors might receive larger monosynaptic facilitation and extensors stronger disynaptic inhibition in both monkeys (Phillips and Porter, 1964) and humans (Palmer and Ashby, 1992), though other work has suggested no difference (Park et al., 2004). Stimulation of the reticular formation in monkeys typically evokes bilateral responses, but the prevalent pattern is ipsilateral extensor suppression and flexor facilitation with the opposite pattern occurring contralaterally (Davidson and Buford, 2006, Herbert et al., 2010).

After contralateral CST lesion in monkey, there was no evidence of novel connections from ipsilateral corticospinal fibres that would make any significant contribution to recovery (Zaaimi et al., 2012). In contrast, there was a non-uniform strengthening of brainstem connections, with inputs to forearm flexor and intrinsic hand motorneurons enhanced, whereas connections to extensors remained unchanged (Zaaimi et al., 2012).

Limited CST connections and enhanced RST output has been associated with spasticity in SCI survivors (Sangari and Perez, 2019). Whether reticulospinal reorganization after injury is helpful or detrimental remains a topic of discussion (Karbasforoushan et al., 2019), but many animal models of SCI have provided evidence that it can contribute to functional tasks (Wakabayashi et al., 2001, Ballermann and Fouad, 2006, Filli et al., 2014, May et al., 2017).

Importantly, there is no evidence of increased spasticity in stroke survivors using the wearable device (Choudhury et al., 2020).There were no adverse events of any grade reported during our study with SCI participants.

All this implies that reticulospinal inputs compensate for the loss of corticospinal axons, but may do so preferentially in flexors, which could explain the asymmetrical recovery of biceps and triceps muscles observed in people after SCI (Sangari and Perez, 2020). The lack of these extra inputs to triceps could also explain why our plasticity protocol leads to significantly enhanced motor output in biceps but not triceps. However, it should be noted that given our small number of participants in both studies, we can't rule out a possible effect. After all, Choudhury et al. (2020) showed a significant improvement in hand function in stroke patients after 4 weeks of wearable device usage with a protocol that targeted forearm extensors. Since that study only assessed hand function and not the effects in individual muscles, it is hard to say if the targeted extensors had improved, or whether in fact the protocol led to beneficial changes in flexors, similar to the results reported by Foysal and Baker (2019). There is also the possibility that there is an inherent difference between distal forearm extensors and the more proximal elbow extensor, something that would need to be investigated in future studies.

CHAPTER VI – GENERAL DISCUSSION

Animal studies such as Kuypers' seminal lesion studies (Lawrence and Kuypers, 1968a, Lawrence and Kuypers, 1968b) have shaped our understanding of the motor system as an extensive network of neurons with several distinct and intricate descending pathways. Despite this complexity, existing literature on the human motor system has predominantly focussed on the corticospinal tract (CST). This is in part due to the fact that the CST is the dominant pathway in primates, but also because results obtained from human studies are usually indirect and determining the extent to which other pathways contribute is often impossible.

While animal experiments are important in providing insight into the motor system both anatomically and functionally, there are considerable inter-species differences that limit the degree to which these findings can be translated. In the end, study of the human motor system will always have to involve humans.

This has been made possible in no small part thanks to the introduction of non-invasive brain stimulation methods, such as transcranial magnetic stimulation (TMS), transcranial electrical stimulation (TES) and cervicomedullary junction stimulation. Following their invention in the 1980s, these techniques have now found widespread use in both basic science and clinical settings and have significantly expanded our basic understanding of the human motor system.

Nevertheless, great care needs to be taken when interpreting their effects, since a motor evoked potential (MEP) following a single stimulus often reflects confounding activation of multiple structures or brain areas, with substantial interplay of different circuits. For example, TMS evokes a series of distinct volleys that differ in latency, activation threshold and most likely arise at least in part from different neural circuits (Di Lazzaro et al., 2012). However, the exact physiologic mechanisms behind TMS still remain unclear and the cortical circuits involved are poorly defined.

In addition to cortical circuits, TMS over the motor cortex is capable of activating reticular formation cells (Fisher et al., 2012). Therefore, subcortical effects in TMS measures cannot be excluded.

Non-invasive stimulation can be used not only to probe neural pathways, but also to modify them using the principles of spike-timing dependent plasticity.

Plasticity at various levels of the motor system underlie skilled motor learning and recovery after injuries and is essential for our motor system to adapt throughout life. Neuronal connections can be strengthened if a postsynaptic neuron is activated consistently after a presynaptic input (Markram et al., 1997); this is known as spike-timing dependent plasticity.

Paired associative stimulation (PAS) refers to a known protocol to induce plasticity non-invasively by giving two appropriately-timed stimuli that converge on a common target circuit (Stefan et al., 2000). Several PAS studies have since been reported in literature which showed that plasticity can be induced by repetitive TMS (Huang et al., 2005), or by pairing TMS with a peripheral stimulus (Stefan et al., 2000, Taylor and Martin, 2009, Urbin et al., 2017), with natural activity generated during voluntary movements (Buetefisch et al., 2015, Edwardson et al., 2014, Thabit et al., 2010), or with motor imagery (Foysal and Baker, 2020, Kraus et al., 2016).

These existing non-invasive stimulation protocols can generate plasticity in the motor cortex and its corticospinal projections, but techniques for inducing plasticity in sub-cortical circuits and alternative descending pathways such as the reticulospinal tract (RST) are less well developed.

As mentioned above, one approach which efficiently stimulates the reticulospinal tract is to activate the motor cortex with TMS. Another promising stimulus to target RST neurons is a loud auditory stimulus (LAS), capable of evoking the startle reflex, which is known to involve the nucleus reticularis pontis caudalis (Leitner et al., 1980, Davis et al., 1982, Brown et al., 1991) and its reticulospinal projection.

In one of our studies, we paired LAS with TMS and observed enhanced motor output in healthy human volunteers. The most likely substrate for these plastic changes, consistent with our electrophysiological measurements in humans and direct measurements in monkeys, appears to be an increase in the efficacy of corticoreticular connections.

A major drawback of existing PAS neurostimulation protocols is the need for bulky and expensive equipment, such as a TMS machine, which limits their application to the laboratory and restricts the intervention to brief periods.

As an alternative, we used a wearable electronic device (previously developed in our group), which is capable of delivering stimuli outside the lab and allows continuous stimulation over many days. The device pairs electrical stimulation to the motor point of a muscle with auditory

clicks. These two stimuli were chosen based on the fact that reticulospinal neurons receive extensive afferent input (Leiras et al., 2010) and auditory stimuli excite reticular neurons (Fisher et al., 2012).

This approach has previously been shown to induce plastic changes in the long-latency stretch reflex in healthy volunteers (Foysal et al., 2016), which in biceps likely has a subcortical component. Here we extended the evidence in support of a subcortical origin of plasticity after paired stimulation and tested different stimulus rates.

Although less widespread than those available for the CST, non-invasive electrophysiological techniques can be used to study the reticulospinal tract. In addition to TMS and TES, these include combining auditory startling stimuli with a reaction time task (StartReact paradigm) to shorten reaction time, or TMS to transiently modulate MEPs. However, it must be noted that contributions from other circuits cannot be excluded. As mentioned before, non-invasive measures in humans are rarely completely unambiguous, but convergent results using multiple measurements build a more convincing case than any single finding.

Applying this wearable device protocol in stroke survivors produced a small but significant improvement in upper limb function (Choudhury et al., 2020). We therefore wanted to translate the paradigm to spinal cord injury (SCI) survivors. The trial in stroke survivors targeted forearm muscles and all our previous work on healthy volunteers was done in biceps. Neither of these muscles provide a particularly good therapeutic target for chronic cervical SCI. Elbow extensor muscles show notoriously limited recovery in individuals with cervical SCI, while elbow flexors can recover fairly well. In the face of such asymmetrical recovery, strengthening extensors such as the triceps would provide the most functional benefits.

The RST is of interest after SCI, because reticulospinal connections to motoneurons can strengthen after CST lesions, partially restoring lost synaptic drive (Zaaimi et al., 2012). Following extensive CST damage such as after stroke or SCI, the reticulospinal tract may be the only remaining major descending motor pathway.

Prior studies usually attempted to boost functional recovery using neurostimulation targeted cortical changes, and while there typically are a small subset of spared or ipsilateral CST fibers after SCI, this was often met with disappointing results (Rothwell, 2016). The ability to manipulate plasticity in a sub-cortical target may thus be capable of achieving gains not accessible by other means.

Despite evidence that both proximal and distal muscles are innervated by the two pathways, the RST won't be able to replace a damaged CST. In contrast to CST, RST fibres branch extensively to innervate multiple motor neuron pools (Peterson et al., 1975, Matsuyama and Drew, 1997, Matsuyama et al., 1999), which limits its ability for fractionated output. After a CST lesion, the RST strengthens asymmetrically, which leads to an imbalanced restoration of muscle activity between different muscle groups.

We also need to keep in mind that enhanced RST output together with limited CST connections is associated with spasticity and there is an ongoing discussion about the potential negative impact of reticulospinal reorganization after CST damage on recovery. However, there is evidence from animal models (Wakabayashi et al., 2001, Ballermann and Fouad, 2006, Filli et al., 2014, May et al., 2017) and patient studies (Baker and Perez, 2017, Choudhury et al., 2020) that favour the interpretation that new RST connections can contribute to functional recovery after SCI. Importantly, spasticity did not increase in stroke survivors using the wearable device.

Due to the small number of chronic cervical SCI participants in our study, it is hard to draw decisive conclusions about the benefits of our plasticity protocol. We didn't observe the same changes expected from our biceps results. In addition to the limited number of participants, the considerable variability of impairment amongst SCI individuals as a factor cannot be understated. Each SCI lesion is highly individualized in regards to severity of impairment and which particular descending tracts are spared. Extensive damage to the CST during SCI almost certainly means other tracts, including the RST, suffered damage as well. Therefore, it would make sense that individuals with more severe damage to their RST won't benefit from boosting this particular connection and we need to increase our knowledge of the systemic reorganization that takes place after injury to be able to screen which patients will respond to which protocols.

In order to narrow down the heterogeneity of SCI study participants, a more thorough clinical assessment during recruitment is needed, with subjects having to fit into more restrictive inclusion criteria that are tailored to the target muscle. A subject with ASIA grade C or D, but normal motor function in the target muscle, is unlikely to show changes in that muscle after wearable device stimulation. Another way to stratify participants would be to screen for existing RST outflow. The StartReact paradigm in particular would lend itself to this task, as it is very simple and quick to complete. Subjects demonstrating a nonexistent or diminished

StartReact effect, could be argued to have severely damaged RST connections and hence be unlikely to benefit from this particular plasticity protocol.

It has also become clear that certain plasticity protocols won't work on all muscles equally. There appears to be a hierarchy in the ability to induce plastic changes across muscle groups, with extensors showing a lower potential compared with intrinsic hand muscles and flexors (Foysal and Baker, 2019). This difference was only seen in protocols that require integration of sensory input, but could explain our own results since the wearable device relies on precise timing of afferent and auditory input.

Interestingly, when targeting forearm extensors in stroke survivors, the protocol still led to significant improvement in upper limb function (Choudhury et al., 2020). This discrepancy might be explained with the fact that stimulation of extensors actually led to enhanced outputs of flexors, as seen in a previous study (Foysal and Baker, 2019), which then improved function. Alternatively, we might have to consider that distal extensor muscles are inherently different from more proximal extensors.

Despite the biceps usually recovering better compared to the more distal hand muscles, we observed the same MEP latency differences in both the biceps and the 1DI muscle and these differences decreased significantly after SCI, reflecting the global impact SCI has on the motor system.

Neurostimulation protocols have great potential to aid recovery after damage to the motor system, especially with the advancement of wearable technology that allows usage at home. However, depending on the exact type of injury and muscle groups targeted, different plasticity protocols might be of benefit, to target specific motor pathways. We need to keep in mind that these pathways are not redundant, but rather each functionally relevant, contributing uniquely to the motor system. There still remain considerable gaps in our knowledge that would enable us to use personalized treatments in order to increase both corticospinal and reticulospinal engagement at the right level to help recovery of motor function.

References

ALEXEEVA, N., BROTON, J. G. & CALANCIE, B. 1998. Latency of changes in spinal motoneuron excitability evoked by transcranial magnetic brain stimulation in spinal cord injured individuals. *Electroencephalogr Clin Neurophysiol,* 109**,** 297-303.

AMASSIAN, V. E., EBERLE, L., MACCABEE, P. J. & CRACCO, R. Q. 1992. Modelling magnetic coil excitation of human cerebral cortex with a peripheral nerve immersed in a brain-shaped volume conductor: the significance of fiber bending in excitation. *Electroencephalogr Clin Neurophysiol,* 85**,** 291-301.

AMASSIAN, V. E., STEWART, M., QUIRK, G. J. & ROSENTHAL, J. L. 1987. Physiological basis of motor effects of a transient stimulus to cerebral cortex. *Neurosurgery,* 20**,** 74-93.

ANDERSON, K. D. 2004. Targeting recovery: priorities of the spinal cord-injured population. *J Neurotrauma,* 21**,** 1371-83.

ANGELI, C. A., EDGERTON, V. R., GERASIMENKO, Y. P. & HARKEMA, S. J. 2014. Altering spinal cord excitability enables voluntary movements after chronic complete paralysis in humans. *Brain,* 137**,** 1394-409.

ARAI, N., OKABE, S., FURUBAYASHI, T., TERAO, Y., YUASA, K. & UGAWA, Y. 2005. Comparison between short train, monophasic and biphasic repetitive transcranial magnetic stimulation (rTMS) of the human motor cortex. *Clin Neurophysiol,* 116**,** 605-13.

BAKER, S. N. 2011. The primate reticulospinal tract, hand function and functional recovery. *J Physiol,* 589**,** 5603-12.

BAKER, S. N., OLIVIER, E. & LEMON, R. N. 1995. Task-Related Modulation in the Amplitude of the Direct Volley Evoked by Transcranial Magnetic Stimulation of the Motor Cortex and Recorded from the Medullary Pyramid in the Monkey. *Journal of Physiology-London,* 487p**,** P69-P70.

BAKER, S. N. & PEREZ, M. A. 2016. Evidence for a Contribution of the Reticulospinal Tract to Hand Control in Humans with Spinal Cord Injury *Journal of Neuroscience,* In submission.

BAKER, S. N. & PEREZ, M. A. 2017. Reticulospinal Contributions to Gross Hand Function after Human Spinal Cord Injury. *J Neurosci,* 37**,** 9778-9784.

BAKER, S. N., PHILBIN, N., SPINKS, R., PINCHES, E. M., WOLPERT, D. M., MACMANUS, D. G., PAULUIS, Q. & LEMON, R. N. 1999. Multiple single unit recording in the cortex of monkeys using independently moveable microelectrodes. *Journal of Neuroscience Methods,* 94**,** 5-17.

BAKER, S. N., ZAAIMI, B., FISHER, K. M., EDGLEY, S. A. & SOTEROPOULOS, D. S. 2015. Pathways mediating functional recovery. *Prog Brain Res,* 218**,** 389-412.

BALLERMANN, M. & FOUAD, K. 2006. Spontaneous locomotor recovery in spinal cord injured rats is accompanied by anatomical plasticity of reticulospinal fibers. *Eur J Neurosci,* 23**,** 1988-96.

BARKER, A. T., JALINOUS, R. & FREESTON, I. L. 1985. Non-invasive magnetic stimulation of human motor cortex. *Lancet,* 1**,** 1106-7.

BARRIONUEVO, G. & BROWN, T. H. 1983. Associative long-term potentiation in hippocampal slices. *Proc Natl Acad Sci U S A,* 80**,** 7347-51.

BARTHELEMY, D., WILLERSLEV-OLSEN, M., LUNDELL, H., BIERING-SORENSEN, F. & NIELSEN, J. B. 2015. Assessment of transmission in specific descending pathways in relation to gait and balance following spinal cord injury. *Prog Brain Res,* 218**,** 79-101.

BARTHELEMY, D., WILLERSLEV-OLSEN, M., LUNDELL, H., CONWAY, B. A., KNUDSEN, H., BIERING-SORENSEN, F. & NIELSEN, J. B. 2010. Impaired transmission in the corticospinal tract and gait disability in spinal cord injured persons. *J Neurophysiol,* 104**,** 1167-76.

BELHAJ-SAIF, A. & CHENEY, P. D. 2000. Plasticity in the distribution of the red nucleus output to forearm muscles after unilateral lesions of the pyramidal tract. *J Neurophysiol,* 83**,** 3147-53.

BENAVIDES, F. D., JO, H. J., LUNDELL, H., EDGERTON, V. R., GERASIMENKO, Y. & PEREZ, M. A. 2020. Cortical and Subcortical Effects of Transcutaneous Spinal Cord Stimulation in Humans with Tetraplegia. *J Neurosci,* 40**,** 2633-2643.

BENJAMINI, Y. & HOCHBERG, Y. 1995. Controlling the False Discovery Rate - a Practical and Powerful Approach to Multiple Testing. *Journal of the Royal Statistical Society Series B-Statistical Methodology,* 57**,** 289-300.

BERARDELLI, A., INGHILLERI, M., ROTHWELL, J. C., CRUCCU, G. & MANFREDI, M. 1991. Multiple firing of motoneurones is produced by cortical stimulation but not by direct activation of descending motor tracts. *Electroencephalogr Clin Neurophysiol,* 81**,** 240-2.

BERNHARD, C. G. & BOHM, E. 1954. Cortical representation and functional significance of the corticomotoneuronal system. *AMA Arch Neurol Psychiatry,* 72**,** 473-502.

BERREVOETS, C. E. & KUYPERS, H. G. 1975. Pericruciate cortical neurons projecting to brain stem reticular formation, dorsal column nuclei and spinal cord in the cat. *Neurosci Lett,* 1**,** 257-62.

BI, G. & POO, M. 2001. Synaptic modification by correlated activity: Hebb's postulate revisited. *Annu Rev Neurosci,* 24**,** 139-66.

BI, G. Q. & POO, M. M. 1998. Synaptic modifications in cultured hippocampal neurons: dependence on spike timing, synaptic strength, and postsynaptic cell type. *J Neurosci,* 18**,** 10464-72.

BLESCH, A. & TUSZYNSKI, M. H. 2009. Spinal cord injury: plasticity, regeneration and the challenge of translational drug development. *Trends Neurosci,* 32**,** 41-7.

BRASILNETO, J. P., COHEN, L. G., PANIZZA, M., NILSSON, J., ROTH, B. J. & HALLETT, M. 1992. Optimal Focal Transcranial Magnetic Activation of the Human Motor Cortex - Effects of Coil Orientation, Shape of the Induced Current Pulse, and Stimulus-Intensity. *Journal of Clinical Neurophysiology,* 9**,** 132-136.

BROUWER, B., BUGARESTI, J. & ASHBY, P. 1992. Changes in corticospinal facilitation of lower limb spinal motor neurons after spinal cord lesions. *J Neurol Neurosurg Psychiatry,* 55**,** 20-4.

BROWN, P. 1994. Pathophysiology of spasticity. *J Neurol Neurosurg Psychiatry,* 57**,** 773-7.

BROWN, P. 2002. Neurophysiology of the startle syndrome and hyperekplexia. *Adv Neurol,* 89**,** 153-9.

BROWN, P., ROTHWELL, J. C., THOMPSON, P. D., BRITTON, T. C., DAY, B. L. & MARSDEN, C. D. 1991. New observations on the normal auditory startle reflex in man. *Brain,* 114 (Pt 4)**,** 1891-902.

BUETEFISCH, C. M., HOWARD, C., KORB, C., HAUT, M. W., SHUSTER, L., PERGAMI, P., SMITH, C. & HOBBS, G. 2015. Conditions for enhancing the encoding of an elementary motor memory by rTMS. *Clin Neurophysiol,* 126**,** 581-93.

BUNDAY, K. L. & PEREZ, M. A. 2012. Impaired crossed facilitation of the corticospinal pathway after cervical spinal cord injury. *J Neurophysiol,* 107**,** 2901-11.

BUNGE, R. P., PUCKETT, W. R., BECERRA, J. L., MARCILLO, A. & QUENCER, R. M. 1993. Observations on the pathology of human spinal cord injury. A review and classification

of 22 new cases with details from a case of chronic cord compression with extensive focal demyelination. *Adv Neurol,* 59**,** 75-89.

BUONOMANO, D. V. & MERZENICH, M. M. 1998. Cortical plasticity: from synapses to maps. *Annu Rev Neurosci,* 21**,** 149-86.

BUYS, E. J., LEMON, R. N., MANTEL, G. W. & MUIR, R. B. 1986. Selective facilitation of different hand muscles by single corticospinal neurones in the conscious monkey. *J Physiol,* 381**,** 529-49.

CALANCIE, B., ALEXEEVA, N., BROTON, J. G., SUYS, S., HALL, A. & KLOSE, K. J. 1999. Distribution and latency of muscle responses to transcranial magnetic stimulation of motor cortex after spinal cord injury in humans. *J Neurotrauma,* 16**,** 49-67.

CALANCIE, B., MOLANO, M. R. & BROTON, J. G. 2004. EMG for assessing the recovery of voluntary movement after acute spinal cord injury in man. *Clin Neurophysiol,* 115**,** 1748-59.

CARIGA, P., CATLEY, M., NOWICKY, A. V., SAVIC, G., ELLAWAY, P. H. & DAVEY, N. J. 2002. Segmental recording of cortical motor evoked potentials from thoracic paravertebral myotomes in complete spinal cord injury. *Spine (Phila Pa 1976),* 27**,** 1438-43.

CARLSEN, A., CHUA, R., INGLIS, J. T., SANDERSON, D. J. & FRANKS, I. M. 2004a. Prepared movements are elicited early by startle. *J Mot Behav,* 36**,** 253-64.

CARLSEN, A. N., CHUA, R., INGLIS, J. T., SANDERSON, D. J. & FRANKS, I. M. 2004b. Can prepared responses be stored subcortically? *Exp Brain Res,* 159**,** 301-9.

CARLSEN, A. N., CHUA, R., INGLIS, J. T., SANDERSON, D. J. & FRANKS, I. M. 2009. Differential effects of startle on reaction time for finger and arm movements. *J Neurophysiol,* 101**,** 306-14.

CAURAUGH, J., LIGHT, K., KIM, S., THIGPEN, M. & BEHRMAN, A. 2000. Chronic motor dysfunction after stroke: recovering wrist and finger extension by electromyography-triggered neuromuscular stimulation. *Stroke,* 31**,** 1360-4.

CHARLTON, C. S., RIDDING, M. C., THOMPSON, P. D. & MILES, T. S. 2003. Prolonged peripheral nerve stimulation induces persistent changes in excitability of human motor cortex. *J Neurol Sci,* 208**,** 79-85.

CHEERAN, B., TALELLI, P., MORI, F., KOCH, G., SUPPA, A., EDWARDS, M., HOULDEN, H., BHATIA, K., GREENWOOD, R. & ROTHWELL, J. C. 2008. A common polymorphism in the brain-derived neurotrophic factor gene (BDNF) modulates human cortical plasticity and the response to rTMS. *J Physiol,* 586**,** 5717-25.

CHEN, R., YUNG, D. & LI, J. Y. 2003. Organization of ipsilateral excitatory and inhibitory pathways in the human motor cortex. *J Neurophysiol,* 89**,** 1256-64.

CHENEY, P. D., FETZ, E. E. & MEWES, K. 1991. Neural mechanisms underlying corticospinal and rubrospinal control of limb movements. *Prog Brain Res,* 87**,** 213-52.

CHOKROVERTY, S., WALCZAK, T. & HENING, W. 1992. Human startle reflex: technique and criteria for abnormal response. *Electroencephalogr Clin Neurophysiol,* 85**,** 236-42.

CHOUDHURY, S., SHOBHANA, A., SINGH, R., SEN, D., ANAND, S. S., SHUBHAM, S., BAKER, M. R., KUMAR, H. & BAKER, S. N. 2019. The Relationship Between Enhanced Reticulospinal Outflow and Upper Limb Function in Chronic Stroke Patients. *Neurorehabil Neural Repair,* 33**,** 375-383.

CHOUDHURY, S., SINGH, R., SHOBHANA, A., SEN, D., ANAND, S. S., SHUBHAM, S., GANGOPADHYAY, S., BAKER, M. R., KUMAR, H. & BAKER, S. N. 2020. A Novel Wearable Device for Motor Recovery of Hand Function in Chronic Stroke Survivors. *Neurorehabil Neural Repair,* 34**,** 600-608.

CIRILLO, J., CALABRO, F. J. & PEREZ, M. A. 2016. Impaired Organization of Paired-Pulse TMS-Induced I-Waves After Human Spinal Cord Injury. *Cereb Cortex,* 26**,** 2167-77.

CIRILLO, J. & PEREZ, M. A. 2015. Subcortical contribution to late TMS-induced I-waves in intact humans. *Front Integr Neurosci,* 9**,** 38.

COLEBATCH, J. G. & GANDEVIA, S. C. 1989. The distribution of muscular weakness in upper motor neuron lesions affecting the arm. *Brain,* 112 (Pt 3)**,** 749-63.

CORTES, J. C., GOLDSMITH, J., HARRAN, M. D., XU, J., KIM, N., SCHAMBRA, H. M., LUFT, A. R., CELNIK, P., KRAKAUER, J. W. & KITAGO, T. 2017. A Short and Distinct Time Window for Recovery of Arm Motor Control Early After Stroke Revealed With a Global Measure of Trajectory Kinematics. *Neurorehabil Neural Repair,* 31**,** 552-560.

CURT, A., KECK, M. E. & DIETZ, V. 1998. Functional outcome following spinal cord injury: significance of motor-evoked potentials and ASIA scores. *Arch Phys Med Rehabil,* 79**,** 81-6.

CURT, A., VAN HEDEL, H. J., KLAUS, D., DIETZ, V. & GROUP, E.-S. S. 2008. Recovery from a spinal cord injury: significance of compensation, neural plasticity, and repair. *J Neurotrauma,* 25**,** 677-85.

DARLING, W. G., GE, J., STILWELL-MORECRAFT, K. S., ROTELLA, D. L., PIZZIMENTI, M. A. & MORECRAFT, R. J. 2018. Hand Motor Recovery Following Extensive Frontoparietal Cortical Injury Is Accompanied by Upregulated Corticoreticular Projections in Monkey. *J Neurosci,* 38**,** 6323-6339.

DAVEY, N. J., ROMAIGUERE, P., MASKILL, D. W. & ELLAWAY, P. H. 1994. Suppression of voluntary motor activity revealed using transcranial magnetic stimulation of the motor cortex in man. *J Physiol,* 477**,** 223-35.

DAVEY, N. J., SMITH, H. C., SAVIC, G., MASKILL, D. W., ELLAWAY, P. H. & FRANKEL, H. L. 1999. Comparison of input-output patterns in the corticospinal system of normal subjects and incomplete spinal cord injured patients. *Exp Brain Res,* 127**,** 382-90.

DAVEY, N. J., SMITH, H. C., WELLS, E., MASKILL, D. W., SAVIC, G., ELLAWAY, P. H. & FRANKEL, H. L. 1998. Responses of thenar muscles to transcranial magnetic stimulation of the motor cortex in patients with incomplete spinal cord injury. *J Neurol Neurosurg Psychiatry,* 65**,** 80-7.

DAVIDSON, A. G. & BUFORD, J. A. 2004. Motor outputs from the primate reticular formation to shoulder muscles as revealed by stimulus-triggered averaging. *J Neurophysiol,* 92**,** 83-95.

DAVIDSON, A. G. & BUFORD, J. A. 2006. Bilateral actions of the reticulospinal tract on arm and shoulder muscles in the monkey: stimulus triggered averaging. *Exp Brain Res,* 173**,** 25-39.

DAVIDSON, A. G., SCHIEBER, M. H. & BUFORD, J. A. 2007. Bilateral spike-triggered average effects in arm and shoulder muscles from the monkey pontomedullary reticular formation. *J Neurosci,* 27**,** 8053-8.

DAVIS, M., GENDELMAN, D. S., TISCHLER, M. D. & GENDELMAN, P. M. 1982. A primary acoustic startle circuit: lesion and stimulation studies. *J Neurosci,* 2**,** 791-805.

DAY, B. L., DRESSLER, D., MAERTENS DE NOORDHOUT, A., MARSDEN, C. D., NAKASHIMA, K., ROTHWELL, J. C. & THOMPSON, P. D. 1989. Electric and magnetic stimulation of human motor cortex: surface EMG and single motor unit responses. *J Physiol,* 412**,** 449-73.

DEAN, L. R. & BAKER, S. N. 2017. Fractionation of muscle activity in rapid responses to startling cues. *J Neurophysiol,* 117**,** 1713-1719.

DELWAIDE, P. J. & SCHEPENS, B. 1995. Auditory startle (audio-spinal) reaction in normal man: EMG responses and H reflex changes in antagonistic lower limb muscles. *Electroencephalogr Clin Neurophysiol,* 97**,** 416-23.

DI LAZZARO, V., OLIVIERO, A., PROFICE, P., SATURNO, E., PILATO, F., INSOLA, A., MAZZONE, P., TONALI, P. & ROTHWELL, J. C. 1998a. Comparison of descending volleys evoked by

transcranial magnetic and electric stimulation in conscious humans. *Electroencephalogr Clin Neurophysiol,* 109**,** 397-401.

DI LAZZARO, V., OLIVIERO, A., SATURNO, E., PILATO, F., INSOLA, A., MAZZONE, P., PROFICE, P., TONALI, P. & ROTHWELL, J. C. 2001. The effect on corticospinal volleys of reversing the direction of current induced in the motor cortex by transcranial magnetic stimulation. *Exp Brain Res,* 138**,** 268-73.

DI LAZZARO, V., PROFICE, P., RANIERI, F., CAPONE, F., DILEONE, M., OLIVIERO, A. & PILATO, F. 2012. I-wave origin and modulation. *Brain Stimul,* 5**,** 512-25.

DI LAZZARO, V., RESTUCCIA, D., OLIVIERO, A., PROFICE, P., FERRARA, L., INSOLA, A., MAZZONE, P., TONALI, P. & ROTHWELL, J. C. 1998b. Effects of voluntary contraction on descending volleys evoked by transcranial stimulation in conscious humans. *J Physiol,* 508 (Pt 2)**,** 625-33.

DI LAZZARO, V., ROTHWELL, J. & CAPOGNA, M. 2018. Noninvasive Stimulation of the Human Brain: Activation of Multiple Cortical Circuits. *Neuroscientist,* 24**,** 246-260.

DI LAZZARO, V. & ROTHWELL, J. C. 2014. Corticospinal activity evoked and modulated by non-invasive stimulation of the intact human motor cortex. *J Physiol,* 592**,** 4115-28.

DI LAZZARO, V. & ZIEMANN, U. 2013. The contribution of transcranial magnetic stimulation in the functional evaluation of microcircuits in human motor cortex. *Front Neural Circuits,* 7**,** 18.

DI LAZZARO, V., ZIEMANN, U. & LEMON, R. N. 2008. State of the art: Physiology of transcranial motor cortex stimulation. *Brain Stimul,* 1**,** 345-62.

DITUNNO, J. F., JR., COHEN, M. E., HAUCK, W. W., JACKSON, A. B. & SIPSKI, M. L. 2000. Recovery of upper-extremity strength in complete and incomplete tetraplegia: a multicenter study. *Arch Phys Med Rehabil,* 81**,** 389-93.

DITUNNO, J. F., JR., STOVER, S. L., FREED, M. M. & AHN, J. H. 1992. Motor recovery of the upper extremities in traumatic quadriplegia: a multicenter study. *Arch Phys Med Rehabil,* 73**,** 431-6.

DREW, T., DUBUC, R. & ROSSIGNOL, S. 1986. Discharge patterns of reticulospinal and other reticular neurons in chronic, unrestrained cats walking on a treadmill. *J Neurophysiol,* 55**,** 375-401.

EDGLEY, S. A., EYRE, J. A., LEMON, R. N. & MILLER, S. 1990. Excitation of the corticospinal tract by electromagnetic and electrical stimulation of the scalp in the macaque monkey. *J Physiol,* 425**,** 301-20.

EDGLEY, S. A., EYRE, J. A., LEMON, R. N. & MILLER, S. 1997. Comparison of activation of corticospinal neurons and spinal motor neurons by magnetic and electrical transcranial stimulation in the lumbosacral cord of the anaesthetized monkey. *Brain,* 120 (Pt 5)**,** 839-53.

EDWARDSON, M. A., AVERY, D. H. & FETZ, E. E. 2014. Volitional muscle activity paired with transcranial magnetic stimulation increases corticospinal excitability. *Front Neurosci,* 8**,** 442.

ELLAWAY, P. H., ANAND, P., BERGSTROM, E. M., CATLEY, M., DAVEY, N. J., FRANKEL, H. L., JAMOUS, A., MATHIAS, C., NICOTRA, A., SAVIC, G., SHORT, D. & THEODOROU, S. 2004. Towards improved clinical and physiological assessments of recovery in spinal cord injury: a clinical initiative. *Spinal Cord,* 42**,** 325-37.

ELLAWAY, P. H., CATLEY, M., DAVEY, N. J., KUPPUSWAMY, A., STRUTTON, P., FRANKEL, H. L., JAMOUS, A. & SAVIC, G. 2007. Review of physiological motor outcome measures in spinal cord injury using transcranial magnetic stimulation and spinal reflexes. *J Rehabil Res Dev,* 44**,** 69-76.

ESTORES, I. M. 2003. The consumer's perspective and the professional literature: What do persons with spinal cord injury want? *Journal of Rehabilitation Research and Development,* 40**,** 93-98.

FEDERICO, P. & PEREZ, M. A. 2017. Distinct Corticocortical Contributions to Human Precision and Power Grip. *Cereb Cortex,* 27**,** 5070-5082.

FELLOWS, S. J., TOPPER, R., SCHWARZ, M., THILMANN, A. F. & NOTH, J. 1996. Stretch reflexes of the proximal arm in a patient with mirror movements: absence of bilateral long-latency components. *Electroencephalogr Clin Neurophysiol,* 101**,** 79-83.

FILLI, L., ENGMANN, A. K., ZORNER, B., WEINMANN, O., MORAITIS, T., GULLO, M., KASPER, H., SCHNEIDER, R. & SCHWAB, M. E. 2014. Bridging the gap: a reticulo-propriospinal detour bypassing an incomplete spinal cord injury. *J Neurosci,* 34**,** 13399-410.

FISHER, K. M., CHINNERY, P. F., BAKER, S. N. & BAKER, M. R. 2013. Enhanced reticulospinal output in patients with (REEP1) hereditary spastic paraplegia type 31. *J Neurol,* 260**,** 3182-4.

FISHER, K. M., JILLANI, N. E., OLUOCH, G. O. & BAKER, S. N. 2015. Blocking central pathways in the primate motor system using high-frequency sinusoidal current. *J Neurophysiol,* 113**,** 1670-80.

FISHER, K. M., ZAAIMI, B. & BAKER, S. N. 2012. Reticular formation responses to magnetic brain stimulation of primary motor cortex. *J Physiol,* 590**,** 4045-60.

FISHER, K. M., ZAAIMI, B., EDGLEY, S. A. & BAKER, S. N. 2021. Extensive Cortical Convergence to Primate Reticulospinal Pathways. *J Neurosci,* 41**,** 1005-1018.

FITZPATRICK, R. C. & DAY, B. L. 2004. Probing the human vestibular system with galvanic stimulation. *J Appl Physiol (1985),* 96**,** 2301-16.

FITZPATRICK, S. C., LUU, B. L., BUTLER, J. E. & TAYLOR, J. L. 2016. More conditioning stimuli enhance synaptic plasticity in the human spinal cord. *Clin Neurophysiol,* 127**,** 724-731.

FOYSAL, K. M., DE CARVALHO, F. & BAKER, S. N. 2016. Spike Timing-Dependent Plasticity in the Long-Latency Stretch Reflex Following Paired Stimulation from a Wearable Electronic Device. *J Neurosci,* 36**,** 10823-10830.

FOYSAL, K. M. R. & BAKER, S. N. 2019. A hierarchy of corticospinal plasticity in human hand and forearm muscles. *J Physiol,* 597**,** 2729-2739.

FOYSAL, K. M. R. & BAKER, S. N. 2020. Induction of plasticity in the human motor system by motor imagery and transcranial magnetic stimulation. *J Physiol,* 598**,** 2385-2396.

FREGOSI, M., CONTESTABILE, A., HAMADJIDA, A. & ROUILLER, E. M. 2017. Corticobulbar projections from distinct motor cortical areas to the reticular formation in macaque monkeys. *Eur J Neurosci,* 45**,** 1379-1395.

FUJIYAMA, H., HYDE, J., HINDER, M. R., KIM, S. J., MCCORMACK, G. H., VICKERS, J. C. & SUMMERS, J. J. 2014. Delayed plastic responses to anodal tDCS in older adults. *Front Aging Neurosci,* 6**,** 115.

FURUBAYASHI, T., UGAWA, Y., TERAO, Y., HANAJIMA, R., SAKAI, K., MACHII, K., MOCHIZUKI, H., SHIIO, Y., UESUGI, H., ENOMOTO, H. & KANAZAWA, I. 2000. The human hand motor area is transiently suppressed by an unexpected auditory stimulus. *Clin Neurophysiol,* 111**,** 178-83.

GALEA, M. P. & DARIAN-SMITH, I. 1994. Multiple corticospinal neuron populations in the macaque monkey are specified by their unique cortical origins, spinal terminations, and connections. *Cereb Cortex,* 4**,** 166-94.

GANDEVIA, S. C., PETERSEN, N., BUTLER, J. E. & TAYLOR, J. L. 1999. Impaired response of human motoneurones to corticospinal stimulation after voluntary exercise. *J Physiol,* 521 Pt 3**,** 749-59.

GERMANN, M. & BAKER, S. N. 2021. Evidence for Subcortical Plasticity after Paired Stimulation from a Wearable Device. *J Neurosci,* 41**,** 1418-1428.

GOLDSMITH, J. & KITAGO, T. 2016. Assessing systematic effects of stroke on motorcontrol by using hierarchical function-on-scalar regression. *J R Stat Soc Ser C Appl Stat,* 65**,** 215-236.

GRIFFITHS, I. R. & MCCULLOCH, M. C. 1983. Nerve-Fibers in Spinal-Cord Impact Injuries .1. Changes in the Myelin Sheath during the Initial 5 Weeks. *Journal of the Neurological Sciences,* 58**,** 335-349.

GROPPA, S., WERNER-PETROLL, N., MUNCHAU, A., DEUSCHL, G., RUSCHWORTH, M. F. & SIEBNER, H. R. 2012. A novel dual-site transcranial magnetic stimulation paradigm to probe fast facilitatory inputs from ipsilateral dorsal premotor cortex to primary motor cortex. *Neuroimage,* 62**,** 500-9.

HAMADA, M., MURASE, N., HASAN, A., BALARATNAM, M. & ROTHWELL, J. C. 2013. The role of interneuron networks in driving human motor cortical plasticity. *Cereb Cortex,* 23**,** 1593-605.

HAMMOND, G. R. 1973. Lesions of pontine and medullary reticular formation and prestimulus inhibition of the acoustic startle reaction in rats. *Physiol Behav,* 10**,** 239-43.

HANNAH, R. & ROTHWELL, J. C. 2017. Pulse Duration as Well as Current Direction Determines the Specificity of Transcranial Magnetic Stimulation of Motor Cortex during Contraction. *Brain Stimul,* 10**,** 106-115.

HEBB, D. O. 1949. *The organisation of behaviour: a neuropsychological theory*, Science Editions New York.

HERBERT, W. J., DAVIDSON, A. G. & BUFORD, J. A. 2010. Measuring the motor output of the pontomedullary reticular formation in the monkey: do stimulus-triggered averaging and stimulus trains produce comparable results in the upper limbs? *Exp Brain Res,* 203**,** 271-83.

HOLSTEGE, G. & KUYPERS, H. G. 1982. The anatomy of brain stem pathways to the spinal cord in cat. A labeled amino acid tracing study. *Prog Brain Res,* 57**,** 145-75.

HOLSTEGE, J. C. & KUYPERS, H. G. 1987. Brainstem projections to spinal motoneurons: an update. *Neuroscience,* 23**,** 809-21.

HONEYCUTT, C. F., KHAROUTA, M. & PERREAULT, E. J. 2013. Evidence for reticulospinal contributions to coordinated finger movements in humans. *J Neurophysiol,* 110**,** 1476-83.

HONEYCUTT, C. F. & PERREAULT, E. J. 2012. Planning of ballistic movement following stroke: insights from the startle reflex. *PLoS One,* 7**,** e43097.

HUANG, Y. Z., EDWARDS, M. J., ROUNIS, E., BHATIA, K. P. & ROTHWELL, J. C. 2005. Theta burst stimulation of the human motor cortex. *Neuron,* 45**,** 201-6.

ILIC, T. V., MEINTZSCHEL, F., CLEFF, U., RUGE, D., KESSLER, K. R. & ZIEMANN, U. 2002. Short-interval paired-pulse inhibition and facilitation of human motor cortex: the dimension of stimulus intensity. *J Physiol,* 545**,** 153-67.

IRVINE, D. R. & JACKSON, G. D. 1983. Auditory input to neurons in mesencephalic and rostral pontine reticular formation: an electrophysiological and horseradish peroxidase study in the cat. *J Neurophysiol,* 49**,** 1319-33.

ISA, T. & SASAKI, S. 2002. Brainstem control of head movements during orienting; organization of the premotor circuits. *Prog Neurobiol,* 66**,** 205-41.

IWAMOTO, Y., SASAKI, S. & SUZUKI, I. 1990. Input-output organization of reticulospinal neurones, with special reference to connexions with dorsal neck motoneurones in the cat. *Exp Brain Res,* 80**,** 260-76.

JANKOWSKA, E., HAMMAR, I., SLAWINSKA, U., MALESZAK, K. & EDGLEY, S. A. 2003. Neuronal basis of crossed actions from the reticular formation on feline hindlimb motoneurons. *J Neurosci,* 23**,** 1867-78.

JANKOWSKA, E., PADEL, Y. & TANAKA, R. 1975. The mode of activation of pyramidal tract cells by intracortical stimuli. *J Physiol,* 249**,** 617-36.

JINNAI, K. 1984. Electrophysiological study on the corticoreticular projection neurons of the cat. *Brain Res,* 291**,** 145-9.

JO, H. J., DI LAZZARO, V. & PEREZ, M. A. 2018. Effect of coil orientation on motor-evoked potentials in humans with tetraplegia. *J Physiol,* 596**,** 4909-4921.

JONES, B. E. & YANG, T. Z. 1985. The efferent projections from the reticular formation and the locus coeruleus studied by anterograde and retrograde axonal transport in the rat. *J Comp Neurol,* 242**,** 56-92.

JUNG, N. H., DELVENDAHL, I., PECHMANN, A., GLEICH, B., GATTINGER, N., SIEBNER, H. R. & MALL, V. 2012. Transcranial magnetic stimulation with a half-sine wave pulse elicits direction-specific effects in human motor cortex. *BMC Neurosci,* 13**,** 139.

KAKULAS, B. A. 1999. A review of the neuropathology of human spinal cord injury with emphasis on special features. *J Spinal Cord Med,* 22**,** 119-24.

KAKULAS, B. A. 2004. Neuropathology: the foundation for new treatments in spinal cord injury. *Spinal Cord,* 42**,** 549-63.

KAMPER, D. G., HARVEY, R. L., SURESH, S. & RYMER, W. Z. 2003. Relative contributions of neural mechanisms versus muscle mechanics in promoting finger extension deficits following stroke. *Muscle Nerve,* 28**,** 309-18.

KARBASFOROUSHAN, H., COHEN-ADAD, J. & DEWALD, J. P. A. 2019. Brainstem and spinal cord MRI identifies altered sensorimotor pathways post-stroke. *Nat Commun,* 10**,** 3524.

KEIZER, K. & KUYPERS, H. G. 1989. Distribution of corticospinal neurons with collaterals to the lower brain stem reticular formation in monkey (Macaca fascicularis). *Exp Brain Res,* 74**,** 311-8.

KENNEDY, P. R. 1990. Corticospinal, rubrospinal and rubro-olivary projections: a unifying hypothesis. *Trends Neurosci,* 13**,** 474-9.

KERNELL, D. & CHIEN-PING, W. U. 1967. Responses of the pyramidal tract to stimulation of the baboon's motor cortex. *J Physiol,* 191**,** 653-72.

KIMURA, T., HAGGARD, P. & GOMI, H. 2006. Transcranial magnetic stimulation over sensorimotor cortex disrupts anticipatory reflex gain modulation for skilled action. *J Neurosci,* 26**,** 9272-81.

KITAGO, T., GOLDSMITH, J., HARRAN, M., KANE, L., BERARD, J., HUANG, S., RYAN, S. L., MAZZONI, P., KRAKAUER, J. W. & HUANG, V. S. 2015. Robotic therapy for chronic stroke: general recovery of impairment or improved task-specific skill? *J Neurophysiol,* 114**,** 1885-94.

KRAUS, D., NAROS, G., BAUER, R., KHADEMI, F., LEAO, M. T., ZIEMANN, U. & GHARABAGHI, A. 2016. Brain State-Dependent Transcranial Magnetic Closed-Loop Stimulation Controlled by Sensorimotor Desynchronization Induces Robust Increase of Corticospinal Excitability. *Brain Stimul,* 9**,** 415-424.

KUHN, A. A., SHAROTT, A., TROTTENBERG, T., KUPSCH, A. & BROWN, P. 2004. Motor cortex inhibition induced by acoustic stimulation. *Exp Brain Res,* 158**,** 120-4.

KUMPULAINEN, S., MRACHACZ-KERSTING, N., PELTONEN, J., VOIGT, M. & AVELA, J. 2012. The optimal interstimulus interval and repeatability of paired associative stimulation when the soleus muscle is targeted. *Exp Brain Res,* 221**,** 241-9.

KURTZER, I. L. 2014. Long-latency reflexes account for limb biomechanics through several supraspinal pathways. *Front Integr Neurosci,* 8**,** 99.

KUYPERS, H. 1981a. Anatomy of Descending Pathways: American Physiological Society. *Bethesda, MD*.

KUYPERS, H. 1981b. Anatomy of the descending pathways. *Handbook of Physiology-the nervous system II.*, 56-59.

LACROIX, S., HAVTON, L. A., MCKAY, H., YANG, H., BRANT, A., ROBERTS, J. & TUSZYNSKI, M. H. 2004. Bilateral corticospinal projections arise from each motor cortex in the macaque monkey: a quantitative study. *J Comp Neurol,* 473**,** 147-61.

LADPLI, R. & BRODAL, A. 1968. Experimental studies of commissural and reticular formation projections from the vestibular nuclei in the cat. *Brain Res,* 8**,** 65-96.

LAWRENCE, D. G. & KUYPERS, H. G. 1968a. The functional organization of the motor system in the monkey. I. The effects of bilateral pyramidal lesions. *Brain,* 91**,** 1-14.

LAWRENCE, D. G. & KUYPERS, H. G. 1968b. The functional organization of the motor system in the monkey. II. The effects of lesions of the descending brain-stem pathways. *Brain,* 91**,** 15-36.

LEIRAS, R., VELO, P., MARTIN-CORA, F. & CANEDO, A. 2010. Processing afferent proprioceptive information at the main cuneate nucleus of anesthetized cats. *J Neurosci,* 30**,** 15383-99.

LEITNER, D. S., POWERS, A. S. & HOFFMAN, H. S. 1980. The neural substrate of the startle response. *Physiol Behav,* 25**,** 291-7.

LEMON, R. N. 2008. Descending pathways in motor control. *Annu Rev Neurosci,* 31**,** 195-218.

LINGENHOHL, K. & FRIAUF, E. 1992. Giant neurons in the caudal pontine reticular formation receive short latency acoustic input: an intracellular recording and HRP-study in the rat. *J Comp Neurol,* 325**,** 473-92.

LISSENS, M. A. & VANDERSTRAETEN, G. G. 1996. Motor evoked potentials of the respiratory muscles in tetraplegic patients. *Spinal Cord,* 34**,** 673-8.

LONG, J., FEDERICO, P. & PEREZ, M. A. 2017. A novel cortical target to enhance hand motor output in humans with spinal cord injury. *Brain,* 140**,** 1619-1632.

MAERTENS DE NOORDHOUT, A., ROTHWELL, J. C., DAY, B. L., DRESSLER, D., NAKASHIMA, K., THOMPSON, P. D. & MARSDEN, C. D. 1992. Effect of digital nerve stimuli on responses to electrical or magnetic stimulation of the human brain. *J Physiol,* 447**,** 535-48.

MAIER, M. A., OLIVIER, E., BAKER, S. N., KIRKWOOD, P. A., MORRIS, T. & LEMON, R. N. 1997. Direct and indirect corticospinal control of arm and hand motoneurons in the squirrel monkey (Saimiri sciureus). *J Neurophysiol,* 78**,** 721-33.

MARINO, R. J., SHEA, J. A. & STINEMAN, M. G. 1998. The Capabilities of Upper Extremity instrument: reliability and validity of a measure of functional limitation in tetraplegia. *Arch Phys Med Rehabil,* 79**,** 1512-21.

MARKRAM, H., LUBKE, J., FROTSCHER, M. & SAKMANN, B. 1997. Regulation of synaptic efficacy by coincidence of postsynaptic APs and EPSPs. *Science,* 275**,** 213-5.

MARTIN, G. F., VERTES, R. P. & WALTZER, R. 1985. Spinal projections of the gigantocellular reticular formation in the rat. Evidence for projections from different areas to laminae I and II and lamina IX. *Exp Brain Res,* 58**,** 154-62.

MATSUMOTO, J., FUHR, P., NIGRO, M. & HALLETT, M. 1992. Physiological abnormalities in hereditary hyperekplexia. *Ann Neurol,* 32**,** 41-50.

MATSUYAMA, K. & DREW, T. 1997. Organization of the projections from the pericruciate cortex to the pontomedullary brainstem of the cat: a study using the anterograde tracer Phaseolus vulgaris-leucoagglutinin. *J Comp Neurol,* 389**,** 617-41.

MATSUYAMA, K. & DREW, T. 2000. Vestibulospinal and reticulospinal neuronal activity during locomotion in the intact cat. II. Walking on an inclined plane. *J Neurophysiol,* 84**,** 2257-76.

MATSUYAMA, K., MORI, F., KUZE, B. & MORI, S. 1999. Morphology of single pontine reticulospinal axons in the lumbar enlargement of the cat: A study using the anterograde tracer PHA-L. *Journal of Comparative Neurology,* 410**,** 413-430.

MAY, Z., FENRICH, K. K., DAHLBY, J., BATTY, N. J., TORRES-ESPIN, A. & FOUAD, K. 2017. Following Spinal Cord Injury Transected Reticulospinal Tract Axons Develop New Collateral Inputs to Spinal Interneurons in Parallel with Locomotor Recovery. *Neural Plast,* 2017**,** 1932875.

MAZEVET, D., MEUNIER, S., PRADAT-DIEHL, P., MARCHAND-PAUVERT, V. & PIERROT-DESEILLIGNY, E. 2003. Changes in propriospinally mediated excitation of upper limb motoneurons in stroke patients. *Brain,* 126**,** 988-1000.

MCDONNELL, M. N. & RIDDING, M. C. 2006. Afferent stimulation facilitates performance on a novel motor task. *Exp Brain Res,* 170**,** 109-15.

MCKAY, D., BROOKER, R., GIACOMIN, P., RIDDING, M. & MILES, T. 2002. Time course of induction of increased human motor cortex excitability by nerve stimulation. *Neuroreport,* 13**,** 1271-3.

MCKAY, W. B., LIM, H. K., PRIEBE, M. M., STOKIC, D. S. & SHERWOOD, A. M. 2004. Clinical neurophysiological assessment of residual motor control in post-spinal cord injury paralysis. *Neurorehabil Neural Repair,* 18**,** 144-53.

MCKAY, W. B., OVECHKIN, A. V., VITAZ, T. W., TERSON DE PALEVILLE, D. G. & HARKEMA, S. J. 2011. Neurophysiological characterization of motor recovery in acute spinal cord injury. *Spinal Cord,* 49**,** 421-9.

MCNEIL, C. J., BUTLER, J. E., TAYLOR, J. L. & GANDEVIA, S. C. 2013. Testing the excitability of human motoneurons. *Front Hum Neurosci,* 7**,** 152.

MERTON, P. A. & MORTON, H. B. 1980. Stimulation of the cerebral cortex in the intact human subject. *Nature,* 285**,** 227.

MIDDLETON, J., TRAN, Y. & CRAIG, A. 2007. Relationship between quality of life and self-efficacy in persons with spinal cord injuries. *Arch Phys Med Rehabil,* 88**,** 1643-8.

MILLS, K. R., BONIFACE, S. J. & SCHUBERT, M. 1992. Magnetic brain stimulation with a double coil: the importance of coil orientation. *Electroencephalogr Clin Neurophysiol,* 85**,** 17-21.

MIN, Y. S., CHANG, Y., PARK, J. W., LEE, J. M., CHA, J., YANG, J. J., KIM, C. H., HWANG, J. M., YOO, J. N. & JUNG, T. D. 2015. Change of Brain Functional Connectivity in Patients With Spinal Cord Injury: Graph Theory Based Approach. *Ann Rehabil Med,* 39**,** 374-83.

MRACHACZ-KERSTING, N., FONG, M., MURPHY, B. A. & SINKJAER, T. 2007. Changes in excitability of the cortical projections to the human tibialis anterior after paired associative stimulation. *J Neurophysiol,* 97**,** 1951-8.

MURAKAMI, T., SAKUMA, K., NOMURA, T., UEMURA, Y., HASHIMOTO, I. & NAKASHIMA, K. 2008. Changes in somatosensory-evoked potentials and high-frequency oscillations after paired-associative stimulation. *Exp Brain Res,* 184**,** 339-47.

MURRAY, E. A. & COULTER, J. D. 1981. Organization of corticospinal neurons in the monkey. *J Comp Neurol,* 195**,** 339-65.

NAKAJIMA, T., TAZOE, T., SAKAMOTO, M., ENDOH, T., SHIBUYA, S., ELIAS, L. A., MEZZARANE, R. A., KOMIYAMA, T. & OHKI, Y. 2017. Reassessment of Non-Monosynaptic Excitation from the Motor Cortex to Motoneurons in Single Motor Units of the Human Biceps Brachii. *Front Hum Neurosci,* 11**,** 19.

NAKASHIMA, K., WANG, Y., SHIMODA, M., SHIMOYAMA, R., YOKOYAMA, Y. & TAKAHASHI, K. 1994. Auditory effects on the motor responses after magnetic cortical stimulation and on the H-reflexes in patients with Parkinson's disease. *J Neurol Sci,* 122**,** 15-9.

NATHAN, P. W. & SMITH, M. C. 1955. Long descending tracts in man. I. Review of present knowledge. *Brain,* 78**,** 248-303.

NI, Z., CHARAB, S., GUNRAJ, C., NELSON, A. J., UDUPA, K., YEH, I. J. & CHEN, R. 2011. Transcranial magnetic stimulation in different current directions activates separate cortical circuits. *J Neurophysiol,* 105**,** 749-56.

NITSCHE, M. A. & PAULUS, W. 2000. Excitability changes induced in the human motor cortex by weak transcranial direct current stimulation. *J Physiol,* 527 Pt 3**,** 633-9.

NONNEKES, J., GEURTS, A. C., NIJHUIS, L. B., VAN GEEL, K., SNIJDERS, A. H., BLOEM, B. R. & WEERDESTEYN, V. 2014a. Reduced StartReact effect and freezing of gait in Parkinson's disease: two of a kind? *J Neurol,* 261**,** 943-50.

NONNEKES, J., OUDE NIJHUIS, L. B., DE NIET, M., DE BOT, S. T., PASMAN, J. W., VAN DE WARRENBURG, B. P., BLOEM, B. R., WEERDESTEYN, V. & GEURTS, A. C. 2014b. StartReact restores reaction time in HSP: evidence for subcortical release of a motor program. *J Neurosci,* 34**,** 275-81.

ONODERA, S. & HICKS, T. P. 2010. Carbocyanine dye usage in demarcating boundaries of the aged human red nucleus. *PLoS One,* 5**,** e14430.

OZDEMIR, R. A. & PEREZ, M. A. 2018. Afferent input and sensory function after human spinal cord injury. *J Neurophysiol,* 119**,** 134-144.

PALMER, E. & ASHBY, P. 1992. Corticospinal projections to upper limb motoneurones in humans. *J Physiol,* 448**,** 397-412.

PARE, D., SMITH, Y., PARENT, A. & STERIADE, M. 1988. Projections of brainstem core cholinergic and non-cholinergic neurons of cat to intralaminar and reticular thalamic nuclei. *Neuroscience,* 25**,** 69-86.

PARK, M. C., BELHAJ-SAIF, A. & CHENEY, P. D. 2004. Properties of primary motor cortex output to forelimb muscles in rhesus macaques. *J Neurophysiol,* 92**,** 2968-84.

PATTON, H. D. & AMASSIAN, V. E. 1954. Single and multiple-unit analysis of cortical stage of pyramidal tract activation. *J Neurophysiol,* 17**,** 345-63.

PEREZ, M. A. 2012. Transcranial Magnetic Stimulation and Spinal Cord Injury. *In:* CHEN, R. & ROTHWELL, J. C. (eds.) *Cortical Connectivity.* Berlin, Heidelberg: Springer Berlin Heidelberg.

PERLMUTTER, S. I., MAIER, M. A. & FETZ, E. E. 1998. Activity of spinal interneurons and their effects on forearm muscles during voluntary wrist movements in the monkey. *Journal of Neurophysiology,* 80**,** 2475-2494.

PESTRONK, A. & DRACHMAN, D. B. 1988. Motor nerve outgrowth: reduced capacity for sprouting in the terminals of longer axons. *Brain Res,* 463**,** 218-22.

PETERSEN, J. A., WILM, B. J., VON MEYENBURG, J., SCHUBERT, M., SEIFERT, B., NAJAFI, Y., DIETZ, V. & KOLLIAS, S. 2012. Chronic cervical spinal cord injury: DTI correlates with clinical and electrophysiological measures. *J Neurotrauma,* 29**,** 1556-66.

PETERSEN, N. T., TAYLOR, J. L. & GANDEVIA, S. C. 2002. The effect of electrical stimulation of the corticospinal tract on motor units of the human biceps brachii. *J Physiol,* 544**,** 277-84.

PETERSON, B. W. & ABZUG, C. 1975. Properties of projections from vestibular nuclei to medial reticular formation in the cat. *J Neurophysiol,* 38**,** 1421-35.

PETERSON, B. W., MAUNZ, R. A., PITTS, N. G. & MACKEL, R. G. 1975. Patterns of projection and braching of reticulospinal neurons. *Exp Brain Res,* 23**,** 333-51.

PETTERSSON, L. G., BLAGOVECHTCHENSKI, E., PERFILIEV, S., KRASNOCHOKOVA, E. & LUNDBERG, A. 2000. Recovery of food-taking in cats after lesions of the corticospinal (complete) and rubrospinal (complete and incomplete) tracts. *Neurosci Res,* 38**,** 109-12.

PHILLIPS, C. G. & PORTER, R. 1964. The pyramidal projection to motoneurones of some muscle groups of the baboon's forelimb. *Prog Brain Res,* 12**,** 222-245.

PITCHER, J. B., RIDDING, M. C. & MILES, T. S. 2003. Frequency-dependent, bi-directional plasticity in motor cortex of human adults. *Clin Neurophysiol,* 114**,** 1265-71.

PORTER, R. & LEMON, R. 1993. *Corticospinal function and voluntary movement*, Oxford University Press, USA.

PRENTICE, S. D. & DREW, T. 2001. Contributions of the reticulospinal system to the postural adjustments occurring during voluntary gait modifications. *J Neurophysiol,* 85**,** 679-98.

PYNDT, H. S. & RIDDING, M. C. 2004. Modification of the human motor cortex by associative stimulation. *Exp Brain Res,* 159**,** 123-8.

RAO, J. S., LIU, Z., ZHAO, C., WEI, R. H., ZHAO, W., YANG, Z. Y. & LI, X. G. 2016. Longitudinal evaluation of functional connectivity variation in the monkey sensorimotor network induced by spinal cord injury. *Acta Physiol (Oxf),* 217**,** 164-73.

RIDDING, M. C., BROUWER, B., MILES, T. S., PITCHER, J. B. & THOMPSON, P. D. 2000. Changes in muscle responses to stimulation of the motor cortex induced by peripheral nerve stimulation in human subjects. *Exp Brain Res,* 131**,** 135-43.

RIDDING, M. C., MCKAY, D. R., THOMPSON, P. D. & MILES, T. S. 2001. Changes in corticomotor representations induced by prolonged peripheral nerve stimulation in humans. *Clin Neurophysiol,* 112**,** 1461-9.

RIDDING, M. C. & UY, J. 2003. Changes in motor cortical excitability induced by paired associative stimulation. *Clin Neurophysiol,* 114**,** 1437-44.

RIDDLE, C. N. & BAKER, S. N. 2010. Convergence of pyramidal and medial brain stem descending pathways onto macaque cervical spinal interneurons. *J Neurophysiol,* 103**,** 2821-32.

RIDDLE, C. N., EDGLEY, S. A. & BAKER, S. N. 2009. Direct and indirect connections with upper limb motoneurons from the primate reticulospinal tract. *J Neurosci,* 29**,** 4993-9.

ROSENGREN, S. M., WELGAMPOLA, M. S. & COLEBATCH, J. G. 2010. Vestibular evoked myogenic potentials: past, present and future. *Clin Neurophysiol,* 121**,** 636-51.

ROSENTHAL, J., WALLER, H. J. & AMASSIAN, V. E. 1967. An analysis of the activation of motor cortical neurons by surface stimulation. *J Neurophysiol,* 30**,** 844-58.

ROSENZWEIG, E. S., COURTINE, G., JINDRICH, D. L., BROCK, J. H., FERGUSON, A. R., STRAND, S. C., NOUT, Y. S., ROY, R. R., MILLER, D. M., BEATTIE, M. S., HAVTON, L. A., BRESNAHAN, J. C., EDGERTON, V. R. & TUSZYNSKI, M. H. 2010. Extensive spontaneous plasticity of corticospinal projections after primate spinal cord injury. *Nat Neurosci,* 13**,** 1505-10.

ROSSIGNOL, S. & JONES, G. M. 1976. Audio-spinal influence in man studied by the H-reflex and its possible role on rhythmic movements synchronized to sound. *Electroencephalogr Clin Neurophysiol,* 41**,** 83-92.

ROTHWELL, J., BURKE, D., HICKS, R., STEPHEN, J., WOODFORTH, I. & CRAWFORD, M. 1994. Transcranial electrical stimulation of the motor cortex in man: further evidence for the site of activation. *J Physiol,* 481 (Pt 1)**,** 243-50.

ROTHWELL, J. C. 2006. The startle reflex, voluntary movement, and the reticulospinal tract. *Suppl Clin Neurophysiol,* 58**,** 223-31.

ROTHWELL, J. C. 2016. Can Motor Recovery in Stroke Be Improved by Non-invasive Brain Stimulation? *Adv Exp Med Biol,* 957**,** 313-323.

ROTHWELL, J. C., HALLETT, M., BERARDELLI, A., EISEN, A., ROSSINI, P. & PAULUS, W. 1999. Magnetic stimulation: motor evoked potentials. The International Federation of Clinical Neurophysiology. *Electroencephalogr Clin Neurophysiol Suppl,* 52**,** 97-103.

ROTHWELL, J. C., THOMPSON, P. D., DAY, B. L., BOYD, S. & MARSDEN, C. D. 1991. Stimulation of the human motor cortex through the scalp. *Exp Physiol,* 76**,** 159-200.

ROY, F. D., ZEWDIE, E. T. & GORASSINI, M. A. 2011. Short-interval intracortical inhibition with incomplete spinal cord injury. *Clin Neurophysiol,* 122**,** 1387-95.

RUDELL, A. P. & EBERLE, L. P. 1985. Acoustic facilitation of the Hoffmann reflex. *Exp Neurol,* 89**,** 592-602.

SAKAI, K., UGAWA, Y., TERAO, Y., HANAJIMA, R., FURUBAYASHI, T. & KANAZAWA, I. 1997. Preferential activation of different I waves by transcranial magnetic stimulation with a figure-of-eight-shaped coil. *Exp Brain Res,* 113**,** 24-32.

SANGARI, S. & PEREZ, M. A. 2019. Imbalanced Corticospinal and Reticulospinal Contributions to Spasticity in Humans with Spinal Cord Injury. *J Neurosci,* 39**,** 7872-7881.

SANGARI, S. & PEREZ, M. A. 2020. Distinct Corticospinal and Reticulospinal Contributions to Voluntary Control of Elbow Flexor and Extensor Muscles in Humans with Tetraplegia. *J Neurosci,* 40**,** 8831-8841.

SCHABRUN, S. M. & RIDDING, M. C. 2007. The influence of correlated afferent input on motor cortical representations in humans. *Exp Brain Res,* 183**,** 41-9.

SCHAEFER, D. M., FLANDERS, A., NORTHRUP, B. E., DOAN, H. T. & OSTERHOLM, J. L. 1989. Magnetic resonance imaging of acute cervical spine trauma. Correlation with severity of neurologic injury. *Spine (Phila Pa 1976),* 14**,** 1090-5.

SCHEPENS, B. & DREW, T. 2004. Independent and convergent signals from the pontomedullary reticular formation contribute to the control of posture and movement during reaching in the cat. *J Neurophysiol,* 92**,** 2217-38.

SCHEPENS, B. & DREW, T. 2006. Descending signals from the pontomedullary reticular formation are bilateral, asymmetric, and gated during reaching movements in the cat. *J Neurophysiol,* 96**,** 2229-52.

SCHIRMER, C. M., SHILS, J. L., ARLE, J. E., COSGROVE, G. R., DEMPSEY, P. K., TARLOV, E., KIM, S., MARTIN, C. J., FELTZ, C., MOUL, M. & MAGGE, S. 2011. Heuristic map of myotomal innervation in humans using direct intraoperative nerve root stimulation. *J Neurosurg Spine,* 15**,** 64-70.

SHEMMELL, J., AN, J. H. & PERREAULT, E. J. 2009. The differential role of motor cortex in stretch reflex modulation induced by changes in environmental mechanics and verbal instruction. *J Neurosci,* 29**,** 13255-63.

SHINODA, Y., OHGAKI, T., SUGIUCHI, Y., FUTAMI, T. & KAKEI, S. 1992. Functional synergies of neck muscles innervated by single medial vestibulospinal axons. *Ann N Y Acad Sci,* 656**,** 507-18.

SIMMONS, Z. 2013. Electrodiagnosis of brachial plexopathies and proximal upper extremity neuropathies. *Phys Med Rehabil Clin N Am,* 24**,** 13-32.

SJOSTROM, P. J., TURRIGIANO, G. G. & NELSON, S. B. 2001. Rate, timing, and cooperativity jointly determine cortical synaptic plasticity. *Neuron,* 32**,** 1149-64.

SMITH, H. C., SAVIC, G., FRANKEL, H. L., ELLAWAY, P. H., MASKILL, D. W., JAMOUS, M. A. & DAVEY, N. J. 2000. Corticospinal function studied over time following incomplete spinal cord injury. *Spinal Cord,* 38**,** 292-300.

SMITH, V., MASLOVAT, D. & CARLSEN, A. N. 2019. StartReact effects are dependent on engagement of startle reflex circuits: support for a subcortically mediated initiation pathway. *J Neurophysiol,* 122**,** 2541-2547.

SOTEROPOULOS, D. S., WILLIAMS, E. R. & BAKER, S. N. 2012. Cells in the monkey ponto-medullary reticular formation modulate their activity with slow finger movements. *J Physiol,* 590**,** 4011-27.

STEFAN, K., KUNESCH, E., BENECKE, R., COHEN, L. G. & CLASSEN, J. 2002. Mechanisms of enhancement of human motor cortex excitability induced by interventional paired associative stimulation. *J Physiol,* 543**,** 699-708.

STEFAN, K., KUNESCH, E., COHEN, L. G., BENECKE, R. & CLASSEN, J. 2000. Induction of plasticity in the human motor cortex by paired associative stimulation. *Brain,* 123 Pt 3**,** 572-84.

STERIADE, M., PARE, D., PARENT, A. & SMITH, Y. 1988. Projections of cholinergic and non-cholinergic neurons of the brainstem core to relay and associational thalamic nuclei in the cat and macaque monkey. *Neuroscience,* 25**,** 47-67.

STONEY, S. D., JR., THOMPSON, W. D. & ASANUMA, H. 1968. Excitation of pyramidal tract cells by intracortical microstimulation: effective extent of stimulating current. *J Neurophysiol,* 31**,** 659-69.

TAPIA, J. A., TOHYAMA, T., POLL, A. & BAKER, S. N. submitted. The StartReact Effect Measures Reticulospinal Drive to Movement.

TATE, D. G., KALPAKJIAN, C. Z. & FORCHHEIMER, M. B. 2002. Quality of life issues in individuals with spinal cord injury. *Archives of Physical Medicine and Rehabilitation,* 83**,** S18-S25.

TAYLOR, J. L. 2006. Stimulation at the cervicomedullary junction in human subjects. *J Electromyogr Kinesiol,* 16**,** 215-23.

TAYLOR, J. L. & MARTIN, P. G. 2009. Voluntary motor output is altered by spike-timing-dependent changes in the human corticospinal pathway. *J Neurosci,* 29**,** 11708-16.

TAZOE, T. & PEREZ, M. A. 2017. Cortical and reticular contributions to human precision and power grip. *J Physiol,* 595**,** 2715-2730.

TERAO, Y. & UGAWA, Y. 2002. Basic mechanisms of TMS. *J Clin Neurophysiol,* 19**,** 322-43.

THABIT, M. N., UEKI, Y., KOGANEMARU, S., FAWI, G., FUKUYAMA, H. & MIMA, T. 2010. Movement-related cortical stimulation can induce human motor plasticity. *J Neurosci,* 30**,** 11529-36.

THE STATIONERY OFFICE 2005. *Control of Noise at Work Regulations*.

THOMAS, C. K., ZAIDNER, E. Y., CALANCIE, B., BROTON, J. G. & BIGLAND-RITCHIE, B. R. 1997. Muscle weakness, paralysis, and atrophy after human cervical spinal cord injury. *Exp Neurol,* 148**,** 414-23.

THURET, S., MOON, L. D. & GAGE, F. H. 2006. Therapeutic interventions after spinal cord injury. *Nat Rev Neurosci,* 7**,** 628-43.

TOHYAMA, T., KINOSHITA, M., KOBAYASHI, K., ISA, K., WATANABE, D., KOBAYASHI, K., LIU, M. & ISA, T. 2017. Contribution of propriospinal neurons to recovery of hand dexterity after corticospinal tract lesions in monkeys. *Proc Natl Acad Sci U S A,* 114**,** 604-609.

TOKIMURA, H., RIDDING, M. C., TOKIMURA, Y., AMASSIAN, V. E. & ROTHWELL, J. C. 1996. Short latency facilitation between pairs of threshold magnetic stimuli applied to human motor cortex. *Electromyography and Motor Control-Electroencephalography and Clinical Neurophysiology,* 101**,** 263-272.

TOTOIU, M. O. & KEIRSTEAD, H. S. 2005. Spinal cord injury is accompanied by chronic progressive demyelination. *J Comp Neurol,* 486**,** 373-83.

TWITCHELL, T. E. 1951. The restoration of motor function following hemiplegia in man. *Brain,* 74**,** 443-80.

UCHINO, Y., SATO, H., SASAKI, M., IMAGAWA, M., IKEGAMI, H., ISU, N. & GRAF, W. 1997. Sacculocollic reflex arcs in cats. *J Neurophysiol,* 77**,** 3003-12.

UENO, S., TASHIRO, T. & HARADA, K. 1988. Localized Stimulation of Neural Tissues in the Brain by Means of a Paired Configuration of Time-Varying Magnetic-Fields. *Journal of Applied Physics,* 64**,** 5862-5864.

UGAWA, Y., ROTHWELL, J. C., DAY, B. L., THOMPSON, P. D. & MARSDEN, C. D. 1991. Percutaneous electrical stimulation of corticospinal pathways at the level of the pyramidal decussation in humans. *Ann Neurol,* 29**,** 418-27.

URBIN, M. A., OZDEMIR, R. A., TAZOE, T. & PEREZ, M. A. 2017. Spike-timing-dependent plasticity in lower-limb motoneurons after human spinal cord injury. *J Neurophysiol,* 118**,** 2171-2180.

VALLS-SOLE, J., KUMRU, H. & KOFLER, M. 2008. Interaction between startle and voluntary reactions in humans. *Exp Brain Res,* 187**,** 497-507.

VALLS-SOLE, J., ROTHWELL, J. C., GOULART, F., COSSU, G. & MUNOZ, E. 1999a. Patterned ballistic movements triggered by a startle in healthy humans. *J Physiol,* 516 (Pt 3)**,** 931-8.

VALLS-SOLE, J., SOLE, A., VALLDEORIOLA, F., MUNOZ, E., GONZALEZ, L. E. & TOLOSA, E. S. 1995. Reaction time and acoustic startle in normal human subjects. *Neurosci Lett,* 195**,** 97-100.

VALLS-SOLE, J., VALLDEORIOLA, F., MOLINUEVO, J. L., COSSU, G. & NOBBE, F. 1999b. Prepulse modulation of the startle reaction and the blink reflex in normal human subjects. *Exp Brain Res,* 129**,** 49-56.

VAVREK, R., PEARSE, D. D. & FOUAD, K. 2007. Neuronal populations capable of regeneration following a combined treatment in rats with spinal cord transection. *J Neurotrauma,* 24**,** 1667-73.

VOLZ, L. J., HAMADA, M., ROTHWELL, J. C. & GREFKES, C. 2015. What Makes the Muscle Twitch: Motor System Connectivity and TMS-Induced Activity. *Cereb Cortex,* 25**,** 2346-53.

WAKABAYASHI, Y., KOMORI, H., KAWA-UCHI, T., MOCHIDA, K., TAKAHASHI, M., QI, M., OTAKE, K. & SHINOMIYA, K. 2001. Functional recovery and regeneration of descending tracts in rats after spinal cord transection in infancy. *Spine (Phila Pa 1976),* 26**,** 1215-22.

WATSON, S. R. & COLEBATCH, J. G. 1998a. Vestibular-evoked electromyographic responses in soleus: a comparison between click and galvanic stimulation. *Exp Brain Res,* 119**,** 504-10.

WATSON, S. R. & COLEBATCH, J. G. 1998b. Vestibulocollic reflexes evoked by short-duration galvanic stimulation in man. *J Physiol,* 513 (Pt 2)**,** 587-97.

WERHAHN, K. J., FONG, J. K., MEYER, B. U., PRIORI, A., ROTHWELL, J. C., DAY, B. L. & THOMPSON, P. D. 1994. The effect of magnetic coil orientation on the latency of surface EMG and single motor unit responses in the first dorsal interosseous muscle. *Electroencephalogr Clin Neurophysiol,* 93**,** 138-46.

WIETHOFF, S., HAMADA, M. & ROTHWELL, J. C. 2014. Variability in response to transcranial direct current stimulation of the motor cortex. *Brain Stimul,* 7**,** 468-75.

WILKINS, D. E., HALLETT, M. & WESS, M. M. 1986. Audiogenic startle reflex of man and its relationship to startle syndromes. A review. *Brain,* 109 (Pt 3)**,** 561-73.

WILLIAMS, E. R., SOTEROPOULOS, D. S. & BAKER, S. N. 2010. Spinal interneuron circuits reduce approximately 10-Hz movement discontinuities by phase cancellation. *Proc Natl Acad Sci U S A,* 107**,** 11098-103.

YOSHINO-SAITO, K., NISHIMURA, Y., OISHI, T. & ISA, T. 2010. Quantitative inter-segmental and inter-laminar comparison of corticospinal projections from the forelimb area of the primary motor cortex of macaque monkeys. *Neuroscience,* 171**,** 1164-79.

ZAAIMI, B., EDGLEY, S. A., SOTEROPOULOS, D. S. & BAKER, S. N. 2012. Changes in descending motor pathway connectivity after corticospinal tract lesion in macaque monkey. *Brain,* 135**,** 2277-89.

ZAAIMI, B., SOTEROPOULOS, D. S., FISHER, K. M., RIDDLE, C. N. & BAKER, S. N. 2018. Classification of Neurons in the Primate Reticular Formation and Changes after Recovery from Pyramidal Tract Lesion. *J Neurosci,* 38**,** 6190-6206.

ZIEMANN, U. & ROTHWELL, J. C. 2000. I-waves in motor cortex. *J Clin Neurophysiol,* 17**,** 397-405.

ZIEMANN, U., TERGAU, F., WASSERMANN, E. M., WISCHER, S., HILDEBRANDT, J. & PAULUS, W. 1998a. Demonstration of facilitatory I wave interaction in the human motor cortex by paired transcranial magnetic stimulation. *J Physiol,* 511 (Pt 1)**,** 181-90.

ZIEMANN, U., TERGAU, F., WISCHER, S., HILDEBRANDT, J. & PAULUS, W. 1998b. Pharmacological control of facilitatory I-wave interaction in the human motor cortex. A paired transcranial magnetic stimulation study. *Electroencephalogr Clin Neurophysiol,* 109**,** 321-30.

ZORNER, B., BACHMANN, L. C., FILLI, L., KAPITZA, S., GULLO, M., BOLLIGER, M., STARKEY, M. L., ROTHLISBERGER, M., GONZENBACH, R. R. & SCHWAB, M. E. 2014. Chasing central nervous system plasticity: the brainstem's contribution to locomotor recovery in rats with spinal cord injury. *Brain,* 137**,** 1716-32.